MAGYAR ÁLLAMI
EÖTVÖS LORÁND
GEOFIZIKAI INTÉZET

EÖTVÖS LORÁND
GEOPHYSICAL INSTITUTE
OF HUNGARY

GEOFIZIKAI KÖZLEMÉNYEK

GEOPHYSICAL TRANSACTIONS

ВЕНГЕРСКИЙ
ГЕОФИЗИЧЕСКИЙ
ИНСТИТУТ
ИМ Л. ЭТВЕША

ГЕОФИЗИЧЕСКИЙ
БЮЛЛЕТЕНЬ

BUDAPEST

CONTENTS

VOL. 36. NO. 1–2. JUNE 1991(ISSN 0016–7177)

CONTENTS continued

TARTALOMJEGYZÉK

СОДЕРЖАНИЕ

Licensed to cruise at super seismic speeds

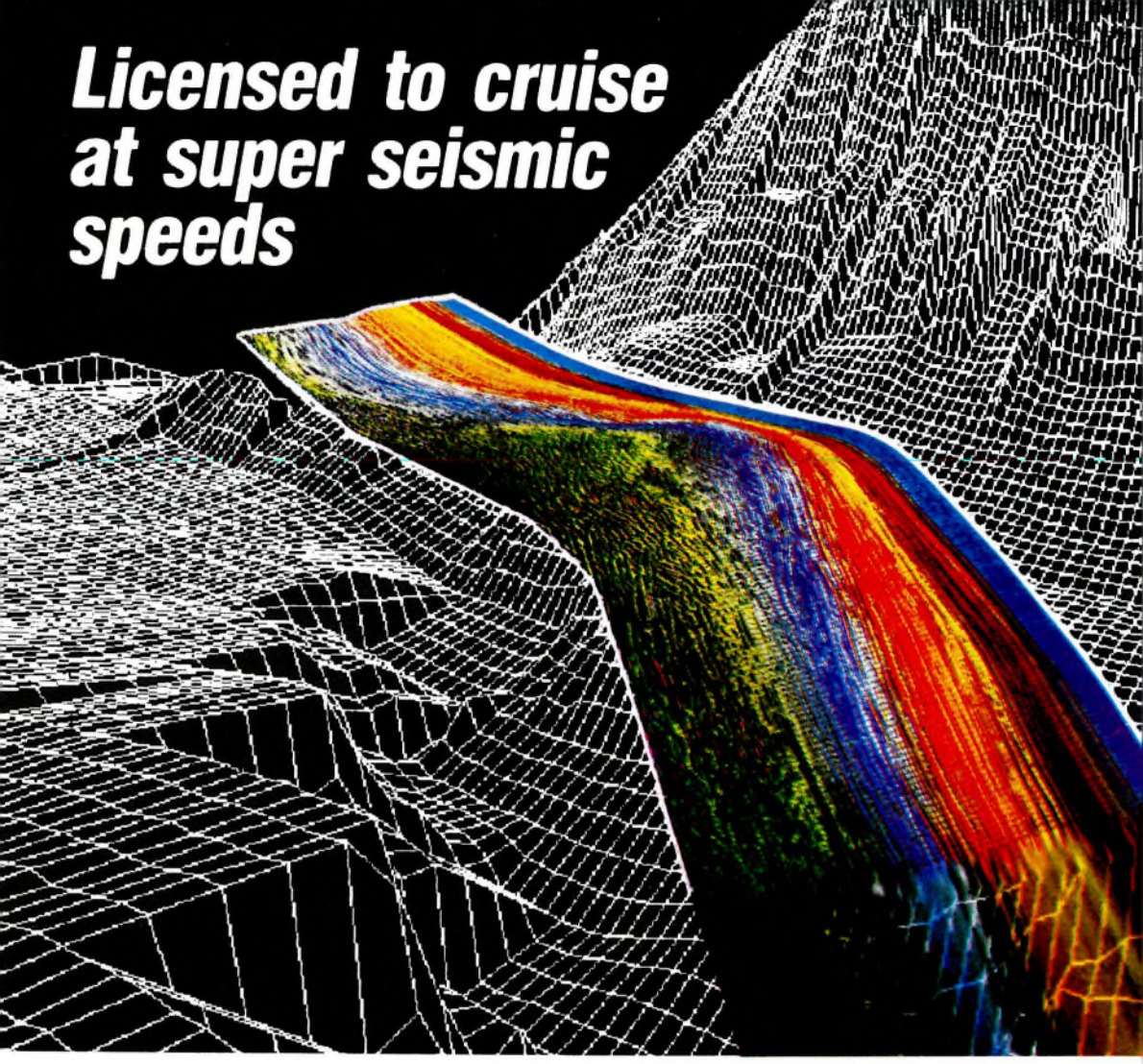

If your seismic data processing gets stuck in first gear when entering complex geological zones, consider licensing seismic processing software from Western Geophysical.

Western software is being used to process data from geologic provinces throughout the world. In fact, more miles of seismic data are processed with Western software, at the highest efficiency level, than any other software.

Western seismic processing software operates on vector supercomputers as well as scalar mainframes and departmental minicomputers. Every user has access to Western's comprehensive program library designed for effective and efficient processing of 2-D and 3-D surveys on land, at sea, and across shallow-water transition zones.

The latest software enhancements, released on a continuous basis by Western's R&D and Computer Science departments, are available through the Software Subscription Service. If you run into a problem, our Rapid Response teams are on alert to clear any processing flightpaths.

Whether you need a basic processing package or full facility management, call Western Geophysical and shift your seismic center into high gear.

Western Atlas International
A Litton/Dresser Company

WESTERN GEOPHYSICAL

Wesgeco House
PO Box 18
455 London Road
Isleworth, Middlesex
England TW7 5AB
(081) 560-3160
Fax (081) 847-3131

Houston	(713) 789-9600
Denver	(303) 770-8660
Calgary	(403) 291-8100
Singapore	65-258-3455
Caracas	58-2-262-0272
Bogota	57-1-267-6199
Rio de Janeiro	55-21-541-1599

EÖTVÖS L. GEOPHYSICAL INSTITUTE OF HUNGARY

THE OLDEST INSTITUTION FOR APPLIED GEOPHYSICS OFFERS THE LATEST ACHIEVEMENTS FOR GROUND-WATER PROSPECTING and ENVIRONMENTAL PROTECTION

The most often occurring demands:

- local geophysical measurements for the water supply of small communities by a few wells
- regional geophysical mapping to determine hydrological conditions for irrigation, regional agricultural development,
- large-scale exploration for the water supply of towns, extended areas i.e. regional waterworks,
- determination of bank storage of river terraces, planning of bank filtered well systems,
- thermal water exploration for use as an energy source, agricultural use or community utilization,
- cold and warm karst water prospecting,
- water engineering problems, water construction works

The Maxi-Probe electromagnetic sounding and mapping system – produced under licence by Geoprobe Ltd. Canada – is an ideal tool for shallow depths, especially in areas where seismic results are poor or unobtainable.

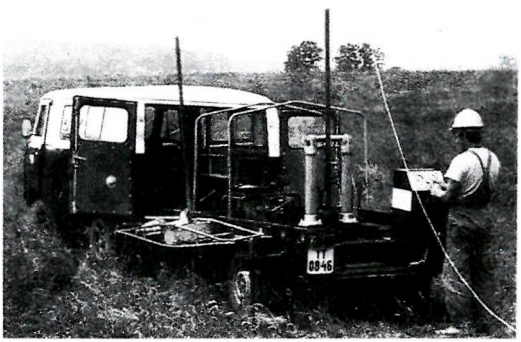

ELGI has a vast experience in solving problems of environmental protection such as control of surface waters, reservoir construction, industrial and communal waste disposal, protection of surface and ground water etc. ELGI's penetrologger provides in-situ information – up to a maximum depth of 30 m – on the strength, sand/shale ratio and density without costly drilling.

Field work with ELGI's 24-channel portable seismograph

ELGI offers contracts with co-operating partners to participate in the whole complex process of exploration–drilling–production.

For further information ask for our booklets on instruments and applications. Let us know your problem and we will select the appropriate method and the best instrument for your purpose.

Our address: ELGI POB 35. Budapest, H–1440. HUNGARY
Telex: 22-6194 elgi h

PREFACE

The Austrian Geologische Bundesanstalt and the Hungarian Central Office of Geology have regularly cooperated since agreeing — in 1968 — on the mutual exchange of scientific results between the geoscientific institutes of the two countries. Geology is not concerned with state borders in view of which the cooperation has meant that several research tasks have been solved together, and in a number of cases a third country was also asked to participate in the investigations.

The present volume contains all the results of these joint activities of the recent past that are ready for publication. The construction of the pre-Tertiary basement contour map or the delineation of the crust–mantle boundary were typically such tasks that required multilateral cooperation. Palaeomagnetic studies of the Eastern Alps and the geomagnetic investigation of the Penninic Unit represent other examples involving the common interpretation of geoscientific problems. Within geophysical methodological research there have also been several other topics in which the geophysicists of the cooperating countries could complement each other's knowledge.

There is little doubt that far better results are achieved when experts or expert teams have the possibility to discuss their problems with others who are similarly engaged. Such an approach has even more significance in small countries such as Austria or Hungary where one often has to seek for colleagues beyond national borders. It is earnestly hoped that these joint activities and similar collaboration in the future will continue to promote successful research.

Dr. Károly Posgay

GEOPHYSICAL TRANSACTIONS 1991
Vol. 36. No. 1–2. pp. 7–13

CONTOUR MAP OF THE MOHOROVIČIĆ DISCONTINUITY BENEATH CENTRAL EUROPE

Károly POSGAY*, István ALBU**, Milica MAYEROVÁ+, Zelenka NAKLÁDALOVÁ+, Ivan IBRMAJER+, Milan BLIŽKOVSKÝ+, Kay ARIC++, Rudolf GUTDEUTSCH++

A Moho contour map was compiled by using data from various geophysical measurements performed in Austria, Czechoslovakia and Hungary. The intention in publishing the map of crustal thickness (Moho depth) is to increase the available information on the Alp-Carpathian mountain system and the young (Neogene) Pannonian basin. It is hoped that apart from contributing towards the knowledge of the area, this work will promote further structural analyses.

Keywords: deep seismic sounding, Mohorovičić discontinuity, crustal thickness, Alps, Carpathians, Pannonian basin

1. Introduction

Based on seismic measurements taken in and before 1984 we have compiled a map of the Earth's crust–mantle boundary (Mohorovičić–discontinuity) for the area of Austria, Czechoslovakia and Hungary. The data were obtained in different ways and thus differed in quality and accuracy. It is mentioned that apart from providing information on crustal thickness, the map reflects all shortcomings: lack of data — especially in Austria — irregular distribution of data, non-uniform reliability.

2. Data acquisition and compilation of the map

The first experiments to study the Earth's crust by the seismic reflection method started in Hungary in 1954. The results showed that the crust is substantially thinner in the Pannonian basin than in the surrounding areas [GÁLFI and STEGENA 1955]. Individual reflections gave only approximate information on the depth of deep reflectors and this gave no clue as to the velocity distribution within and below the crust. Experiments were continued by using refraction seismics and later by combined refraction and reflection measurements [MITUCH et al. 1964].

* Eötvös Loránd Geophysical Institute of Hungary, Budapest, POB 35, H–1440, Hungary
** Central Office of Geology, Budapest, Arany János u. 25, H–1051, Hungary
+ Geofyzika n.p. Brno, Brno-Řečkovice, Ječná ul. 29a, 612 46 Brno 12, Czechoslovakia
++ Institute of Meteorology and Geophysics, University of Vienna, A–1190 Wien, Hohe Warte 38, Austria
Manuscript received: 16 May, 1989

Since the early 70s multiple coverage reflection measurements have been made in Hungary using digital seismic stations. Furthermore reflection arrivals enabled us to draw conclusions concerning the structure and the velocity of the lithosphere [POSGAY 1975].

Data gained from a network of regional seismic profiles [RÁNER et al. 1972] and magnetotelluric soundings [RÁNER et al. 1983] contributed to the integrated study of the structure of the crust and upper mantle in Hungary, (also involving heat flow data) and resulted in the compilation of a depth contour map of the Mohorovičić discontinuity. Further results of this study revealed tectonic features and geophysical parameters within the investigated depth range [POSGAY et al. 1986]. It was concluded that the crust was separated from the upper mantle by a transition zone which has changed in both depth and thickness throughout geological time. The contour lines of the Moho map reflect the lower boundary of this transition zone.

The first international DSS profile (No VI) crossing the GDR, Czechoslovakia and Hungary was carried out in the early 60s. The results of the international co-operation creating a network of deep seismic profiles in Central and Eastern Europe appeared in the following monographs: Eds. SOLLOGUB et al. 1971, 1978, 1980, Crustal Monograph 1972.

Hungary also participated in the project of ALP75 longitudinal profile [MILLER 1976, MILLER et al. 1977]. This cooperation enabled us to combine Hungarian and Austrian data.

In Czechoslovakia, investigation of the deeper parts of the Earth's crust, including the Moho relief, began in 1962 as part of a project prepared by the European Seismological Commission in 1959. Czechoslovakia participated in DSS measurements along profiles VI, V and VII until 1972 (see *Fig. 1*).

From 1975 to 1980 measurements were carried out on national regional profiles KIII, KII, 100R an KI (Fig. 1) in the Czechoslovakian West Carpathians [BERÁNEK and ZÁTOPEK 1981]. The purpose of these measurements was to trace refraction boundaries, to determine the velocity distribution in the crust and to gather information on the relief and depth of the Moho. In 1979 seismic measurements were also conducted along the Czech part of the Fennolora profile [BERÁNEK et al. 1983].

In the period 1971–1984 the information on the Moho from international and regional Carpathian profiles was complemented systematically by recording seismic waves generated by industrial blasts [BERÁNEK et al. 1973]. In this case measurements were carried out using seismic sounding at discrete points (Fig. 1). The methodology and first results of processing these records were described by BERÁNEK and ZOUNKOVÁ [1977].

The Moho map taken from earlier works [BERÁNEK and ZOUNKOVÁ 1977, BERÁNEK and ZÁTOPEK 1981] has gradually been complemented. The depth to the Moho was computed on the assumption of a smooth seismic boundary and therefore individual data were processed using a smoothing program. The Moho depths were given in relation to the sea level and corrections for the unconsolidated part of the Earth's crust were introduced. The first arrivals of

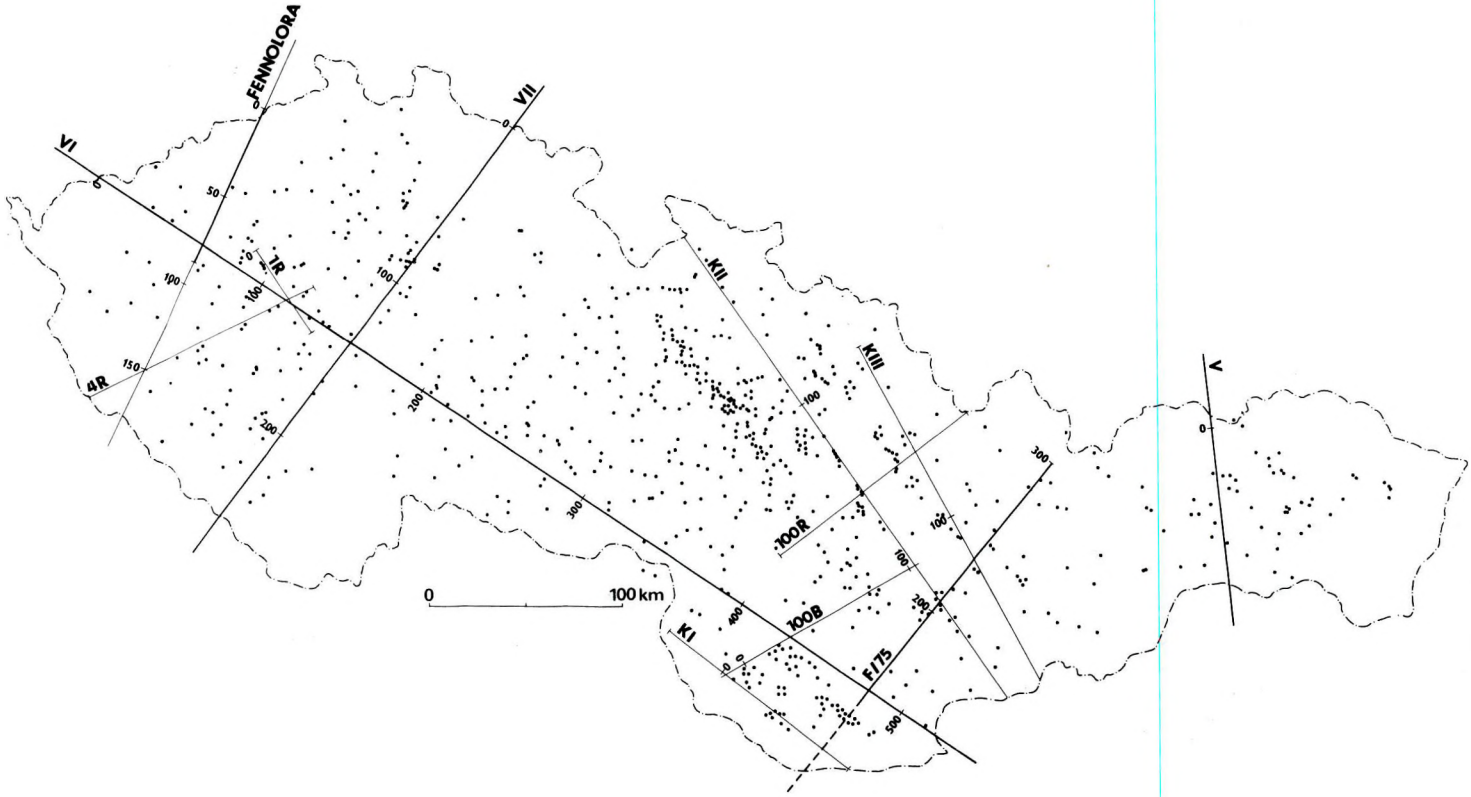

Fig. 1. Location map of seismic measurements for crustal investigation in Czechoslovakia

1. ábra. Földkéregkutató szeizmikus mérések helyszínrajza Csehszlovákiában

Рис. 1. План ситуации сейсмических измерений для изучения земной коры на территории Чехо-Словакии

the groups of P_M-waves were used for the map. The corrected arrival times were converted to depth data at individual points. The average velocity of 6.3 km/s was used for the Bohemian Massif and also for the Carpathian system [MAYEROVA et al. 1985].

During the period 1980–1987 about 800 km of seismic reflection profiles were shot in Czehoslovakia with recording times up to 16 sec. The majority of them contains recognizable reflections originating at the Moho. Depth data derived from these profiles are incorporated into the contour map *(Encl. 1)*.

During these years seismic crustal investigations in countries of western and southern Europe were carried out partly on a national basis and partly with support of the European Seismological Committee [GIESE et al. 1973]. Longitudinal profiles along the Alps [MILLER 1976, MILLER et al. 1978] provided information about the structure of the Mohorovičić discontinuity from France to Hungary. These data mainly come from a reinterpretation of profile ALP75, where two-dimensional models of the crust were calculated using the ray-tracing method [ARIC 1981]. These models, constructed on the basis of travel time measurements, were tested and improved by the interpretation of amplitudes, while Q-values for the upper and lower crust were also calculated [LENHARDT 1983].

Additional information was provided by short seismic profiles [ARIC et al. 1987] as well as by the near SNEALP 77 earthquake array perpendicular to ALP75 [LIDSTER et al. 1979]. OSTERODE [1976] used teleseismic signals observed in Vienna in order to obtain details on the crustal structure and Moho depth from the crust's transmission function. Reflection seismic measurements in near vertical and wide angle ranges [WEBER et al. 1981, MAURITSCH et al. 1986, ARIC 1981] as well as near earthquake measurements on local arrays [GEBRANDE et al. 1978] provided complementary Moho depth data.

Gravity measurements carried out in the Eastern Alps published by PARTSCH [1971], MAKRIS [1971], GÖTZE [1984] and MEURERS et al. [1987] should be mentioned here as they provide some indications on the Moho relief. The Moho map of MAKRIS is partly supported by models suggested by GIESE [1968] from older refraction seismic profiles perpendicular to the Alps. The link between gravity and seismic interpretation comes from empirical relations between Moho depths and $\Delta g''$ along these profiles. GÖTZE refers to the same source. MEURERS et al. fit their model, which covers a smaller area (50 km broad at about 11° longitude), to the seismic model provided by ALP75 [MILLER 1976]. Recently GRANSER [1986], GRANSER et al. [1988] and STEINHAUSER and PUSTIZEK [1987] have published maps of the M–discontinuity on the basis of $\Delta g''$ data using an inversion method.

The fundamental approach in gravity modelling differs from that used in seismics. That is why for this map we do not use models based on gravity data in order to prevent an undesirable mixture of information of different quality.

3. Conclusion

Data presented on the final map of the Moho (Encl. 1) come from areas of completely different tectonic units. Therefore the acoustic parameters which led to its construction vary between wide limits and so does the density of source data. In spite of this, the final map should be appreciated as the first one in Central Europe which shows the Moho relief on a 1:1,000,000 scale. There are gaps in the data mainly between the Alps and the Czech border. Additional measurements on several short profiles will be necessary in order to check the depth of the Moho in the northern part of Austria.

REFERENCES

ARIC K. 1981: Deutung krustenseismischer und seismologischer Ergebnisse im Zusammenhang mit der Tektonik des Alpenostrandes. Österr. Akad. d. Wiss. Smn. 190–13, Springer Verlag, Wien

ARIC K., GUTDEUTSCH R., KLINGER G., LENHARDT W. 1987: Seismological Studies in the Eastern Alps. In: Geodynamic of the Eastern Alps. (Eds. Flügel H. W. and Faupl P.) Deuticke Verlag, Wien, pp. 326–333

BERÁNEK B., ZOUNKOVÁ M., PETR W. 1973: Erforschung des Tiefbaus der Erdkruste in der CSSR unter Ausnützung industriemassiger Sprengungen. Proceedings of the Xth Congress CBGA 1973. Sec. VIII. Geophysics. GUDS Bratislava, 103 p.

BERÁNEK B. and ZOUNKOVÁ M. 1977: Investigations of the earth's crust in Czechoslovakia using industrial blasting. Studia geophys. et geod. **21,** 3–4, pp. 273–280

BERÁNEK B., SCHENK V., FIRBAS P., MAYEROVÁ M., ZÁTOPEK A. and SCHULZE A. 1983: The Fennolora experiment and crustal structure in the Bohemian massif. Proc. of the 17th Assembly of the ESC, Budapest 1980, pp. 479–481

BERÁNEK B. and ZÁTOPEK A. 1981: Earth's crust structure in Czechoslovakia and in Central Europe by methods of explosion seismology. In: Geophysical Syntheses in Czechoslovakia (Ed. Zátopek A.), Veda, Bratislava, pp. 243–264

Crustal Monograph 1972: The crustal structure of central and southeastern Europe based on the results of explosion seismology. In: Geofizikai Közlemények, Special issue (ed. Szénás Gy.) 172 p.

GÁLFI J. and STEGENA L. 1955: Deep reflections in the region of Hajdúszoboszló (in Hungarian with English abstract). Geofizikai Közlemények **6,** 1–2, pp. 53–60

GEBRANDE H., HÖGE H., MILLER H., MÜLLER G. and SCHMEDES E. 1978: Aftershock investigations and fault-plane solutions of the Friuli earthquakes 1976. In Alps, Apennines, Hellenides; Verlag Schweizerbart, Stuttgart, pp. 173–189

GIESE P. 1968: Versuch einer Gliederung der Erdkruste in nördlichen Alpenvorland, in der Ostalpen und in Teilen der Westalpen mit Hilfe charakteristischer Refraktions–Laufzeit–Kurven sowie eine geologische Deutung. Geophysikalische Abhandlungen 1, 2, Verlag von D. Reimer in Berlin. Monographie. 202 p.

GIESE P., MORELLI C. and STEINMETZ I. 1973: Main features of crustal structure in western and southern Europe based on data of exploration seismology. Tectonophysics **20,** 1–4, pp. 367–379

GÖTZE H. J. 1984: Über den Einsatz interaktiver Computergraphik im Rahmen 3-dimensionaler Interpretations-techniken in Gravimetrie und Magnetik. Habilitation Thesis, Technische Universitat Clausthal. 236 p.

GRANSER H. 1988: Gravimetric studies in the Eastern Alps. Tagungsbericht. 4. Int. Alpen Gravimetric Koll. Wien 1986. Berichte über den Tiefbau der Ostalpen ZAMG, No 323. pp. 89–98.

GRANSER H., MEUVERS B. and STEINHAUSER P. 1988: Apparent density mapping and 3D gravimetry inversion in the Eastern Alps. Geophysical Prospecting **37,** 3, pp. 279–292

LENHARDT W. 1983: Bestimmung der Absorptionseigenschaften der Erdkruste im Bereich der Ostalpen. Ph. D. Thesis, Univ. Wien. 118 p.

LIEDSTER R. C., ARIC K. and KING R. 1979: Preliminary results from a seismic network in the Eastern Alps. EOS Trans., Am. Geoph. Un., **60,** 7, 101 p.

MAYEROVÁ M., NAKLÁDALOVÁ Z., IBRMAJER I. and HERMAN H. 1985: Areal distribution of the Moho discontinuity in Czechoslovakia based on results of DSS profile measurements and quarry blasts. Procc. of 8th Geophysical congress of Cz. geophysicists, České Budějovice (in Czech.)

MAKRIS J. 1971: Aufbau der Kruste in den Ostalpen aus Schweremessungen und Ergebnissen der Refraktions-seismik. Hamburger Geophys. Einzelschriften, **15,** Hamburg

MAURITSCH H. J., SCHMÖLLER R., WALACH G., WEBER F. 1986: Geophysical investigaton of crustal structures in the Eastern Alps and the Alpine–Pannonian transition zone. Arbeiten aus der Zentralanstalt für Meteorologie und Geodynamik **67,** Wien

MEURERS B., RUESS D. and STEINHAUSER P. 1987: The Gravimetric Alpine Traverse. Geodynamics of the Eastern Alps, Deuticke Verl., Wien, pp. 334–344

MILLER H. 1976: A Lithospheric seismic profile along the axis of the Alps, 1975.: Pageoph **114,** 6, pp. 1109–1130

MILLER H., GEBRANDE H. and SCHMEDES E. 1977: Ein verbessertes Strukturmodell für die Ostalpen, abgeleitet aus refraktions-seismischen Daten unter Berücksichtigung des Alpenlangprofiles. Geolog. Rundschau **66,** pp. 289–308

MILLER H., ANSORGE J., ARIC K. and PERRIER G. 1978: Preliminary results of the lithospheric seismic Alpine longitudinal profile 1975, from France to Hungary. In: Alps, Appenines, Hellenides; Verlag Schweizerbart, Stuttgart

MITUCH E., POSGAY K. and SÉDY L. 1964: The use of wide angle reflections for the investigation of the earth's crust (in Hungarian with English abstract). Geofizikai Közlemények **13,** 2, pp. 201–210

OSTERODE W. 1976: Die Krustenstruktur im Raume Wien, abgeleitet aus kurz- und langperiodischen Raumwellen. Ph. D. Thesis, Univ. Wien. 112 p.

PARTSCH W. 1971: Ein gravimetrisches Modell der Erdkruste im Gebiet der Ostalpen. Z. Geophys. **37,** 6, pp. 957–973

POSGAY K. 1975: Mit Reflexionmessungen bestimmte Horizonte und Geschwindigkeitsverteilung in der Erdkruste und im Erdmantel. Geophysical Transactions **23,** 1. pp. 13–27

POSGAY K., ALBU I., RÁNER G. and VARGA G. 1986: Characteristics of the reflecting layers in the Earth's crust and upper mantle in Hungary (in Reflection Seismology; A global perspective.) Geodynamics Series **13,** AGU, Washington

RÁNER G., KÓNYA A. and SZALAY I. 1972: The methodological research of the foregrounds of the Hungarian Central range. Annual Report of ELGI for 1971. In Hungarian pp. 42–46 with English abstract p. 119

RÁNER G., ALBU I., ÁDÁM O., MAJKUTH T., NEMESI L., TÁTRAI M. and VARGA G. 1983: Regional study of the tectonics of Transdanubia. Annual Report of ELGI for 1982. In Hungarian pp. 66–71, with English abstract p. 191

SOLLOGUB V. B., PROSEN D. and MILITZER H. 1971: Crustal structure of Central and Southeastern Europe (in Russian). Naukova dumka, Kiev, 286 p.

SOLLOGUB V. B., GUTERCH A. and PROSEN D. 1978: Structure of the Earth's Crust and Upper Mantle of Central and Eastern Europe (in Russian). Naukova dumka, Kiev, 271 p.

SOLLOGUB V. B., GUTERCH A. and PROSEN D. 1980: Structure of the Earth's Crust in Central and Eastern Europe according to Geophysical Investigations (in Russian). Naukova dumka, Kiev, 206 p.

STEIHAUSER P. and PUSTIZEK A. 1987: Estimation of the mass deficit of the Eastern Alps. Geod. Arbeiten Öst. für die Int. Erdmessung, Neue Folge, **4,** Graz

WEBER F., HANSCHEK H., MAURITSCH H. J., OBERLADSTATTER M., SCHMÖLLER R. and WALACH G. 1981: Activities of the Institute of Geophysics of the Mining University Leoben in the International Geodynamic Project 1972–1979. BMWF, Wien. pp. 35–38

A MOHOROVIČIČ HATÁRFELÜLET KÖZÉP-EURÓPA ALATTI DOMBORZATA

POSGAY Károly, ALBU István
Milica MAYEROVÁ, Zelenka NAKLÁDALOVÁ, Ivan IBRMAJER, Milan BLIŽKOVSKÝ, Kay ARIC, Rudolf GUTDEUTSCH

Ausztria, Csehszlovákia és Magyarország területén különböző időben és módszerekkel készült mérések eredményeinek felhasználásával készítettük el a Mohorovičić határfelület mélységtérképét. A három ország területére szerkesztett kéregvastagság térkép (Moho mélység térkép) publikálásával növelni szándékoztuk az Alp-Kárpáti rendszer és a Pannon medence földtani ismeretességét. Reméljük, hogy térképünk hozzájárul a terület jobb megismeréséhez és elősegíti újabb szerkezeti elemzések megalapozását.

РЕЛЬЕФ ПОВЕРХНОСТИ МОХОРОВИЧИЧА ПОД ЦЕНТРАЛЬНОЙ ЕВРОПОЙ

Карой ПОШГАИ, Иштван АЛЬБУ,
Милица МАЙЕРОВА, Зеленка НАКЛАДАЛОВА, Иван ИБРМАЙЕР,
Милан БЛИЖКОВСКИ, Кай АРИЧ, Рудольф ГУТДАЙЧ

Карта глубины залегания поверхности Мохоровичича составлена с использованием результатов измерений, выполненных в разные периоды с применением различных методов по территории Австрии, Чехо-Словакии и Венгрии. Опубликованием карты мощности земной коры (глубины залегания Мохо) предполагается повысить геологическую изученность Альпийско-Карпатской горной системы и Паннонского бассейна. Можно надеяться, что данная карта окажется вкладом к лучшему познанию региона и будет способствовать обоснованию дальнейших тектонических синтезов.

GEOPHYSICAL TRANSACTIONS 1991
Vol. 36. No. 1–2. pp. 15–36

PRE-TERTIARY BASEMENT CONTOUR MAP OF THE CARPATHIAN BASIN BENEATH AUSTRIA, CZECHOSLOVAKIA AND HUNGARY

Éva KILÉNYI*, Arthur KRÖLL**, Dusan OBERNAUER+, Jan ŠEFARA+, Peter STEINHAUSER++, Zoltán SZABÓ* and Godfrid WESSELY**

Within the cooperation between Bundesanstalt, Austria, Geofyzika n. p. Bratislava Branch, and ELGI, Budapest a unified basement contour map was constructed for that part of the Carpathian basin belonging to the three countries. The Carpathian basin can be divided into several basins, the largest of them being the Pannonian basin, which in turn can further be divided into sub-basins such as the Danube–Rába basin and the Békés basin just to mention the biggest ones. Wrench faulting is an important factor in the forming of these basins; the best-known pull-apart basins are the Vienna basin and the East Slovakian basin. Although the concept is unified as pre-Tertiary basement, both the geological model and the coverage by geophysical measurements are extremely heterogeneous. Four basic models can be assigned to the different sub-basins. The geophysical methods dominating in the map construction are governed by the geological model and the availability of geophysical data.

Keywords: Carpathian basin, Pannonian basin, Vienna basin, wrench faulting, pull-apart basins, pre-Tertiary basement, contour map

1. Introduction

In 1983–84 in the framework of preparing a Geological Atlas of Hungary, the geological map of the basement was constructed by a team of geologists and geophysicists — on a scale of 1:500,000 — and it was presented at the XXVII. International Geological Congress, Moscow, 1984. This map consists of two separate maps: the geological subcrop map and the depth contour map. As the contour map itself contains so much information, we thought it worthwhile to publish it separately. The map was published in Geophysical Transactions Vol. 35. No. 4. [KILÉNYI – RUMPLER 1984] on a scale of 1:1,000,000. In the Introduction it was written of the Pannonian Basin being divided into sub-basins:

> 'All these sub-basins are cut by political borders. Let this paper be an appeal to geologists and geophysicists of the neighbouring countries to join forces and construct a unified map of the whole of the Carpathian basin!'

The first step towards realizing this dream was the co-operation agreement between ELGI and Geofyzika n. p. Bratislava Branch, Czechoslovakia, in 1985.

* Eötvös Loránd Geophysical Institute of Hungary, Budapest, POB 35, H–1440, Hungary
** ÖMV A–1211 Wien, Postfach 200
+ Geofyzika n. p. Bratislava Branch, Bratislava, Geologicka 18, ČSFR
++ Central Institute for Meteorology and Geodynamics POB 342, A–1191, Vienna, Austria
Manuscript received (revised version): 1 November, 1990

The existing basement contour map for Slovakia fitted well with the Hungarian one in the main features, though in detail there were quite a lot of problems to be solved. This work had just started when the annual co-operation discussions took place between representatives of Austrian and Hungarian geoscientists. The suggestion of ELGI for co-operation in unifying the basement contour maps met with the interest of the Austrian party and the topic was included in the co-operation programme.

The result of this trilateral co-operation is presented now (as an Enclosure) on a scale of 1:500,000.

2. Geological–geophysical characteristics

Although the concept is unified as pre-Tertiary basement, both the geological model and the coverage by geophysical measurements are extremely heterogeneous. Four basic models can be assigned to the different sub-basins:

A) Areas of crystalline or Mesozoic carbonate basement filled with Neogene sediments

This model is the most favourable for all geophysical methods: the basin floor forms a sharp physical discontinuity (*Fig. 1*). In such areas the accuracy of the contour map is determined by the density of the reflection seismic network, or by the proportion of direct depth defining methods in the applied geophysical ensemble.

B) Areas of non-carbonate Mesozoic or Palaeozoic basement

This model responds in different ways to different geophysical methods. For example, graphitic schists have low resistivity but high density and velocity. Thus the contradiction between two methods helps us to recognize this model, and the problem can only be solved with the help of an integrated interpretation of several geophysical methods.

C) Areas of inhomogeneous cover containing screening layers

This model is the most difficult and most ambiguous regarding depth determination. Areas of deep basins covered by sediments including Neogene (or Palaeogene) volcanics belong to this model. Tertiary volcanic formations, mostly of the Badenian to Sarmatian age, are a part of the basin fill. The

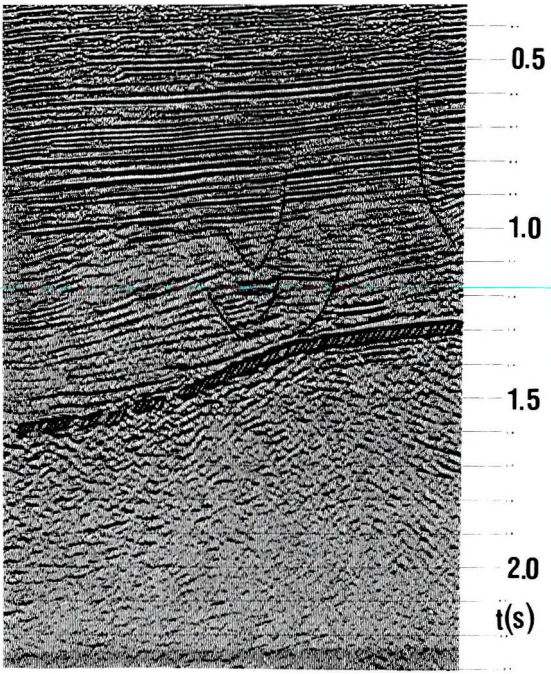

Fig. 1. Migrated time section from the Szeghalom area. Pre-Cambrian crystalline schists form the basin floor [after TAKÁCS E. 1990. Unpublished report of ELGI]

1. ábra. Migrált időszelvény Szeghalom környékéről. Prekambriumi kristályos palák képezik a neogén üledékösszlet aljzatát [TAKÁCS E. 1990 kéziratos jelentése, ELGI Adattár, nyomán]

Рис. 1. Временной разрез с миграцией из окрестностей г. Сегхалом. Фундамент неогеновых отложений сложен докембрийскими кристаллическими сланцами (по рукописному отчету Э. Такача [TAKÁCS E. 1990], фонды Венгерского Геофизического института)

evolution of volcanism exhibits a causality with the relief of the basement forming volcano-tectonic features in the relief (calderas, volcano-tectonic elevations and depressions (*Fig. 2*). Many volcanic formations are covered. On the surface they are most extensive in Central Slovakia.

Another type of area belonging to this class is where the cover contains high density, high velocity limestone layers (generally Eocene). In both cases (volcanics and limestones) the relative position of the screening layer basically affects the problem: if there is a thick enough layer of low resistivity and velocity between the screen and the basement, its depth can be determined by electromagnetic and seismic reflection methods. If, however, the screening layer is deposited directly on the basement, it cannot be separated by any geophysical method.

D) Flysch basins

The pre-Neogene basement of the Vienna Basin is partially formed by the flysch of the Vienna Forest and of the Magura group in the Externides, and the Senonian to Paleogene of the peri-Klippen zone (the Myjava formation) in the Internides (*Fig. 3*). The East Slovakian Basin — which extends partly into the Externides — probably includes the Palaeogene up to the Oligocene [GRECULA et al. 1981] in its basement (*Fig. 4*).

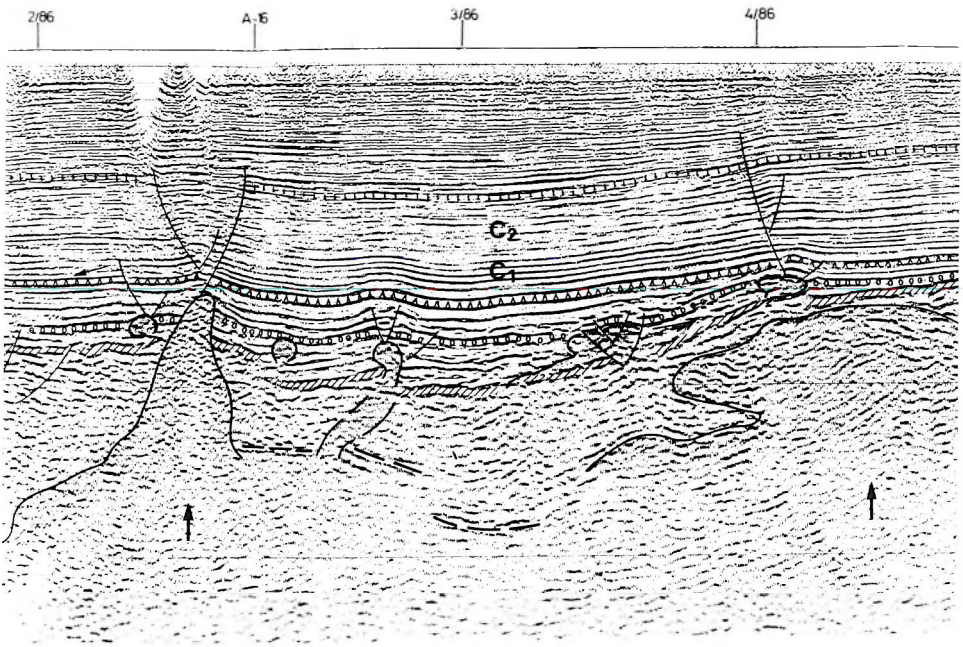

Fig. 2. Migrated time section from the Nyír area to illustrate the connection between volcanism and basement tectonics [after KILÉNYI et al. 1989]

2. ábra. Migrált időszelvény a Nyírségből a vulkanizmus és aljzattektonika kapcsolatának szemléltetésére [KILÉNYI et al. 1989 nyomán]

Рис. 2. Временной разрез с миграцией из Ньирского района, приводимый для иллюстрации соотношений между вулканизмом и тектоникой фундамента (по Э. Киленьи и др. [KILÉNYI et al. 1989])

A special case of this model is the flysch zone of the Great Hungarian Plain. There the problem is not only a stratigraphic one. The northern border of the flysch zone is unknown: no borehole has penetrated the flysch below the thick Miocene volcanic series. Therefore geophysical data are the only sources for the map construction. But for gravity and geoelectric methods the flysch acts as young sediments; for seismic refraction the high velocity horizon is unambiguously the bottom of the flysch. On the other hand, with the seismic reflection method we can follow the surface of the flysch much more easily than its bottom, which can be identified only at the margin (*Fig. 5*). If we were to choose to map the top of the flysch starting from the southern border, we would be unable to connect it to the north, where — in the absence of seismic data — we had to base our map on gravity data, reflecting the older basement.

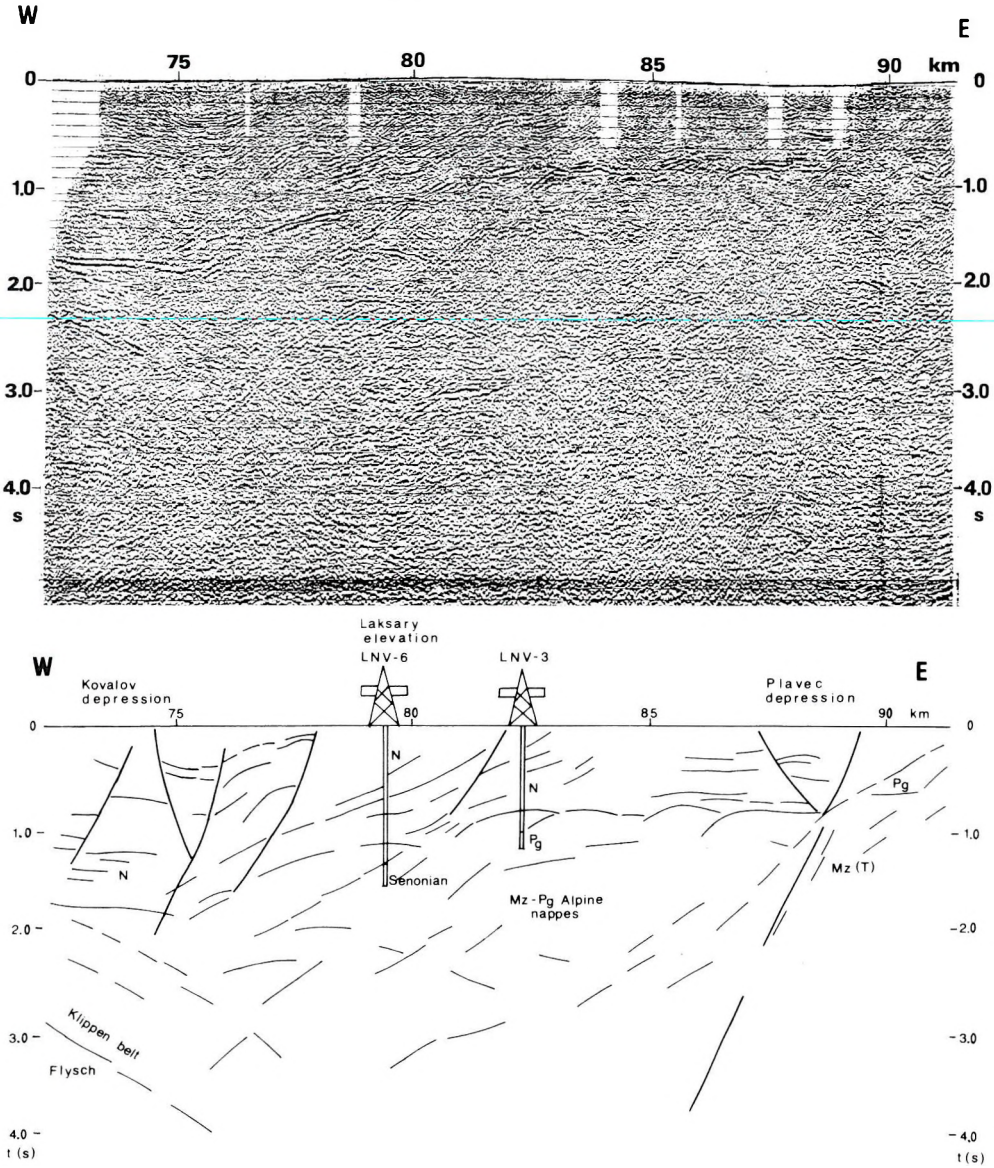

Fig. 3. Unmigrated time section with interpretation from the Vienna basin with Palaeogene (Oligocene) basement [after Томек et al. 1989]

3. ábra. Migrálatlan időszelvény és értelmezése a Bécsi-medencéből paleogén (oligocén) aljzattal [Томек et al. 1989 nyomán]

Рис. 3. Временной разрез без миграции и его интерпретация из Венской впадины с палеогеновым (олигоценовым) фундаментом (по данным Ч. Томека и др. [Томек et al. 1989])

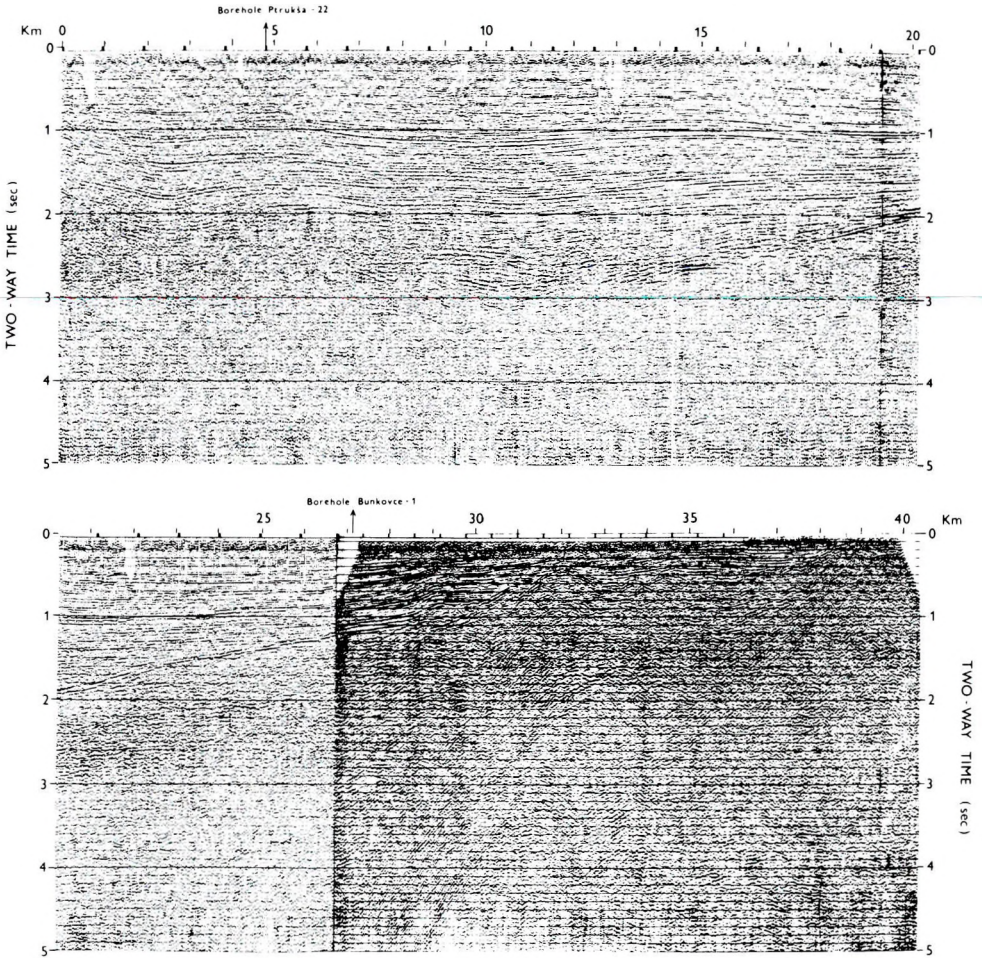

Fig. 4. Unmigrated seismic section from the East Slovakian basin [after Tomek and Thon 1988]
a) time section, b) interpretation with location map

4. ábra. Migrálatlan szeizmikus szelvény a kelet-szlovákiai medencéből
[Tomek és Thon 1988 nyomán]
a) időszelvény, b) értelmezés helyszínrajzzal

Рис. 4. Сейсмический разрез без миграции из Восточно-Словацкой впадины (по данным Томека и Тона (Tomek and Thon 1988])
a) Временной разрез
b) Интерпретация и план ситуации

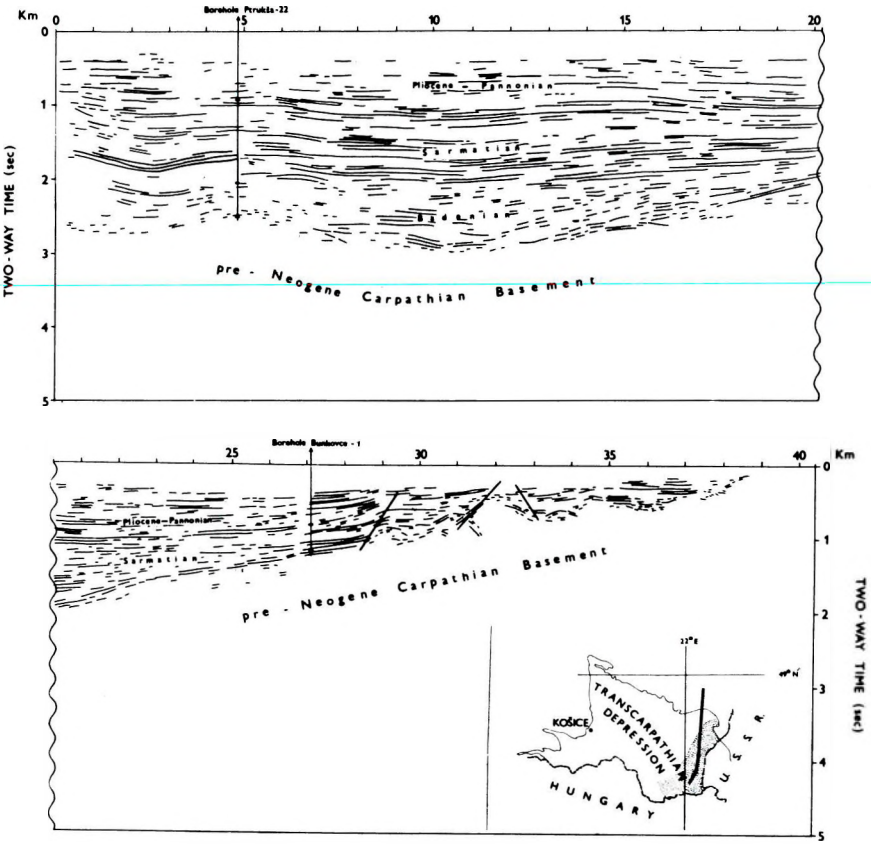

We overcame the difficulty by means of a compromise: as our detailed reflection seismic survey only covers the southern border of the flysch zone (continuous brown line) we present the bottom of the flysch on the contour map and have marked the zone by dots. We must admit, however, that the Hungarian flysch zone represents the least reliable part of the whole map.

These four models are the basic ones; it would be possible to make several subdivisions but our aim is not exact classification, it is rather the presentation of the physical basis of the contour map and the justification for its not being uniform. It is therefore evident that the accuracy of the contour map depends not only on the level of geophysical survey but on the actual model too.

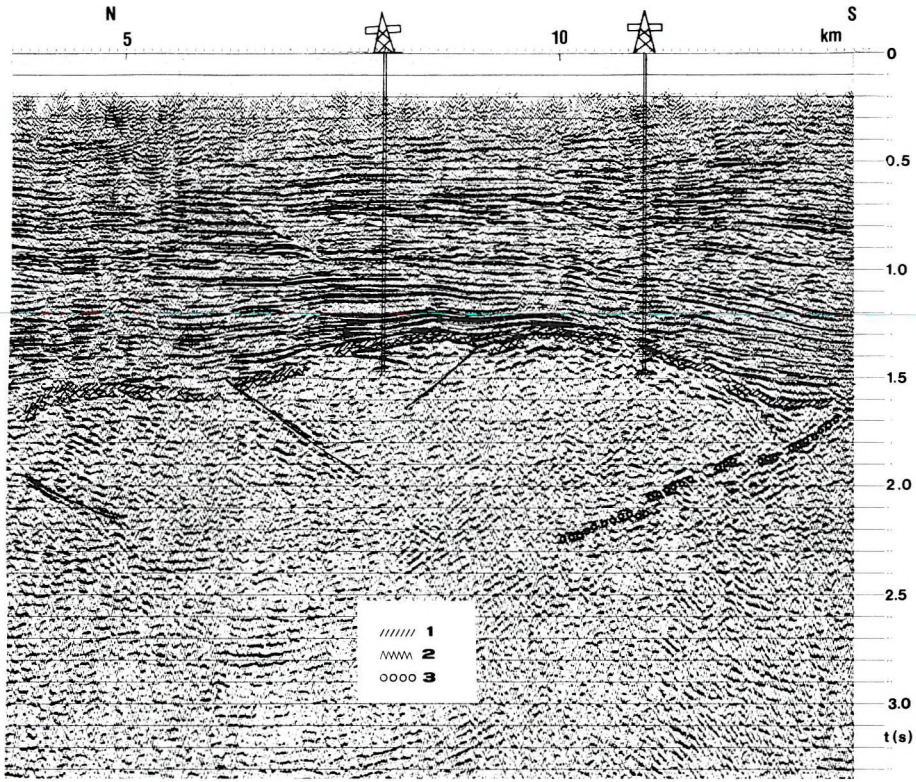

Fig. 5. Migrated time section from the Szolnok area with the southern boundary of the flysch zone [after DETZKY-LŐRINCZ et al. 1989]
1 — base Pannonian; 2 — surface of flysch; 3 — overthrust plane of flysch

5. ábra. Migrált időszelvény Szolnok környékéről a flis zóna déli határával [DETZKYNÉ LŐRINCZ K. et al. 1989 nyomán]
1 — pannon fekü, 2 — flis felszíne; 3 — a flis feltolódási síkja

Рис. 5. Временной разрез с миграцией из окрестностей г. Сольнок с южной границей флишевой зоны (по данным К. Децки-Лёринц и др. [DETZKYNÉ LŐRINCZ K. et al. 1989])
1 — подошва паннона, 2 — поверхность флиша, 3 — плоскость надвигания флиша

3. Geological–geophysical data and the methodology of map construction

Boreholes which have penetrated the pre-Tertiary basement represent a fundamental information set. Their areal distribution is determined by exploration interests, mainly by those of oil, coal, and bauxite prospecting. The majority of boreholes which have reached the basement are located in the Vienna Basin, in the Drava–Mura region, in the SE part of the Great Hungarian Plain; few of them are located in marginal parts of the Rába–Danube Basin, in the northern part of the East Slovakian Basin, and in central Slovakian neovolcanites as well as in the coal-, bauxite-, and ore prospecting areas of the

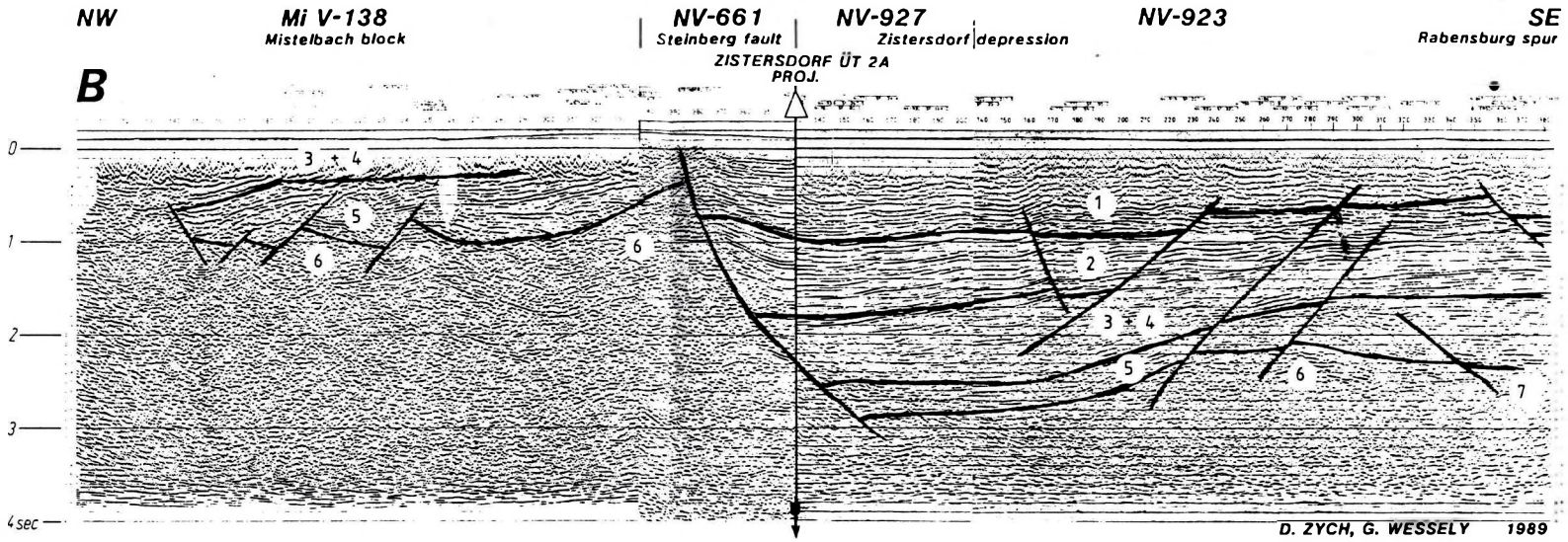

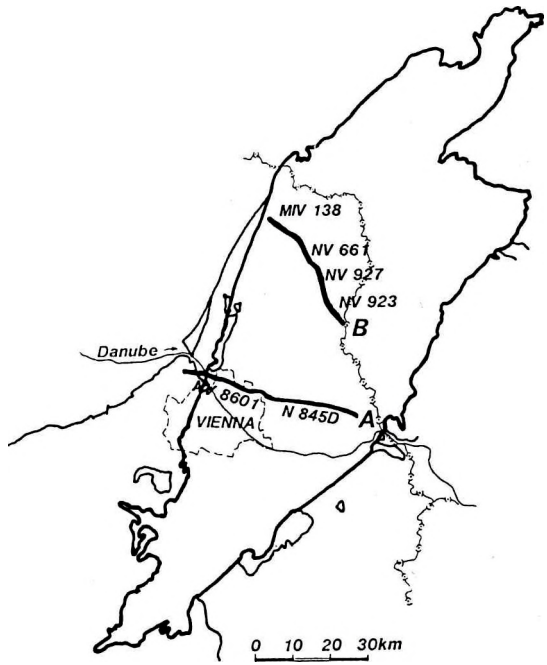

Fig. 6. Migrated time section crossing the Steinberg fault in the Vienna basin [after WESSELY 1990]
1 — Pannonian (Pliocene); 2 — Sarmatian; 3 — Upper Badenian; 4 — Lower Badenian; 5 — Lower Miocene (Karpathian–Eggenburgian); 6 — Flysch belt; 7 — Klippen belt

6. ábra. A Bécsi-medencét átszelő Steinberg vetőt keresztező migrált szeizmikus időszelvény [WESSELY 1990 nyomán]
1 — pannoniai; 2 — szarmata; 3 — felsőbádeni; 4 — alsóbádeni; 5 — alsómiocén (kárpáti–eggenburgi); 6 — flis öv; 7 — szirtöv

Рис. 6. Временной сейсмический разрез с миграцией вкрест Штейнбергскому сдвигу, рассекающему Венскую впадину (по данным Г. Вессели [WESSELY 1990])
1 — паннон; 2 — сармат; 3 — верхний бадений; 4 — нижний бадений; 5 — нижний миоцен (карпат и эггенбург); 6 — флишевая зона; 7 — утесовая зона

Transdanubian Central Range and in the Mecsek Mountains. In nearly all regions there is a lack of drilling data from the deep parts of the basins. The greatest thickness of Neogene sediments (5842.5 m) has been penetrated by a borehole in the Makó depression. Of the other deep boreholes, the LNV–7 in the Czechoslovak part of the Vienna Basin drilled to a depth of 6405 m penetrated the basement already at a depth of 1564 m. In the Austrian part of the basin four wells were drilled to a depth over 6000 metres. The deepest hole is the Zistersdorf UeT2 with a total depth of 8553 metres. A thickness of 4884 metres of Neogene sediments cut by the big 'Steinberg' fault was explored by means of this well *(Fig. 6)*. Seismic data indicate that the greatest thickness of Neogene will be about 5800 metres. These wells have contributed considerably to our knowledge of the structure, stratigraphy and of the facies distribution.

The density of geophysical data is also irregular. The majority of geophysical data, mainly the seismic ones, come from areas promising for oil prospecting. In the neovolcanic regions of Slovakia, in the South Slovakian Basin, and in the interior depressions of the Inner West Carpathians there is coverage by less suitable methods (e.g. VES). In the Transdanubian Central Range and some other parts of Hungary electromagnetic methods play an important role in the ensemble of geophysical methods. Gravimetry is extremely important everywhere, especially in the Czechoslovak part of the West Carpathians (irregular grid, 3–6 points per square kilometre), and in the Vienna basin (up to 12 points per square kilometre).

Let us consider the reliability of the different geophysical methods in determining the depth to the basement. The mapping ability of *gravimetry* decreases with increasing depth to the basement. It has been shown by the data from approximately 200 boreholes in Slovakia [Husák 1986] and 88 boreholes in Hungary [Kilényi 1967] that sediment densities increase with depth, reaching values close to the densities of basements rocks *(Fig. 7)*. Gravity modelling, either 2-D or 3-D [e.g. Gerard and Debeglia 1975], needs a knowledge of both vertical and horizontal density distribution. Such studies were carried out in higher quantity in Slovakia [Grecula et al. 1981] and to a lesser extent in Hungary [Szabó et al. 1984]. It has been proved that ϱ–h curves may differ considerably therefore all gravity modelling should be based on the particular density situation deduced from local borehole data.

As both the basement rock and the sedimentary fill may have a varying density function, for gravity modelling a set of depth points is necessary. These depth points may come either from boreholes or from some depth determining geophysical methods. Unfortunately, most boreholes are located on structural highs leaving the deeper parts of the basin to seismic or geoelectric depth determination thus increasing the ambiguity of gravity modelling.

In some parts of the Pannonian basin Bouguer anomalies do not correlate with the basement topography. Among the causes there may be strong regional effects, special density conditions, etc. If these areas have no satisfactory seismic coverage, the only possibility of mapping the basement topography is to use

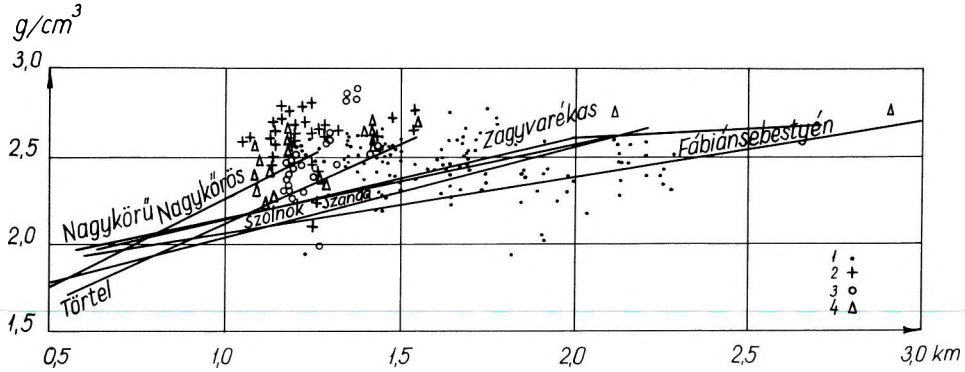

Fig. 7. Smoothed straight lines of the Pannonian density data and the densities of the different elements of the basin floor [after KILÉNYI 1967]
1 — Upper Cretaceous-Palaegoene; 2 — Triassic–Lower Cretaceous; 3 — Permian; 4 — pre-Cambrian

7. ábra. Medencealjzat képződmények sűrűségei az üledékösszlet kiegyenlítő sűrűség–mélység függvényeivel [KILÉNYI 1967 nyomán]
1 — felsőkréta–paleogén; 2 — triász–alsókréta; 3 — perm; 4 — ópaleozoós

Рис. 7. Плотности пород фундамента впадин и выравнивающие функции плотность–глубина для осадочных толщ (по данным Э. Куленьи [KILÉNYI 1967])
1 — верхний мел и палеоген; 2 — триас, юра и нижний мел; 3 — пермь; 4 — нижний палеозой

geoelectric methods. The reliability of different geoelectric methods depends on several factors. Similarly to gravity, the resistivity of both the basement and the sedimentary fill may have an areal variation but, in contrast to gravity, these variations affect data in a more complex way. The accuracy of depth determination depends on the type of geoelectric model, on the interpretation process and last but not least the geological structure with such effects as current channelling. And, on top of all these, we should not forget the phenomenon of equivalence.

The methodology of geoelectrics that proved to be the best in our mapping was the combination of telluric mapping with magnetotelluric (MT) soundings. The telluric isoarea map with the anisotropy ellipses *(Fig. 8)* reflects the main structural directions by the long axes being perpendicular to them, despite the map being distorted by the resistivity variations. MT soundings located on

8. ábra. Kisalföldi tellurikus izoarea térkép az anizotrópia ellipszisekkel [DUDÁS et al. 1987 nyomán]
1 — anizotrópia ellipszis; 2 — mélyfúrás; 3 — tellurikus bázis; 4 — magnetotellurikus szondázás

Рис. 8. Карта теллурических изоареалов по Малой Венгерской впадине с эллипсами анизотропии (по данным И. Дудаша и др. [DUDÁS et al. 1987])
1 — эллипс анизотропии; 2 — буровая скважина; 3 — пункт теллурических измерений; 4 — пункт магнитотеллурических зондирований

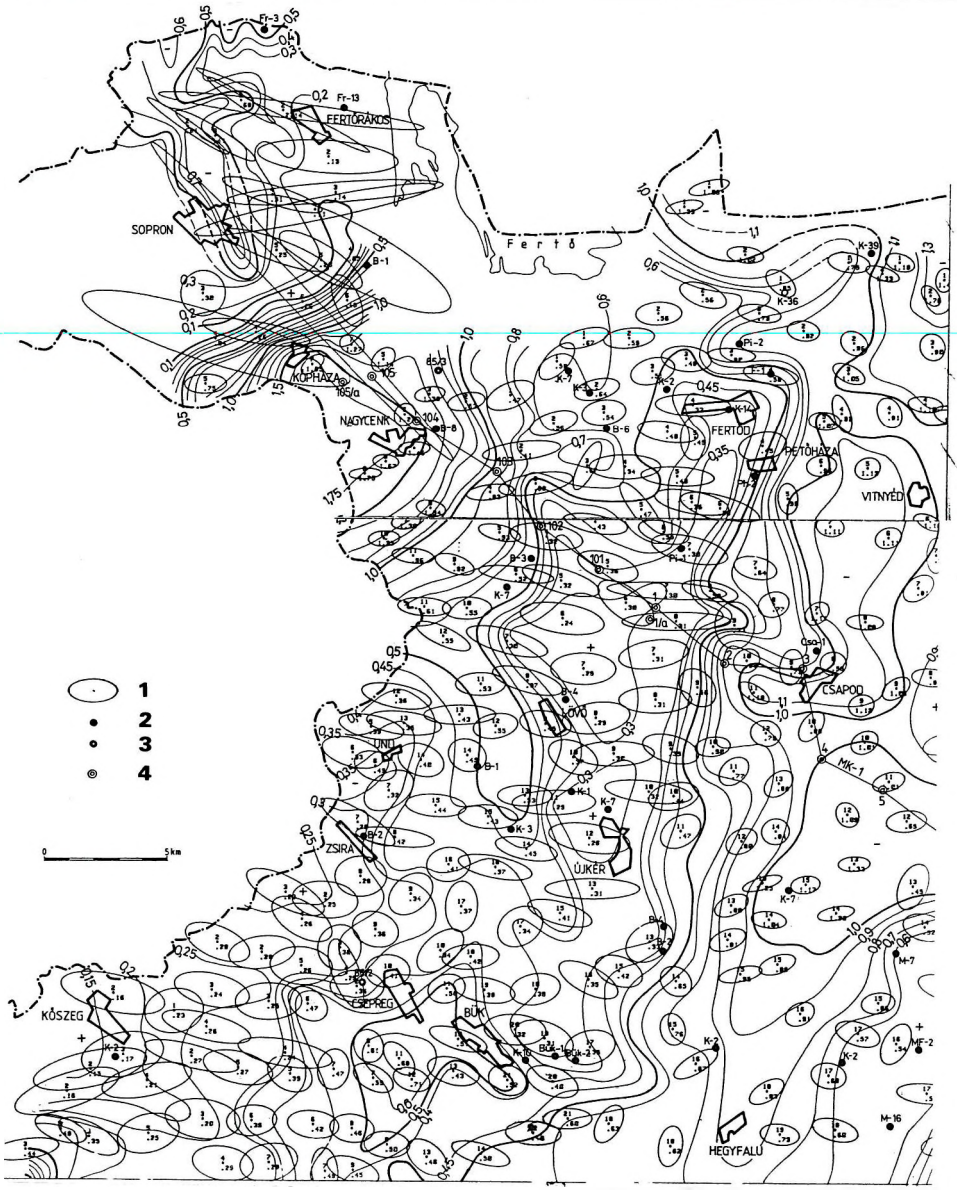

Fig. 8. Telluric isoarea map of the Danube—Rába basin with anisotropy ellipses [after DUDÁS et al. 1987]

1 — anisotropy ellipse; 2 — borehole; 3 — telluric basepoint; 4 — magnetotelluric sounding

characteristic anomalies and in directions parallel and perpendicular to the structural lines give information on the geoelectric model, the resistivity distribution and the depth to basement *(Fig. 9)*.

As far as *seismic methods* are concerned, the coverage is uneven and seismics — similarly to other methods — responds differently to different geological models. Although the velocity function has lost its position as the terror of the seismic reflection method, its effect on the unreliability of depth

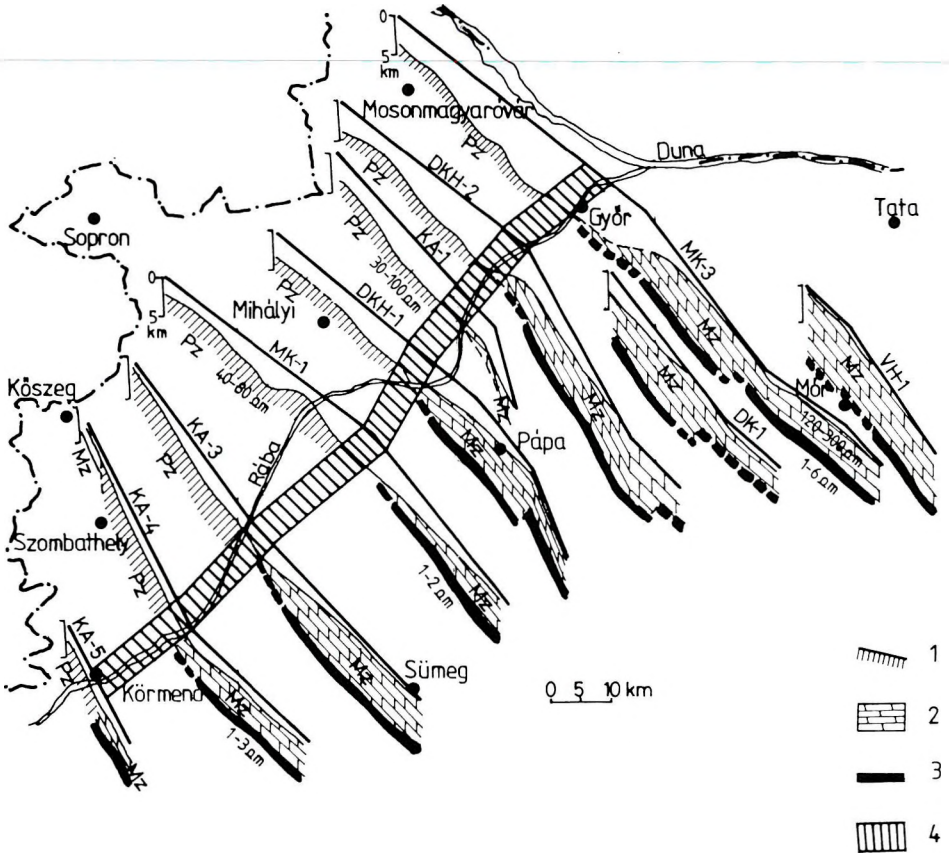

Fig. 9. Interpretation of MT profiles of the Danube–Rába basin [after PÁPA et al. 1990]
1 — Alpine units; 2 — Transdanubian Central Range unit; 3 — conductive zone; 4 — zone of the Rába line

9. ábra. A kisalföldi MT szelvények értelmezése [PÁPA et al. 1990 nyomán]
1 — Alpi egységek; 2 — Dunántúli-középhegység egység; 3 — jólvezető zóna; 4 — a Rába-vonal övezete

Рис. 9. Интерпретация магнитотеллурических разрезов по Малой Венгерской впадине (по данным А. Папы и др. [PÁPA ET AL. 1990])
1 — альпийские единицы; 2 — единица Задунайского среднегорья; 3 — зона высокой электропроводимости; 4 — зона Рабской линии

determination may be as much as 20%. The ever improving quality of reflection seismics has contributed to the recognition of several geological features, the most spectacular of them being wrench-faulting. The finding of flower structures in Pannonian sediments revealed strike-slip movement in the centre of the Carpathian basin as young as 2 Ma *(Fig. 10)*. Similarly the link between wrench-faulting and elongated narrow trenches is a finding of the past few years. Thus topographical features of the basement may be indicators of tectonic movements. In the Vienna Basin a high coverage of good seismic data exists as well as some 3-D areas. Together with the well information these data are in good correlation with the geological reality. The depth determination is exact and depends primarily on the velocity distribution, relief and depth of the pre-Tertiary basement. Within the basin fill, conglomerates exist over wide areas with high velocity (4500–5400 m/sec). The variable thickness (50–400 m) and the time distance between the base of conglomerates and the base of Tertiary occasionally cause difficulties in the seismic correlation.

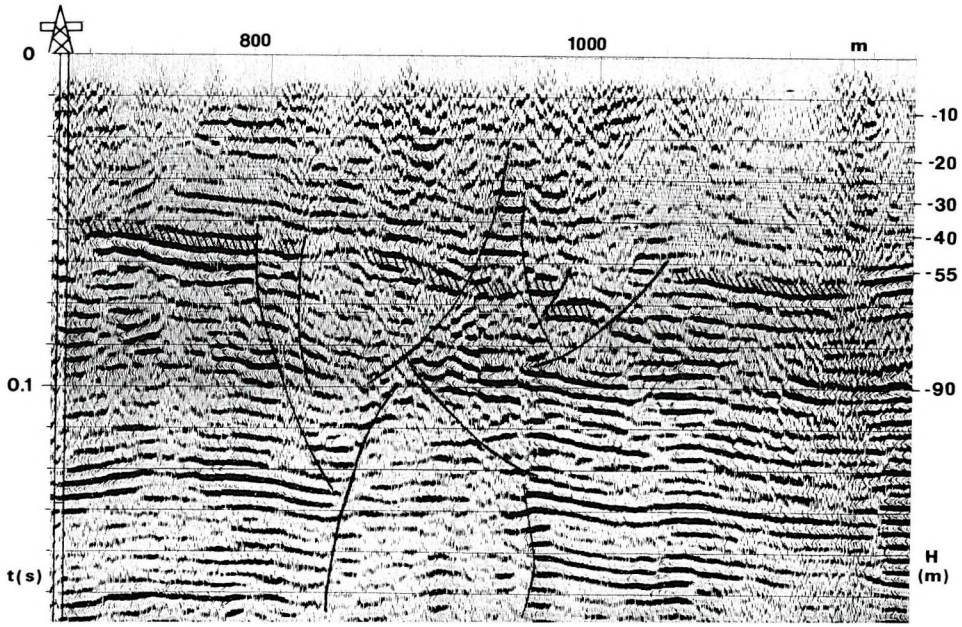

Fig. 10. Migrated shallow-seismic time section crossing the Mid-Hungarian megatectonic zone [after GUTHY and HEGEDÜS 1989]. Correlated horizon: Pleistocene–Upper Pannonian contact

10. ábra. A középmagyarországi megatektonikai vonalat keresztező sekélyszeizmikus migrált időszelvény [GUTHY és HEGEDÜS 1988 nyomán]
Korrelált felület: pleisztocén–felsőpannon határ

Рис. 10. Малоглубинный сейсмический временной разрез с миграцией вкрест Средневенгерской тектонической линии первого порядка (по данным Т. Гути и Э. Хегедюша [GUTHY and HEGEDÜS 1988])
Скоррелированная поверхность — граница плейстоцена с верхним панноном

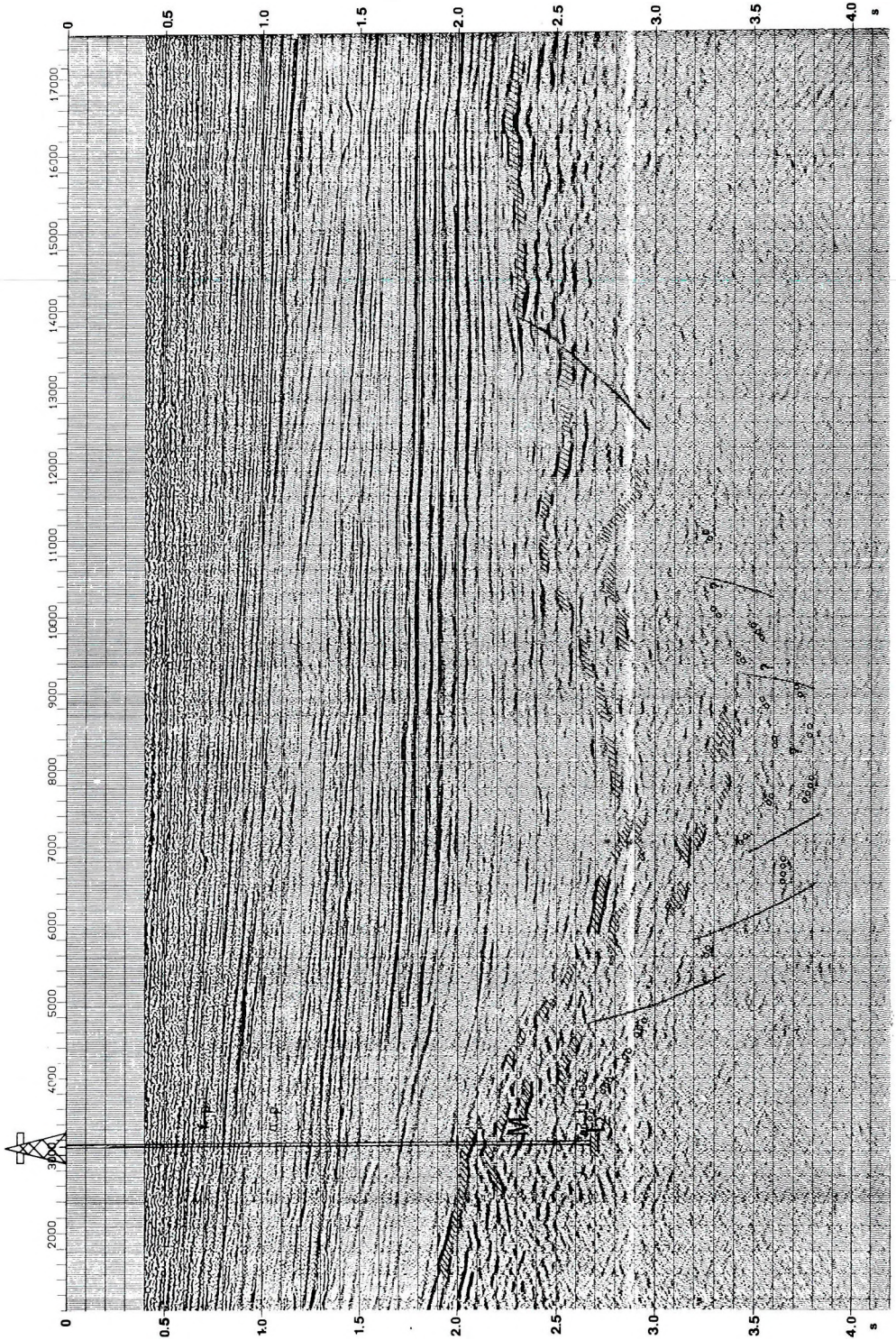
0
0.5
1.0
1.5
2.0
2.5
3.0
3.5
4.0
s
2000
3000
4000
5000
6000
7000
8000
9000
10000
11000
12000
13000
14000
15000
16000
17000

4. Geological interpretation

The question is: What contribution can be expected of a basement contour map (Enclosure) to the understanding of the geological evolution of the region? If we refer to the fact that investigation of the seafloor gave the clue to plate tectonics, the basement of the Carpathian basin, which should be regarded as the floor of the Miocene sea, may help us to delineate the tectonic units and to recognize the main movements.

Even though they are a unity in so far as their formation is connected to the Carpathian arch, the sub-basins of the Carpathian basin differ in many features: age, origin, geothermic conditions, etc. In the following some examples are presented to show this variability.

Valuable evidence on the time–space development of the basin is contained in the pre-Tertiary basement relief map. First of all we can mention the differences in shapes of basins. A basin filled with Palaeogene sediments was deformed during later stages. This kind of deformation took place in the Peri-Klippen zone in the form of overthrusting. Therefore the Neogene basins are the real indicators of basin evolution. They can be divided into graben type basins and subsidence basins with typical disk-like sinking. Of the latter type is the younger part of the Danube–Rába basin which is underlain by a basin with graben disintegration. This disintegration continues to the NE in enclaves which were also developed as graben-type basins synchronously with the Danube–Rába basin subsidence (after Sarmatian). It manifests itself by gravity tectonics revealed by geophysical modelling of their margins. The striking asymmetry of these graben-type basins can be regarded as a consequence of dynamic disintegration of the terrain with listric faults playing an active role. Similar asymmetry can be observed in South Slovakia where the basins perpendicular to the NW–SE trending graben-type ones (e.g. Trencin depression) prevail.

It has long been well known that structural units of different origin are juxtaposed in the basement of the Pannonian Basin [VADÁSZ 1953]. In the latest subcrop map [FÜLÖP–DANK 1987] the line dividing Hungary into two — called the mid-Hungarian megatectonic line — is drawn along the Kapos line in Transdanubia, turns northward near the Danube then again takes a direction of NE–SW and terminates before the buried volcanic area of the Hajdú–Nyír

Fig. 11. North–south directed seismic time section through Kömlő–1 borehole to illustrate the trough [after SZEIDOVITZ et al. 1988. Unpublished report of ELGI]

11. ábra. É–D irányú migrált időszelvény a Kömlő–1 mélyfúrástól D-re eső árok szemléltetésére [SZEIDOVITZ GYNÉ et al. 1988 kéziratos jelentése, ELGI Adattár, nyomán]

Рис. 11. Меридиональный временной разрез с миграцией для иллюстрации строения грабена южнее скважины Кёмлё–1 (по рукописному отчету Сейдовицне и др. [SZEIDOVITZ GY-NÉ et al. 1988], фонды Венгерского Геофизического института)

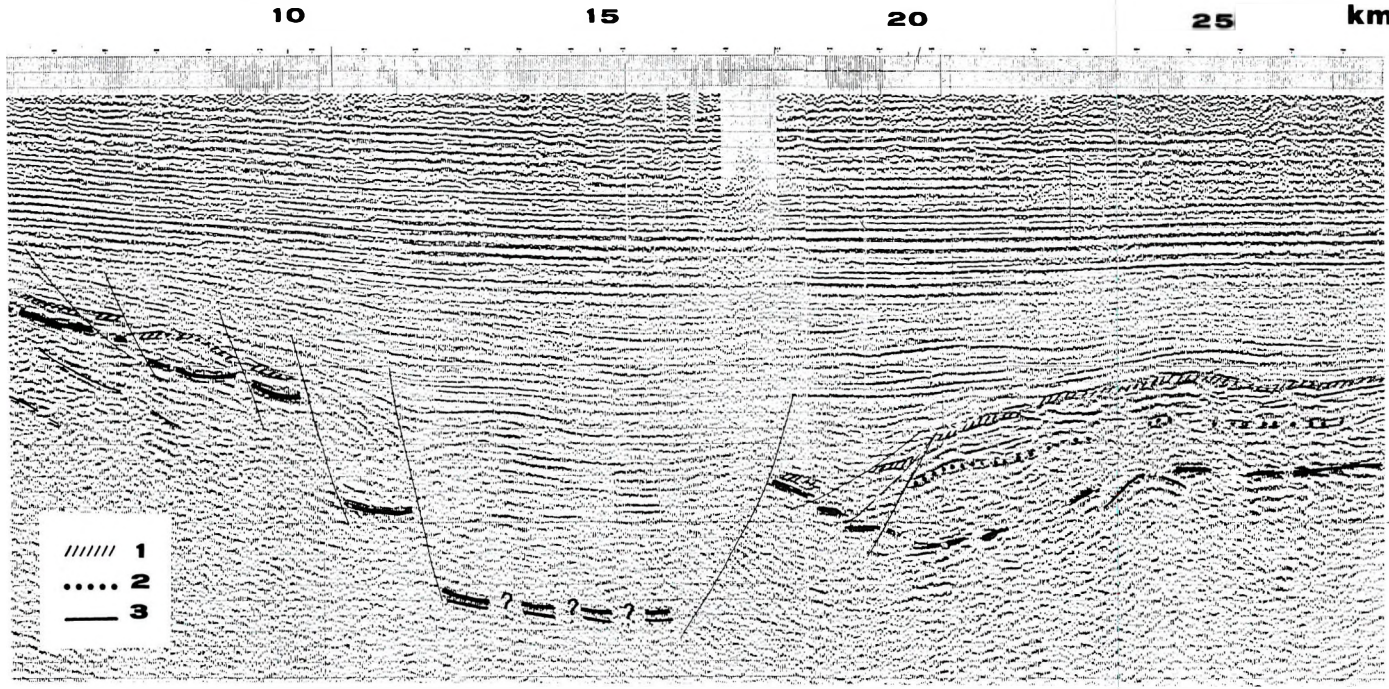

Fig. 12. North–south directed seismic time section near Tiszafüred to illustrate the eastern continuation of the trough system [after KILÉNYI et al. 1987]
1 — base Pannonian; 2 — surface of flysch; 3 — basement

12. ábra. Tiszafüred környéki, közel É–D irányú szelvény az árokrendszer K-i folytatásából [KILÉNYI et al. 1987 nyomán]
1 — pannon fekü; 2 — flis felszíne; 3 — aljzat

Рис. 12. Субмеридиональный разрез из окрестностей г. Тусафюред вкрест восточному продолжению системы грабенов (по данным Э. Киленьи и др. [KILÉNYI et al. 1987])
1 — подошва паннона, 2 — поверхность флиша, 3 — фундамент

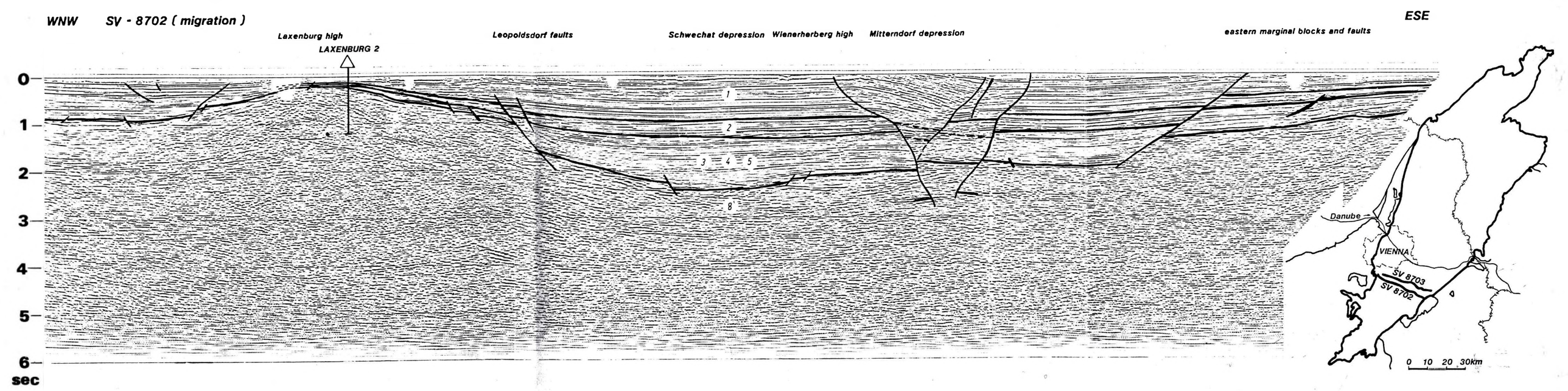

Fig. 13. Migrated time section from the Vienna basin [after HAMILTON et al. 1990]
1 — Pannonian (Pliocene); 2 — Sarmatian; 3 — Upper Badenian; 4 — Lower Badenian; 5 — Lower Miocene (Karpathian–Eggenburgian); 8 — internal Alpine–Carpathian units

13. ábra. Migrált időszelvény a Bécsi-medencéből [HAMILTON et al. 1990 nyomán]
1 — pannoniai; 2 — szarmata; 3 — felső bádeni;
4 — alsó bádeni; 5 — alsó miocén (Kárpáti–Eggenburgi); 8 — belső Alp-Kárpáti egységek

Рис. 13. Временной разрез с миграцией по Венской впадине (по данным Гамильтона и др. [HAMILTON et al. 1990])
1 — паннон (плиоцен); 2 — сармат; 3 — верхний баден;
4 — нижний баден; 5 — нижний миоцен (карпат — эггенбург); 6 — внутренние альпийско-карпатские единицы

region. This termination indicates lack of information rather than real termination of the tectonic line. The line itself was drawn along strong features of the filtered gravity anomaly map [SZABÓ 1989]. As the contour map and the subcrop map were constructed simultaneously and fitted together at the last stage it was certain that the coincidence of the chain of deep grabens along the Mid-Hungarian megatectonic line was not the result of any subjective intention.

The contour maps of the bottom of oceans and seas reveal linear features (ridges or grabens) along major plate movements. Seismic examples of present-day active wrench faults [BALLY 1983] exhibit narrow deep grabens. Thus we think the coincidence of the chain of grabens and the Mid-Hungarian megatectonic line means a strict causative connection.

In the northeastern part where the filtered gravity map lost its strong features because of the great depth to basement, some seismic lines crossed this zone and revealed the characteristics of grabens. Unfortunately the river Tisza flows, for a long stretch, along the tectonic line — not without causative contact. The river hinders seismic surveys, the break of the regular system and cross shooting result in poor quality. Even so, the graben can be seen unambiguously. *Fig. 11* shows the graben near borehole Kömlő–1, *Fig. 12* shows the same or another graben further to the east. The origin of this chain of grabens is connected with the strike-slip movement between the two main structural units: the Alpine type Pelso unit and the southern Tisza unit.

Further, but less direct evidence has been obtained about wrench fault systems in the Little Carpathians–Váh system accompanied by shallow earthquakes (focal depth about 7 km) up to the Žilina area [SCHENKOVÁ et al. 1979, GUTDEUTSCH and ARIC 1988]. Besides geological evidence [BUDAY et al. 1986] a horizontal component of movement was proved [POSPÍŠIL et al. 1985, VASS et al. 1988] by study of the earthquake mechanism. Moreover FUSÁN et al. [1987] presume that in the area near the Little Carpathians the Northern Limestone Alps structures terminate evidently extending into the basement of the Vienna Basin in the form of strike-slip movement.

Among the sub-basins, several have the features characteristic of pull-apart basins. The two big ones — the Vienna basin and the East Slovakian basin — are topics of several past and, most probably, future publications. Some of these papers are included as examples in the list of references [ČEKAN et al. 1990, GRANSER et al. 1990, HAMILTON et al. 1990, JIŘIČEK and TOMEK 1981, KRÖLL and WESSELY 1973, LADWEIN 1988, MEURERS and STEINHAUSER 1985, ROYDEN 1985, WESSELY 1988, WESSELY 1990]. However, some remarks about the Vienna basin are pertinent here. This basin represents an area of major subsidence along the NW-edge of the Alpine–Carpathian internal basin system. The Neogene fill of the basin was deposited on an allochthonous stack of nappes during and after their thrusting over the autochthonous basement (Bohemian massif) covered by Jurassic, Upper Cretaceous and older Tertiary Molasse sediments. The evolution of the basin is closely connected with the Alpine–Carpathian geodynamics. The basin played a specific role within the large Pannonian basin system because

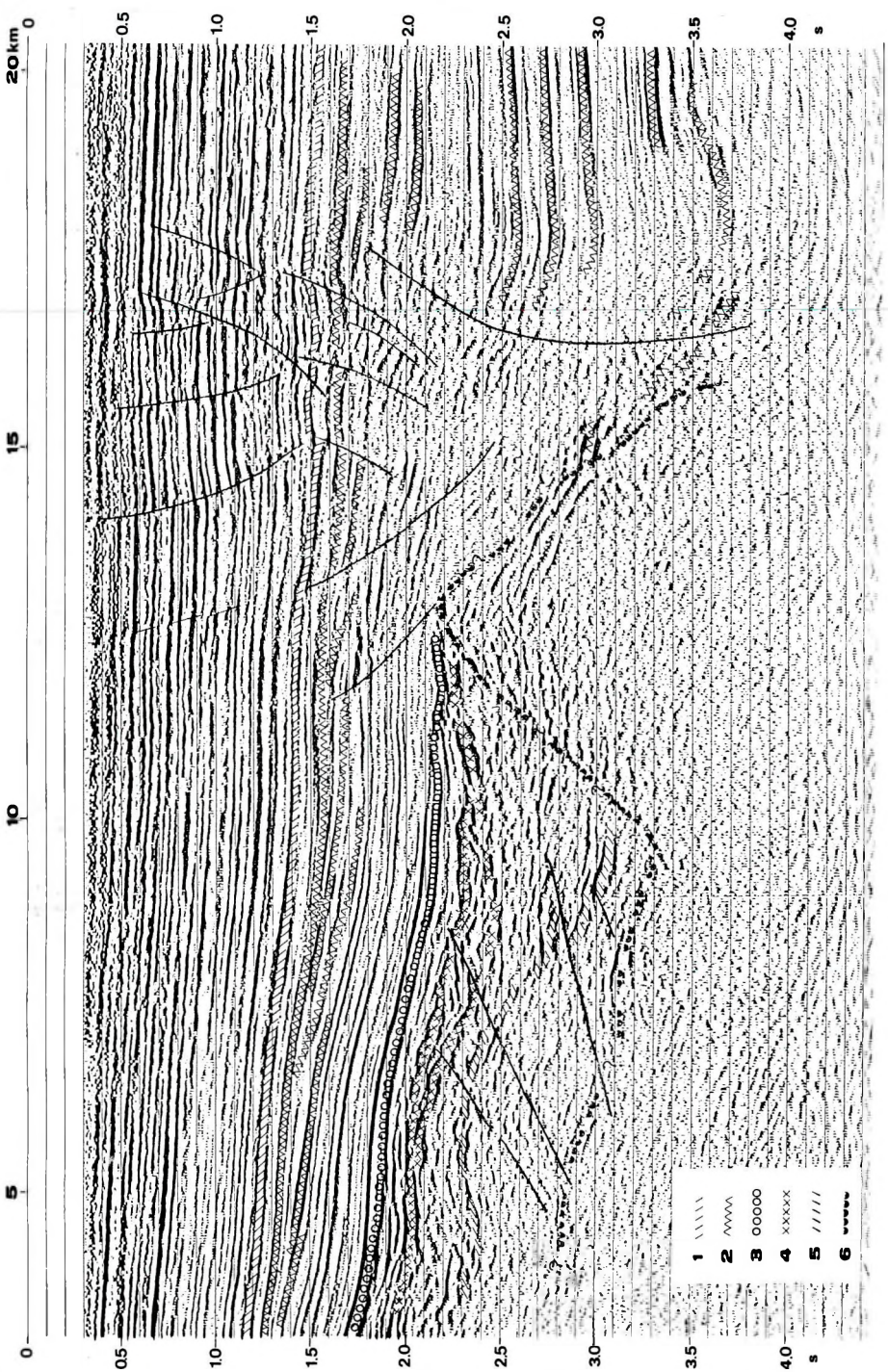
0
5
10
15
20 km
0.5
1.0
1.5
2.0
2.5
3.0
3.5
4.0
s
1
2
3
4
5
6

of its position within the thrust belt. The relatively shallow sub-Alpine–Carpathian basement controlled the mechanism of basin-forming tectonics to a certain extent. The basin has an elongated shape and is filled by Neogene clastic sediments in a very active tectonic environment. Several generations of synsedimentary faults — the most important of them being of Middle and Late Miocene and Pliocene age — created substantial thickness, varying from area to area in the same sedimentary unit *(Figs.* 6 and *13)*. The internal structure is characterized by a large number of faults, fault blocks, and structural ridges. The faults are mostly synsedimentary normal faults, some with a displacement of 4000 to 6000 metres. There are many phenomena which are common in pull-apart basins. The assumption of a pull apart mechanism generating the Vienna basin was documented by ROYDEN [1985]. Although at present this mechanism seems to be more complex its feasibility is increased by regarding the summation of lateral movements along the main Alpine–Carpathian thrust planes. A number of normal faults seem to be restricted to the allochthonous thrust complex, but the autochthonous basement must have controlled the strike of the Alpine–Carpathian thrust front and late Miocene faulting.

Separated from the Vienna basin, about 150 km to the SW, a smaller basin — the Styrian basin — exists with the same geological sequence but with a basin floor formed by crystalline allochthonous Palaeozoic and, to a lesser extent, by Cretaceous. This basin is situated south of the Central-Alpine ridge as a zone of asymmetric subsidence to the SE and is bounded in the east by a SW–NE striking fault system in combination with a high zone (South Burgenland Rise) formed by Palaeozoic and crystalline rocks. This ridge separates the Styrian Basin from the wide Pannonian Basin. The former reaches a maximum depth of 3000 metres and is filled by Neogene sediments including — in some areas — hundreds of metres of volcanics. This fact causes some uncertainties in the interpretation of geophysical data and, consequently, in the determination of depth to the pre-Tertiary basement.

In addition to the large basins we would mention two smaller ones: the Turiec basin in Western Slovakia, where extensive gravity slides and steep marginal fault zones extend into the basement, and the Derecske basin in East Hungary, where the movement involves even Upper Pannonian sediments *(Fig. 14)*.

Fig. 14. Migrated time section crossing the Derecske pull-apart basin. The strike-slip movement causes listric faults even in the Upper Pannonian sediments [after HORVÁTH and RUMPLER 1988]
1 — Upper–Lower Pannonian contact; 2 — Lower Pannonian layers; 3 — Miocene sedimentary and 4 — volcanic series; 5 — Palaeogene flysch; 6 — Mesozoic and crystalline basement

14. ábra. A Derecskei árkot keresztező migrált időszelvény. Az oldaleltolódás még a felsőpannóniai üledékekben is okoz lisztrikus vetőket [HORVÁTH és RUMPLER 1988 nyomán]
1 — alsó–felsőpannon határ; 2 — alsópannoniai rétegek; 3 — miocén üledékes és 4 — vulkáni összlet; 5 — paleogén flis; 6 — mezozoos és kristályos aljzat

Рис. 14. Временной разрез с миграцией вкрест Деречкейскому грабену. Листрические сбросы вызываются сдвигом даже в верхнепаннонских отложениях (по данным Ф. Хорвата и Я. Румплера [HORVÁTH and RUMPLER 1988])
1 — граница нижнего и верхнего паннона; 2 — нижнепаннонские отложения; 3 — миоценовые отложения; 4 — миоценовые вулканиты; 5 — палеогеновый флиш; 6 — мезозойский и палеозойский фундамент

REFERENCES

BALLY A. W. ed. 1983: Seismic expression of structural styles. AAPG publ. Tulsa, Oklahoma

BUDAY T., POSPÍŠIL L., ŠUTORA A. 1986: Geological meaning of some boundaries in Western Slovakia and Eastern Moravia interpreted form satellite images. Mineralia Slov., Bratislava **18,** 6, pp. 481–499

ČEKAN V., KOCÁK A., TOMEK Č., WESSELY G., ZYCH D. 1990: Czechoslovak–Austrian cooperation in geophysical structural exploration in the Vienna basin. *in:* Compendium 30. anniversary of CSSR–Austrian agreement about the exchange of geological experiences, Praha–Wien (in press).

DETZKY-LŐRINCZ K., KILÉNYI É., SZABÓ P., SZEIDOVITZ ZS., VAKARCS G. 1989: The manifestation of a complex wrench-fault system in the seismic reflection data of the Szolnok area. 34th Int. Geophys. Symposium, Budapest, Abstracts and Papers, p. 449

DUDÁS J., FEJES I., HOBOT J., NEMESI L., PÁPA A., and VARGA G. 1987: Regional geophysical prospecting of the Danube–Rába lowland (in Hungarian with English abstract). Ann. Report of ELGI for 1986, pp. 20–26

FUSÁN O., BIELY A., IBRMAJER J., PLANŠÁR J., ROZLOŽNIK L. 1987: Basement of the Tertiary of the Inner Western Carpathians. Geolog. Inst. Dionýza Čtura, Bratislava, 123 p.

FÜLÖP J. and DANK V. 1987: Geological map of Hungary without Cenozoic formations. Publication of the Hung. Geol. Survey, Budapest

GERARD A. and DEBEGLIA N. 1975: Automatic three-dimansional modeling for the interpretation of gravity or magnetic anomalies. Geophysics **40,** 6, pp. 1014–1034

GRANSER H., STEINHAUSER P., RUESS D. and MEURERS B. 1990: Beiträge zur Erkundung der Untergrundstrukturen der Neusiedlersee-Region mit gravimetrischen und magnetischen Methoden. Mitt. Österr. Geol. Ges. (in press).

GRECULA P., KALIČIAK M., TŐZSÉR J. and VARGA I. 1981: Geology of the borderland between the West and Est Carpathians (in Slovak). In: GRECULA (ed.): Geological structure and raw materials in the border zone of the East and West Carpathians, Košice pp. 17–32

GUTDEUTSCH R., ARIC K. 1988: Seismicity and Neotectonics of the East Alpine–Carpathian and Pannonian area. *in:* The Pannonian basin, a study in basin evolution, AAPG Memoir **45,** pp. 183–195, Tulsa–Budapest.

GUTHY T. and HEGEDÜS E. 1988: Age determination of microfaults by high-resolution reflection seismics for seismic hazard investigations. EAEG Abstracts p. 216

HAMILTON W., JIŘIČEK R., WESSELY G. 1990: The Alpine–Carpathian floor of the Vienna basin in Austria and CSFR. *in:* Compendium 30. anniversary of CSFR–Austrian agreement about the exchange of geological experiences, Praha–Wien (in press)

HORVÁTH F. and RUMPLER J. 1988: Some representative seismic reflection lines from the Pannonian basin and their structural interpretaton in the Pannonian Basin (L. H. Royden and F. Horváth eds) AAPG Memoir **45,** pp. 153–169

HUSÁK L. 1986: Density and radioactivity of Inner West Carpathian rock samples (unpublished report in Slovak), Bratislava

JIŘIČEK R. and TOMEK Č. 1981: Sedimentary and structural evolution of the Vienna basin. *in:* Earth evolution sciences 3–4

KILÉNYI É. 1967: Geological–geophysical considerations on the Great Hungarian Plain through a statistical analysis of density data (in Hungarian with English abstract). Geofizikai Közlemények **17,** 4, pp. 41–49

KILÉNYI É. and RUMPLER J. 1984: Pre-Tertiary basement relief map of Hungary. Geophysical Transactions **30,** 4, pp. 425–428

KILÉNYI É., POLCZ I. and SZABÓ Z. 1989: Neogene volcanism of the Nyir region (NE Hungary) as revealed by integrated interpretation of the latest geophysical data. Geophysical Transactions **35,** 1–2, pp. 77–99

KILÉNYI É., OBERNAUER D., RUMPLER J., ŠEFARA J. and SZABÓ Z. 1987: Pre-Tertiary basement contour map of the Alp–Carpathian contact zone and the northern–central part of the Carpathian basin. International Conference on geotectonic development of the Carpatho-Balkan orogenic belt, Oct. 12–15, 1987, Bratislava, CSSR

KRÖLL A. und WESSELY G. 1973: Neue Ergebnisse beim Tiefenaufschluss im Wiener Becken. Erdöl–Erdgas Zeitschrift, **89**, 11, pp. 400–413

LADWEIN W. 1988: Organic geochemistry of Vienna basin: model for hydrocarbon generation in overthrust belts. AAPG Bulletin, **72,** pp. 586–599

MEURERS B. and STEINHAUSER P. 1985: Auflösung tektonischer Strukturen im tertiären Alpenrand durch eine gravimetrische Vermessung am Beispiel des südlichen Wiener Beckens. Ber. Tiefbau Ostalp. **12,** 65–72

PÁPA A., RÁNER G., TÁTRAI M. and VARGA G. 1990: Seismic and magnetotelluric investigation on a network of base lines. Acta Geod, Geophys. et Mont. Hung. **25,** 3–4, pp. 309–323

POSPÍŠIL L., SCHENK V. and SCHENKOVÁ Z. 1985: Relation between seismoactive zones and remote sensing data in the West Carpathians. Proc. 3rd Intern. Symp. Analysis of Seismicity and Seismic Risk, Liblice, Vol. **1,** Prague, pp. 256–263

ROYDEN L. H. 1985: The Vienna basin. A thin skinned pull apart basin. *in:* Strike slip deformation, basin formation and sediments (BIDDLE K. T.–CHRISTIE–BLICK M eds). Society Econ. Paleont. Mineral. Spec. Publ., Tulsa, **37,** pp. 319–338

SCHENKOVÁ Z., KÁRNIK V., SCHENK V. 1979: Earthquake epicentres in Central and Eastern Europe. Studia geoph. et geod. **23,** 2, pp. 197–199, 204 a, b

ŠEFARA J., ŠUTORA A., POSPÍŠIL L., VELICH R., MIKUŠKA J., KURKIN M., OBERNAUER D., FILO M., BIELIK M. 1987: Structural–tectonic map of the Inner West Carpathians — geophysical interpretation (in Slovak). Final Report for the Slovak Geol. Office, Bratislava (unpublished)

SZABÓ Z., KILÉNYI É. and BARDÓCZ B. 1984: Bouguer anomaly–depth to basement relations in the southern part of the Danube–Tisza interfluve, Hungary. Geophysical Transactions **30,** 4, pp. 411–424

SZABÓ Z. 1989: Filtered gravity anomaly map of Hungary. Geophysical Transactions **35,** 1–2, pp. 135–142

TOLLMANN A. 1987: The Alpidic evolution of the Eastern Alps. *in:* Geodynamics of the Eastern Alps; (pp. 361–378) eds: H. W. Flügel and P. Faupl, F. Deuticke, Vienna.

TOMEK Č., DVORÁKOVÁ L. and IBRMAJER I. 1989: Reflection seismic profile in the West Carpathians (in Czech.). In: BLIŽKOVSKÝ M. et al.: Final report of the project: Geophysical investigation of the earth crust for the purpose of the investigation of raw material deposits (unpublished)

TOMEK Č. and THON A. 1988: Interpretation of seismic reflection profiles from the Vienna Basin, the Danube Basin, and the Transcarpathian Depression in Czechoslovakia. *in:* The Pannonian Basin. AAPG Memoir **45,** pp. 171–182

VADÁSZ E. 1953: Geology of Hungary (in Hungarian). Akadémiai Kiadó, Budapest

VASS D., KOVÁČ M., KONEČNÝ V. and LEXA J. 1988: Molasse basins and volcanic activity in West Carpathian Neogene — its evolution and geodynamic character. Geolocky zbornik — Geologica Carpatica **39,** 5, Bratislava, pp. 539–561

WESSELY G. 1988: Structure and development of the Vienna basin in Austria. The Pannonian basin, a study in basin evolution, AAPG Memoir **45,** pp. 333–346, Tulsa–Budapest

WESSELY G. 1990: Geological results of deep exploration in the Vienna basin. Geologische Rundschau **79,** 2

A HARMADKORI MEDENCE ALJZATÁNAK SZINTVONALAS MÉLYSÉGTÉRKÉPE A KÁRPÁT-MEDENCE AUSZTRIAI, CSEHSZLOVÁKIAI ÉS MAGYARORSZÁGI RÉSZÉRE

KILÉNYI Éva, Arthur KRÖLL, Dusan OBERNAUER,
Jan ŠEFARA, Peter STEINHAUSER, SZABÓ Zoltán,
és Godfrid WESSELY

Az ausztriai Bundesanstalt, a csehszlovakiai Geofyzika n. p. Braatislava és az ELGI együttműködése keretében e három országra megszerkesztettük a harmadkori medence aljzatának mélységtérképét. A Kárpát-medence számos medencére osztható, melyek közül a legnagyobb a Pannon-medence, amely viszont tovább osztható részmedencékre, mint a Kisalföldi- és a Békési-medence, csak hogy a legnagyobbakat említsük. A medencék kialakulásában az oldaleltolódásoknak fontos szerepe volt; a legismertebb széthúzási (pull-apart) medencék a Bécsi-medence és a kelet-szlovákiai-medence. Bár a medencealjzat fogalom egységes, mint a harmadkorinál idősebb kőzetek felszíne, mind a földtani modell, mind a geofizikai felmértség rendkívül heterogén. Négy alapmodellt rendelhetünk a különböző rész-medencékhez. A térképszerkesztésben domináló geofizikai módszereket részben a földtani modell, részben a geofizikai adatok léte és hozzáférhetősége határozta meg.

КАРТА ГЛУБИН ФУНДАМЕНТА ТРЕТИЧНЫХ ВПАДИН В ИЗОЛИНИЯХ ПО АВСТРИЙСКОЙ, ЧЕХО-СЛОВАЦКОЙ И ВЕНГЕРСКОЙ ЧАСТЯМ ВНУТРИКАРПАТСКОЙ ДЕПРЕССИИ

Ева КИЛЕНЬИ, Артур КРЁЛЛ, Душан ОБЕРНАУЕР,
Ян ШЕФАРА, Петер ШТЕИНГАУЗЕР, Золтан САБО,
Годфрид ВЕССЕЛИ

В рамках сотрудничества между Геологическим институтом Австрии, предприятием »Геофизика« в Братиславе и Венгерским Геофизическим институтом составлена карта глубин фундамента третичных впадин по этим трем странам. Внутрикарпатская депрессия может быть подразделена на ряд бассейнов, наиболее крупным из которых является Паннонский, в котором в свою очередь могут быть выделены частные впадины, как например Малая Венгерская или Бекешская, чтоб упоминать лишь наиболее крупные. В формировании впадин большую роль играли сдвиги, наиболее известными врадинами этого (pull-apart) типа являются Венская и Восточно-Словацкая. Хотя понятие »фундамент впадин« единообразно в качестве поверхности дотретичных образований, как геологическое строение, так и геофизическая изученность варьируют в широких пределах. Различные частные впадины относятся к четырем основным типам. Набор геофизических методов, игравших определяющую роль в составлении карты, определялся отчасти геологическим строением, отчасти наличием и доступностью геофизических данных.

GEOPHYSICAL TRANSACTIONS 1991
Vol. 36. No. 1–2. pp. 37–48

APPLICATION OF CERTAIN FIELD TRANSFORMATION METHODS TO AEROMAGNETIC DATA FROM THE WESTERN PART OF THE VIENNA BASIN

Károly KIS* and Wolfgang SEIBERL**

Field transformation methods can be applied very successfully in the interpretation of magnetic anomalies. Two transformations, in this paper, the vertical gradient and the reduction to the magnetic pole of the total magnetic anomalies are presented. Since the transformations are based on their transfer functions, the efficiency of the latter is improved by using Gaussian low-pass and band-pass windows as truncation functions. The windowing eliminates the undesirable properties of the transformations, the enhancement of the high frequency noise, and the finite discontinuity of the reduction to the magnetic pole for the zero frequency. The results of the transformations are illustrated by simple model computations and by some field data from an aeromagnetic survey (near Vienna, Austria).

Keywords: aeromagnetic survey, aeromagnetic anomalies, transformations, Gaussian low-pass and band-pass windows, vertical gradient, reduction to the pole, truncation, Vienna Basin

1. Introduction

Nowadays the functional transformations of gravity and magnetic data represent a very important and powerful interpretation tool. In magnetics, calculation of the vertical gradient and reduction to the magnetic pole are widely used to delineate bodies at different depths and to obtain better clustered magnetic anomaly-patterns. In the past these functional transformations had some shortcomings due to the inherent noise in the input data. Additionally in the case of reduction to the magnetic pole there exists a finite discontinuity for the zero frequency.

Calculation of the vertical gradient from potential field data is a very useful tool — especially in applied geophysics — and it is usually used to interpret gravimetric as well as magnetic anomalies. For example BARONGO [1985] suggested a method to estimate the depth of magnetic sources using vertical gradient profiles. Numerous papers and books, e.g. BARANOV [1975], dealing with the mathematical background of the field transformation method have been published. The high level of performance of magnetic instruments enables the vertical gradient over magnetic bodies to be measured directly in the field [MORRIS and PEDERSEN 1961, AITKEN and TITE 1962, RIKITAKE and TANOKA 1960, SLACK et al. 1967, EGGERS and THOMPSON 1984]. Many results of the

* Geophysics Department, Loránd Eötvös University, H–1083 Budapest, Ludovika tér 2, Hungary
** Institute of Meteorology and Geophysics, University of Vienna, A–1180 Wien, Währingerstrasse 17, Austria
Manuscript received (revised version): 9 October, 1990

application of the vertical gradient method in ground magnetic- [e. g. HOOD and MCCLURE 1965], in aeromagnetic surveys [e.g. HOOD et al. 1989], and in marine magnetic surveys [EGGERS and THOMPSON 1984] can be found in the literature.

Because of their vertical magnetization direction, magnetic anomalies are more suitable for interpretation procedures — e.g. comparison with gravimetric data or geological mapping results — BARANOV [1957] introduced a new field transformation method. In this method the total field magnetic anomalies (their shapes are mainly a function of the inducing field and remanent magnetizations) are transformed in such a way that that the magnetization of the magnetic bodies has an inclination of 90 degrees, the inclination at the magnetic pole.

In most of the published papers dealing with the reduction to the magnetic pole (e.g. BHATTACHARYYA [1965], BOTT et al. [1966], KANASEWICH and AGARWAL [1970], WILSON [1970], BARANOV [1975]) this transformation method is based on Poisson's theorem. For example, KIS [1981] obtained the theoretical transfer function of the reduction to the magnetic pole without using Poisson's relation. BARANOV [1975] and SEIBERL [1979] presented coefficients for the reduction to the pole of magnetic anomalies.

2. The vertical gradient

One of the possible methods for computing the vertical gradient is to determine the two-dimensional set of coefficients whose convolution with the input data gives a good approximation to the vertical gradient of the input. The set of coefficients will be obtained from the theoretical transfer function of the derivative with respect to the variable z by numerical inverse Fourier transformation.

Amplification in the high frequency range is undesirable since this range possesses the lowest signal-to-noise ratio. As a consequence, amplification of the high-frequency components usually corresponds to the amplification of the high-frequency noise. In order to remove the high frequencies the theoretical transfer function is multiplied by a Gaussian low-pass window function as suggested by MESKÓ [1984]. The truncated transfer function of the derivative with respect to variable z is

$$S_{tdz}(f_x, f_y) = 2\pi (f_x^2 + f_y^2)^{1/2} \exp(-(36/m)^2(f_x^2 + f_y^2)). \quad (1)$$

The parameter m in Eq. (1) modifies the cut-off frequency of the window. In the course of the computations we chose $m = 9$ for the parameter of the Gaussian window function. The cut-off spatial frequency was defined by -3 dB point. The dimensionless cut-off frequency of the window is $f^c = 0.147$. In *Fig. 1* the theoretical as well as the truncated transfer functions are shown. Both should be close to each other at the origin. For the medium and high-frequency range the contributions to the calculated vertical gradient will be insignificant since the application of the low-pass window introduces continuously increasing attenuation. The actual transfer function is periodic.

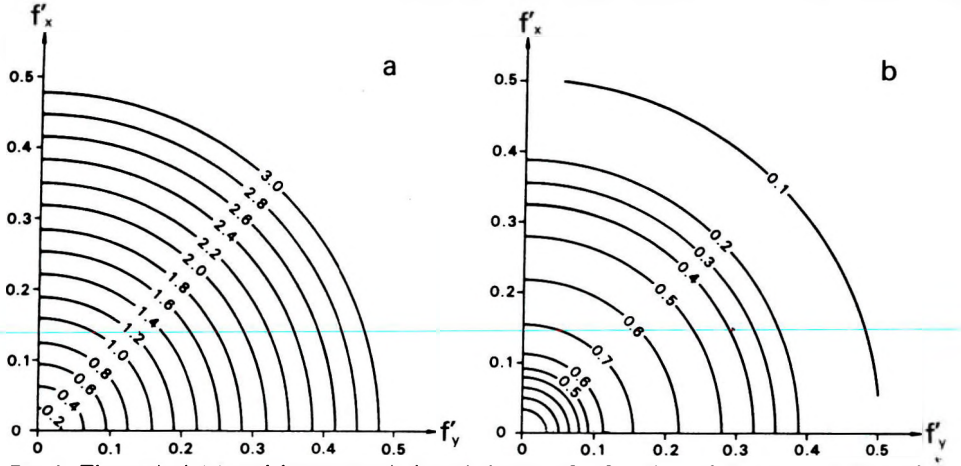

Fig. 1. Theoretical (a) and low-pass windowed (b) transfer function of the computation of the derivatives with respect to z. The independent variables are the dimensionless spatial frequencies f'_x and f'_y

1. ábra. A z-irányú gradienst szolgáltató transzformáció elméleti (a) és felülvágó szűrővel csonkított (b) átviteli függvénye az f'_x és az f'_y dimenziótlan térfrekvenciák függvényében

Рис. 1. Теоретическая (а) и урезанная низкочастотным фильтром (b) функции переноса преобразования с получением градиента по направлению z как функция безразмерных частот поля f'_x и f'_y

The digital weight function (the coefficients) is obtained by inverse Fourier transformation of Eq. (1). The actual calculations were performed for an 11 × 11 set of coefficients and the corresponding results were published by Kis [1983b]. If we wish to obtain the truncated derivative in nTm^{-1}, the results of the convolution of the data with the coefficients have to be divided by the grid spacing (in metres).

In the next step the set of coefficients for calculating the vertical gradient from the total magnetic field data was tested using the theoretical field — and gradient — distributions over a magnetic dipole. As the results of this investigation were good, the set of coefficients was applied to the magnetic field data obtained during an airborne survey near Hollabrunn (Austria). The survey site is shown in *Fig. 2.* The flight-line spacing was 2 km and the flight direction W–E. The survey height was 800 m above mean sea level and the total magnetic field was sampled along the profiles with sampling of approximately 50 m depending on the speed of the aircraft. The sources of the magnetic anomalies (see *Fig. 3a*) in the vicinity of Hollabrunn cannot be found on the surface as this area is covered by thick young sediments (tertiary — quaternary). By extrapolating the strike of the complex anomaly pattern towards NNE it can be correlated with the eastern part of the Boscovician depression, a tectonic feature of southern Czechoslovakia (Moravia). In this area gabbros, diorites, granites and grano-diorites of the Svratka dome [Fuchs and Matura 1976] are outcropping. Another, and rather speculative, explanation of the magnetic anomalies near Hollabrunn are magmatites of late tertiary origin. This type of volcanism is quite common in the eastern part of the Alps.

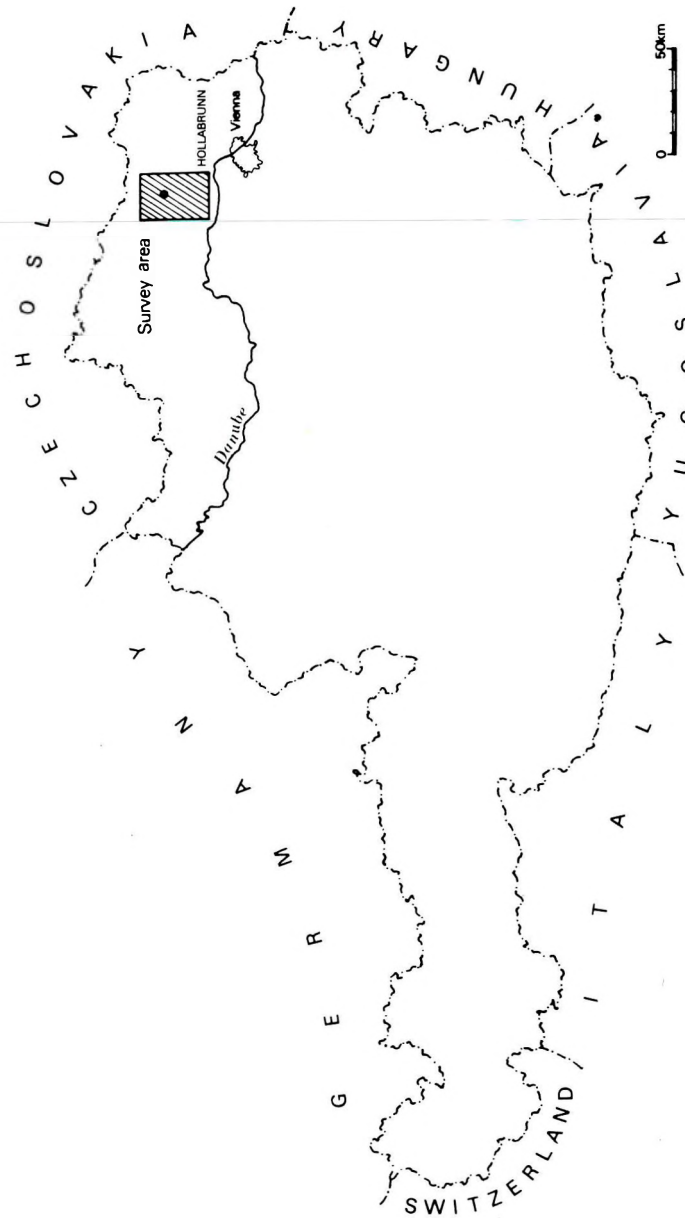

Fig. 2. Location map of the aeromagnetic survey near Hollabrunn

2. ábra. A Hollabrunn kutatási terület

Рис. 2. Площадь работ Голлабрун

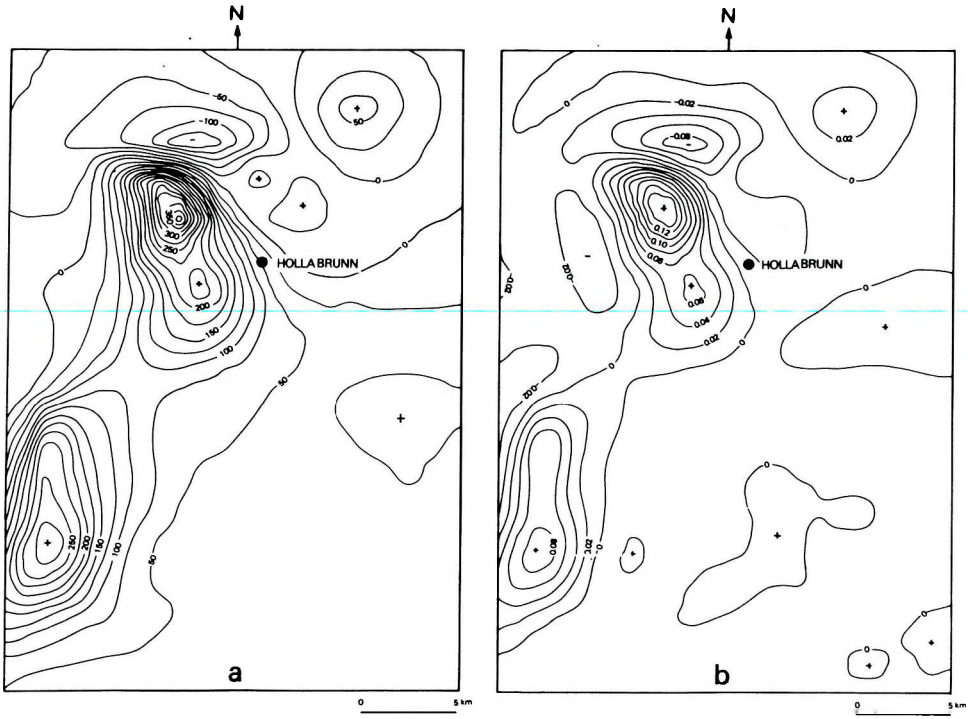

Fig. 3. Total magnetic anomaly map of Hollabrunn area (a), contours are given in nT units, and truncated vertical gradient map of Hollabrunn area (b), contours are given in nTm^{-1} units

3. ábra. A Hollabrunn kutatási terület totális mágneses anomália térképe (a), az izovonalak egysége nT; csonkított vertikális gradiens térképe (b), az izovonalak egysége nTm^{-1}

Рис. 3. Карта полных магнитных аномалий (а, изолинии – в нт) и карта урезанных вертикальных градиентов (в, изолинии – в нт/м) по площади работ Голлабрун

The total magnetic anomaly was sampled in a square grid with the sampling unit of $\xi = 1000$ m, accordingly the cut-off spatial frequency is

$$f_{\text{upper}}^{\square} = \frac{0.147}{\xi} = 0.147 \cdot 10^{-3}\ \text{m}^{-1}. \tag{2}$$

Fig. 3b shows the calculated vertical gradient near Hollabrunn. Usually maps showing the calculated vertical gradient are characterized by a large number of narrow anomalies, which are mainly due to the noise contained in the input data. In the case of the Hollabrunn data this noise is suppressed by the application of a low-pass window function to the theoretical transfer function. The advantage of using a windowed low-pass transfer function is obvious.

3. Reduction to the pole

Similar to the calculation of the vertical gradient the reduction to the magnetic pole may be represented in the frequency domain by its transfer function. By means of inverse Fourier transformation one can calculate the set of coefficients. The reduction to the magnetic pole is performed by convoluting the input data with the just mentioned set of coefficients.

The complex transfer function of the reduction to the pole can be expressed in the form

$$S_T(f_x, f_y) = \frac{f_x^2 + f_y^2}{[N(f_x^2+f_y^2)^{1/2} + j(Lf_x + Mf_y)]\,[n(f_x^2+f_y^2)^{1/2} + j(lf_x + mf_y)]} \tag{3}$$

[e.g. Kis 1983a] where j is the imaginary unit and the direction cosines L, M, N, l, m, and n are

$$\begin{aligned} L &= \cos\alpha\cos\beta & l &= \cos I\cos D \\ M &= \cos\alpha\sin\beta & m &= \cos I\sin D \\ N &= \sin\alpha & n &= \sin I. \end{aligned} \tag{4}$$

In the latter equations I and D are the magnetic inclination and declination of the Earth magnetic field; α and β are the inclination and declination of the remanent magnetization. The transfer function (Eq. 3) depends only on the direction of the induced and remanent magnetization. It is independent of the other parameters of the magnetic source. Uniform magnetization was assumed in order to derive the transfer function (Eq. 3). The transfer function has a finite discontinuity at $f_x = f_y = 0$. In order to calculate the inverse Fourier transform, a suitable window function was applied. The aim of the window function is twofold: it eliminates the discontinuity at the origin ($f_x = f_y = 0$) and it removes the enhancement of the transfer function in the higher frequency range. The conservation of the phase shift properties of the transfer function is also required. Thus, the appropriate truncation function is the band-pass window proposed by Meskó [1984] since this meets the demands mentioned above. The transfer function of the suggested band-pass window is

$$S_{BP}(f_x, f_y) = C\,[\exp(-36^2(f_x^2+f_y^2)/m_1^2) - \exp(-36^2(f_x^2+f_y^2)/m_2^2)]\,. \tag{5}$$

The normalization factor C is

$$C = \frac{1}{\exp(-36^2 f_{rmax}^2/m_1^2) - \exp(-36^2 f_{rmax}^2/m_2^2)}, \tag{6}$$

where

$$f_{rmax} = \frac{m_1 m_2}{36}\left[\frac{2}{m_1^2 - m_2^2}\log\frac{m_1}{m_2}\right]^{1/2} \tag{7}$$

and the $m_1 > m_2$ relation is valid for the parameters of the band-pass window.

In *Fig. 4*, the transfer function of the band-pass window can be seen for the parameters $m_1 = 9$ and $m_2 = 3$. If we again use a -3 dB cut-off criterion the dimensionless cut-off spatial frequencies will be $f^c_{\text{lower}} = 0.0491$ and $f^c_{\text{upper}} = 0.147$.

The transfer function $S_{T_t}(f_x, f_y)$, truncated by a band-pass window, can now be expressed in the form:

$$S_{T_t}(f_x, f_y) = [\text{Re}\{S_T(f_x, f_y)\} + j\,\text{Im}\{S_T(f_x, f_y)\}]S_{BP}(f_x, f_y)\,. \tag{8}$$

This windowed transfer function has no discontinuity because the value of the band-pass filter at the origin is zero (Fig. 4) thereby fulfilling the conditions mentioned above. The coefficients of the digitized weight function can be obtained by the inverse Fourier transform of Eq. (8) in a similar way as the coefficients for the transformation of the truncated vertical gradient. The coefficients were computed for an inclination of 60 degrees and a declination of 0 degrees, respectively. These values are typical for the main magnetic field in eastern Austria (see Kis [1983a] for the set of coefficients).

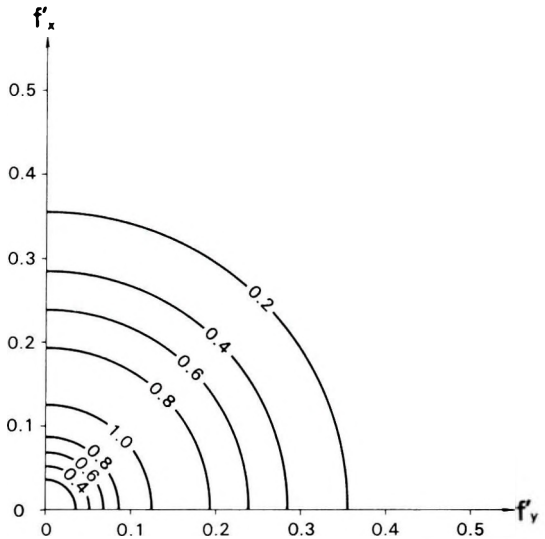

Fig. 4. Transfer function of the band-pass window. The independent variables are the dimensionless spatial frequencies f'_x and f'_y

4. ábra. Az alkalmazott sávszűrő átviteli függvénye az f'_x és az f'_y dimenziótlan térfrekvenciák függvényében

Рис. 4. Функция переноса применяемого полосового фильтра как функция безразмерных частот поля f'_x и f'_y

Similarly to the method of calculating the vertical gradient the set of coefficients for the transformation to the magnetic pole was tested using the field distribution over a 3-D rectangular prism. The prism has its top at a depth of 1000 m, its bottom at 2000 m from the plane of observation. The horizontal dimensions are 4000 m and 6000 m along the x and y axes, respectively. The direction of magnetization is in the direction of the Earth's magnetic field, thus $I = 60$ degrees, $D = 0$ degrees. The magnetization of the prism is 1 A/m. The total magnetic field of this rectangular prism was computed in accordance with the formula given by WHITEHILL [1973].

In *Fig. 5* (*a* and *b*) the total magnetic field over the prism and its band-pass windowed total magnetic field are shown. The band-pass windowed anomaly reduced to the pole as well as the magnetic field for an inclination of 90 degrees over the prism can be seen in Figs. 5c and 5d. The reduction to the pole is a transformation with a phase shift, as can be seen from the model calculation. The maximum of the reduced field is above the centre of the prism and the field is symmetrical.

In the course of the model calculation, the sampling grid was $\xi = 0.5$ km. The lower and upper cut-off frequencies are

$$f^{c}_{\text{lower}} = \frac{0.0491}{\xi} = 0.0981 \text{ km}^{-1} \text{ and } f^{c}_{\text{upper}} = \frac{0.147}{\xi} = 0.294 \text{ km}^{-1}, \qquad (9)$$

respectively.

The same set of coefficients was used to reduce the aeromagnetic data of the area near Hollabrunn to the pole. As was mentioned, the total magnetic anomalies were sampled in a square grid with the sampling unit equal to $\xi = 1$ km, the lower and upper cut-off spatial frequencies of the Gaussian band-pass window are $f^{c}_{\text{lower}} = 0.0491 \text{ km}^{-1}$ and $f^{c}_{\text{upper}} = 0.147 \text{ km}^{-1}$, respectively.

In *Fig. 6* (*a* and *b*) the total magnetic field near Hollabrunn as well as the band-pass windowed field are shown; the field data reduced to the magnetic pole are given in Fig. 6c. The reduction to the magnetic pole was computed assuming that the magnetization was induced, and its direction was given by $I = 60$ degrees, $D = 0$ degrees. If one compares the band-pass windowed anomaly with the reduced one, the phase shift of the reduction is apparent. The reduced anomaly does not have the expected symmetrical shape. This may be due to the fact that the magnetic source has some remanent magnetization.

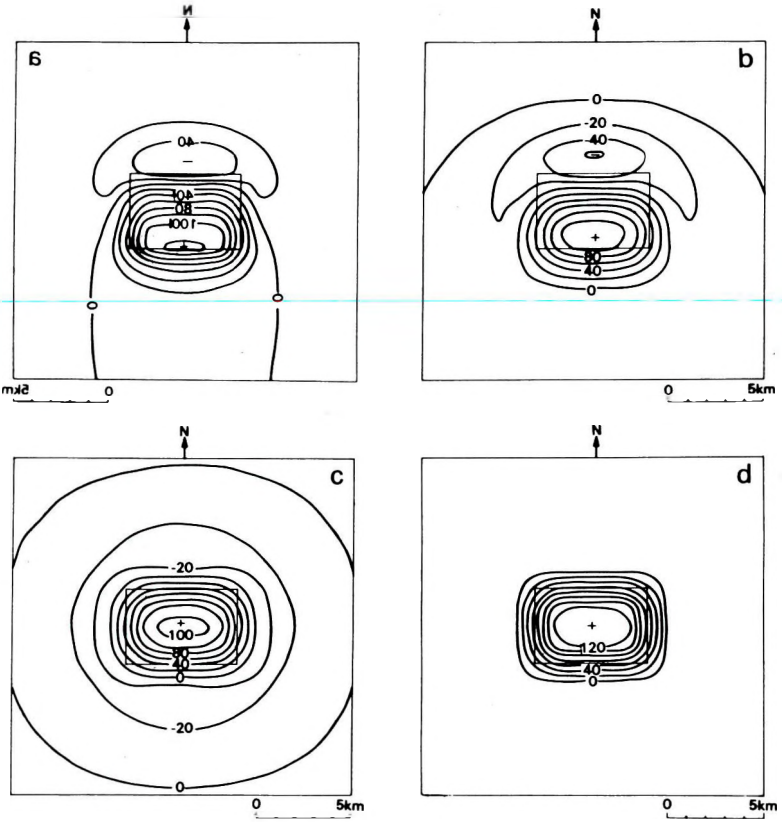

Fig. 5. Total magnetic field due to a three-dimensional rectangular prism ($I = 60°$, $D = 0°$, $J = 1$ A/m) (a), its band-pass windowed total magnetic field (b), its band-pass windowed total magnetic field reduced to the magnetic pole (c), and its total magnetic field with vertical magnetization (d). Contours are given in nT units

5. ábra. Háromdimenziós derékszögű hasáb totális mágneses tere ($I = 60°$, $D = 0°$, $J = 1$ Am^{-1}) (a), sávszűrt totális mágneses tere (b), sávszűrővel csonkított pólusra redukált totális mágneses tere (c), valamint vertikálisan mágnesezett derékszögű hasáb totális mágneses tere (d). Az izovonalak egysége nT

Рис. 5. Полное магнитное поле трехмерной прямоугольной призмы ($I° = 60$, $D° = 0$, $J = 1 Am^{-1}$) (a), то же после полосовой фильтрации (b), то же после урезания полосовой фильтрацией и приведения к полюсу (c) и полное магнитное поле вертикально намагниченной трехмерной прямоуугольной призмы (d). Изолинии — в нт

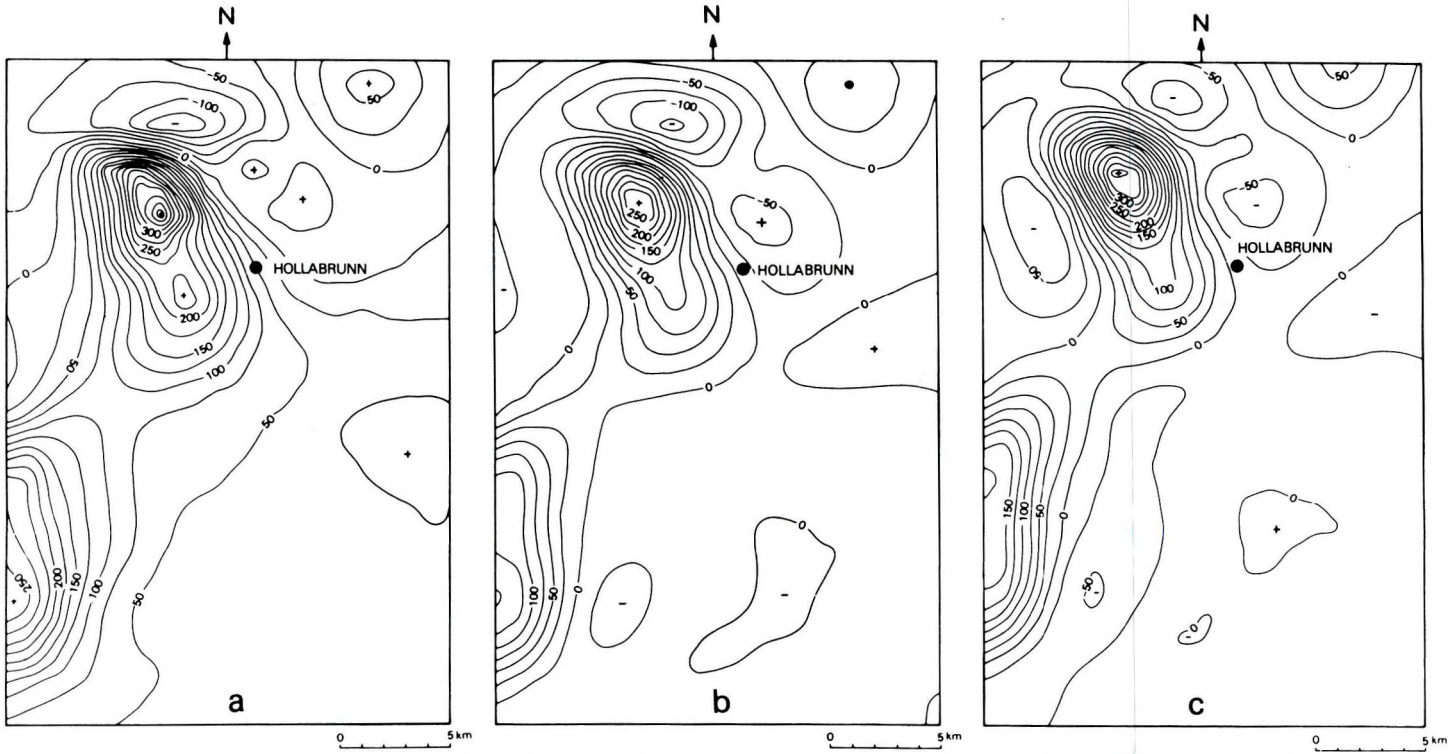

Fig. 6. Total magnetic anomalies of Hollabrunn area (a), its band-pass windowed magnetic anomalies (b), and its band-pass windowed magnetic field reduced to the magnetic pole (c). Contours are given in nT units

6. ábra. A Hollabrunn kutatási terület totális mágneses anomália térképe (a), sávszűrt totális mágneses anomália térképe (b) és sávszűrővel csonkított pólusra redukált totális mágneses anomália térképe (c). Az izovonalak egysége nT

Рис. 6. Карта полных магнитных аномалий по площади работ Голлабрун (a), то же после полосовой фильтрации (b), то же после урезания полосовой фильтрацией и приведения к полюсу (c). Изолинии — в нт

REFERENCES

AITKEN M. J. and TITE M. S. 1962: A gradient magnetometer using free-precession. Journ. Sci. Inst. **39,** pp. 625–629

BARANOV V. 1957: A new method for interpretation of aeromagnetic maps: pseudo-gravimetric anomalies. Geophysics **22,** 2, pp. 359–383

BARANOV V. 1975: Potential fields and their transformation in applied geophysics. Gebrüder Borntraeger, Berlin–Stuttgart

BARONGO J. O. 1985: Method for depth estimation on aeromagnetic vertical gradient anomalies. Geophysics **50,** 6, pp. 963–968

BHATTACHARYYA B. K. 1965: Two-dimensional harmonic analysis as a tool for magnetic interpretation. Geophysics **30,** 5, pp. 829–857

BOTT M. H. D., SMITH R. A. and STACEY R. A. 1966: Estimation of direction of magnetization of a body causing a magnetic anomaly using pseudo-gravity transformation. Geophysics **31,** 4, pp. 803–811

EGGERS D. E. and THOMPSON D. T. 1984: An evalution of the marine magnetic gradiometer. Geophysics **49,** 6, pp. 771–779

FUCHS G. and MATURA A. 1976: Geologische Karte des Kristallins der südlichen Böhmischen Masse 1 : 200.000. Geologische Bundesantalt Wien

HOOD P. and MCCLURE D. J. 1965: Gradient measurement in ground magnetic prospecting. Geophysics **30,** 3, pp. 403–410

HOOD P. J., HOLROYD M. T. and MCGRATH P. H. 1979: Magnetic methods applied to base metal exploration. In: Geophysics and Geochemistry in the Search for Metallic Ores. Econ. Geol. Rep. No. 31, pp. 77–104

KANASEWICH R. G. and AGARWAL E. R. 1970: Analysis of combined gravity and magnetic fields in wave number domain. Journal of Geophysical Research **75,** 29, pp. 5702–5712

KIS K. 1981: Transfer properties of reduction of the magnetic anomalies to the magnetic pole and to the magnetic equator. Annales Univ. Sci. Bp. Geologica **23,** pp. 75–88

KIS K. 1983a: Determination of coefficients reducing magnetic anomalies to the magnetic pole and to the magnetic equator. Acta Geodaet., Geophys. et Montanist. Hung. **18,** 1–2, pp. 173–186

KIS K. 1983b: Determination of coefficients for the computation of derivatives of potential fields with respect to x, y and z. Acta Geodaet., Geophys. et Montanist. Hung. **18,** 4, pp. 501–511

MESKÓ A. 1984: Digital Filtering: Applications in Geophysical Exploration for Oil. Akadémia Kiadó, Budapest, Pitman Publishing Ltd. London, Halsted Press New York, 635 p.

MORRIS R. M. and PEDERSEN B. O. 1961: Design of a second harmonic fluxgate magnetic gradiometer. Rev. Sci. Instruments **32,** pp. 444–448

RIKITAKE T. and TANOKA I. 1960: A differential proton magnetometer. Tokyo Univ. Earthquake Res. Inst. Bull. **38,** pp. 317–328

SLACK H. A., LYNCH V. M. and LAGAN L. 1967: The geomagnetic gradiometer. Geophysics **32,** 5, pp. 877–892

SEIBERL W. 1979: Die Transformation des Schwere- und Magnetfelds im Bereich der Ostalpen. Die Sitzungsberichte der Österreichisen Akademie der Wissenschaften, Mathem–naturw. Klasse, Abteilung II **187,** 1–3

WHITEHILL D. E. 1973: Automated interpretation of magnetic anomalies using the vertical prism model. Geophysics **38,** 6, pp. 1070–1087

WILSON C. D. V. 1970: The use of the Poisson relationship for separating the anomalies due to neighboring bodies and recognizing inhomogeneities and structural deformation. Bolletino di Geofisica **12,** 45–46, pp. 158–182

TRANSZFORMÁCIÓK ALKALMAZÁSA A BÉCSI MEDENCE NYUGATI RÉSZÉNEK LÉGIMÁGNESES ADATAIRA

KIS Károly és Wolfgang SEIBERL

A transzformációs eljárások sikerrel alkalmazhatók a mágneses anomáliák értelmezése során. Jelen tanulmány a mágneses anomáliák vertikális gradiensének meghatározását és pólusra redukálását ismerteti. A transzformációk felhasználhatóságának alapjául az átviteli függvények vizsgálata szolgált. A transzformációk hatékonyságát a felhasznált Gauss-féle (felülvágó és sávszűrő) csonkítófüggvények javították. A csonkítófüggvények kiküszöbölik a transzformációk nemkívánatos tulajdonságait: a nagyfrekvenciás zaj amplitúdójának erősítését és a pólusra redukálás véges szakadását a nulla térfrekvenciánál. A javasolt eljárásokat egyszerű modellszámítások és a Bécsi medence légimágneses adatainak a bemutatott módszerrel történő feldolgozása illusztrálja.

ПРИМЕНЕНИЕ ПРЕОБРАЗОВАНИЙ ДЛЯ ОБРАБОТКИ АЭРОМАГНИТНЫХ ДАННЫХ ПО ЗАПАДНОЙ ЧАСТИ ВЕНСКОЙ ВПАДИНЫ

Карой КИШ, Вольфганг САЙБЕРЛ

Приемы преобразования могут быть успешно применены в интерпретации магнитных аномалий. В настоящей работе излагаются определение вертикального градиента магнитных аномалий и их приведение к полюсю. Основой для применения преобразований служило исследование функций переноса. Эффективность преобразований усиливалась благодаря применению урезающих функций Гаусса (низкочастотное и полосовое фильтрование). Урезающими функциями устраняются нежелательные эффекты от преобразований: усиление амплитуды высокочастотного шума и конечный обрыв приведения к полюсу при нулевых частотах поля. Представленные приемы иллюстрируются простыми расчетами на моделях и обработкой аэромагнитных данных по Венской впадине указанным способом.

GEOPHYSICAL TRANSACTIONS 1991
Vol. 36. No. 1–2. pp. 49–65

PALAEOMAGNETIC INVESTIGATIONS IN HIGHLY METAMORPHOSED ROCKS: EASTERN ALPS (AUSTRIA AND HUNGARY)

Herman J. MAURITSCH*, Emő MÁRTON** and Alfred PAHR***

A palaeomagnetic study was carried out in a tectonically complex area, mainly on highly metamorphosed rocks. Nine sites in the Penninic unit, one site in the Palaeozoic of Graz and one in the Wechsel unit, yielded characteristic remanent magnetizations (ChRM). The ChRMs were further tested in order to estimate the age of acquisition and magnitude of a possible bias of the observed directions due to metamorphism. It is concluded that the studied metamorphic rocks must have been fully overprinted during the last phase of metamorphism in the area and the oriented magnetic fabric could only have had but a minor influence on the direction of remanence.

The directions of the characteristic remanences — both before and after tectonic correction – depart significantly from that of the Earth's present magnetic field observed at the sampling area. The scatter is too high to define palaeomagnetic directions for any of the tectonic units. Tendencies in the declination rotations, however, may be recognized and interpreted as tectonic rotations. Apart from the highest level, the Penninic is clockwise, the top of the Penninic — together with the cover of Karpathian and Badenian age — is counterclockwise rotated. The sense of rotation is uncertain for the Wechsel unit because of the shallowness of the observed inclination. The observed rotations must be mainly due to mid-Miocene tectonic movements, postdating both the deposition of the Karpathian sediments and the last phase of metamorphism at 20 Ma.

Keywords: Palaeomagnetism, metamorphic rocks, Eastern Alps, magnetic fabric, ChRM, tectonic rotation

1. Introduction

The investigated area belongs to the eastern part of the Eastern Alps, where the Penninic crops out *(Fig. 1)* such as the windows of Möltern, Bernstein and Rechnitz [SCHMIDT 1951]. They are parts of a chain of windows exposing the lowermost tectonic unit of the Alps between Genoa, Italy, and Kőszeg, Hungary.

The Penninic unit is characterized by a particular lithology and metamorphism, showing all the elements of an ocean floor development, such as calcareous phyllites, limestone shales, quartzites, greenschists, serpentinites, and metagabbros. The sequence is dated mid-Cretaceous by sponge spiculae in limestone members [SCHÖNLAUB 1973].

The geological environment of the windows of Möltern and Bernstein is dominated by overthrust crystalline rocks of the Lower East-Alpine Wechsel

* Institute of Geophysics, Mining University, Leoben, Franz Josef Street 18, A-8700, Leoben, Austria
** Eötvös Loránd Geophysical Institute, Budapest, POB 35, H-1440, Hungary
*** Geologische Bundesanstalt, 1031 Vienna, Rasumofskygasse 23, Austria
Manuscript received (revised version): 13 October, 1990

unit. The Rechnitz and Eisenberg windows are surrounded by Tertiary sediments of Karpathian through Pannonian age.

The Tertiary cover conceals the tectonic situation in the southern part of the investigated area. Nevertheless, we know from other observations that it is not simple. For instance, the greenschist of Hannersdorf (Fig. 1, site 13) and its surroundings cannot belong to the Penninic in spite of the similar lithology and the present geographic position. The arguments are stratigraphical — as the age of the Hannersdorf dolomite is Devonian in contrast to the Cretaceous age of the Penninic — and geochemical, as the Penninic is derived from the ocean floor whereas the greenschist of Hannersdorf is a metamorphosed intraplate basalt [GRATZER 1985]. Concerning the metamorphism in this area, three main phases have been recognized [LELKES–FELVÁRI 1982, KOLLER 1985]:

a) oceanic metamorphism at high temperatures (500–750° C);

b) metamorphism during subduction at high pressure ($6–8 \times 10^8$ Pa) and low temperature (300–370° C); these conditions require subsidence of the sediments of the Penninic ocean to a depth of about 15–25 km; the metamorphism is dated at 65 ± 6 Ma by the K/Ar method.

c) Regional metamorphism at pressures less than 3×10^8 Pa and temperatures of 390–430° C (greenschist facies); this event is dated at 19–22 Ma by the K/Ar method. It seems that the temperature of the metamorphism increases from north to south.

Based on *b*-axis orientation and the degree of complexity of the metamorphic texture, the Penninic may be subdivided into two nappe systems, both emplaced after the last phase of metamorphism. In the lower unit the *b*-axes are usually N–S oriented, in the upper unit they lie close to the E–W direction [PAHR 1980]. Members of the lower unit may be recognized as such by observing crenulations in addition to the dominant schistosity, since crenulation is totally absent in the upper nappe system.

2. Sampling and analysis of magnetic remanence

Six to twenty-six cores were drilled at twenty four sites in greenschists, calcareous phyllites, quartz phyllites, serpentinites belonging to the Penninic unit (Fig. 1, sites 1–12, 14–18, 24), in amphibolites and albite–chlorite–quartz -schists of the Wechsel unit (Fig. 1, sites 21–23), greenschist belonging to the Palaeozoic of Graz (Fig. 1, site 13,) and in Tertiary sediments (Fig. 1, sites 19 and 25); 332 samples in all. The cores were oriented by a magnetic compass. Orientation of schistosity planes and fold-axes were measured in the field as precisely as possible. These observations were meant to serve a double purpose: firstly, to facilitate full tectonic correction of the palaeomagnetic directions; secondly, to decide whether the site belonged to the lower or the upper nappe system. The serpentinite of Bernstein (Fig. 1, site 24) was the only site at which tectonic elements could not be measured.

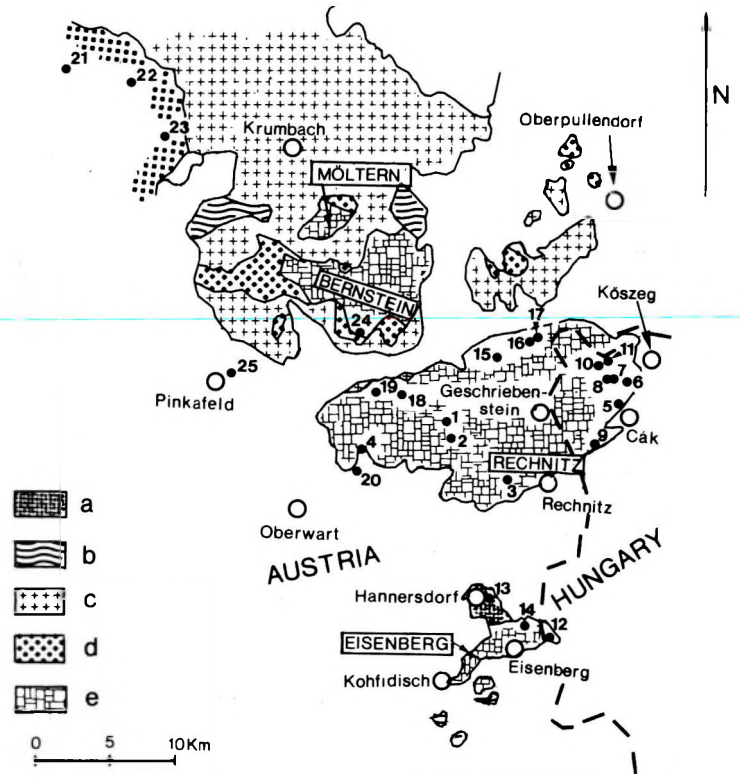

Fig. 1. Geological sketch map of the eastern part of the Eastern Alps with palaeomagnetic sampling sites. Key to geology: a) Upper East-Alpine Palaeozoic, b) Middle East-Alpine Crystalline, c) Lower East-Alpine Grobgneiss unit, d) Lower East-Alpine Wechsel unit, e) Penninic. Sampling sites are in the Penninic of the Rechnitz window (sites 1–11, 18), of the Eisenberg window (sites 12 and 14) and of the Bernstein window (site 24), in the Palaeozoic of Graz (13), in the Wechsel unit (sites 21–23), in Karpathian (site 19) and Badenian (site 25) sediments covering the Grobgneiss unit

1. ábra. Földtani vázlat a Keleti Alpok keleti részéről, a paleomágneses mintavételi helyekkel. Jelmagyarázat: a) Felső Keletalpi paleozoikum, b) Középső Keletalpi kristályos egység, c) Alsó Keletalpi Grobgneiss egység, d) Alsó Keletalpi Wechsel egység, e) Penninikum. Mintavételi helyek a Penninikumon: a Rohonci ablakból (1–11 és 18), a Vashegyi ablakból (12 és 14) és a Bernstein ablakból (24); a grazi paleozoikumon (13), a Wechsel egységen (21–23), és a Grobgneiss egység fedőjét képező kárpáti (19) és bádeni (25) üledékeken

Рис. 1. Геологическая схема восточного окончания Восточных Альп с обозначением пунктов отбора проб на палеомагнитные определения
a) верхне-восточноальпийский палеозой, b) — средневосточноальпийские кристаллические комплексы, c) нижневосточноальпийские грубые гнейсы, d) нижне-восточноальпийский Вехсельский покров, e) Пеннинский покров. Пункты отбора проб из Пеннинского покрова: по Кёсегско-Рехницкому окну (1–11 и 18), по Вашхедьско-Айзенбергскому окну (12 и 14), по Бернштайнскому окну (24); из грацского палеозоя (13); из Вехсельского покрова (21–23); из осадочного чехла единицы грубых гнейсов: по карпатским отложениям (19), по баденским отложениям (25)

The field cores were cut into 2–4 standard-size samples. From each core, sister specimens were subjected to stepwise demagnetization, both by AF and by the thermal method, independently in the palaeomagnetic laboratories in Budapest and at Gams. Full demagnetization was rarely achieved with AF (only at sites 24 and 25, see *Fig. 3*). Thermal demagnetization combined with AF or alone were more efficient (*Fig. 2.* and *Fig. 4*). Where full coercivity or a blocking temperature spectrum was available, palaeomagnetic site mean directions were calculated combining first the characteristic remanences of sister specimens on sample, then on site level (sites 3, 10, 14, 18, 22, 25); samples with sister specimens of different directions (angular difference higher than 25°) were rejected (*Fig. 5*).

Unstable behaviour on cleaning often prevented complete demagnetization. Samples with dominant spurious components were disregarded. Moderate instability, however, was dealt with in the following way. After removing an obviously different and moderately resistant component, remanence directions measured at successive heating steps were averaged to enhance the signal (*Fig. 6*), provided that the susceptibility had not incresased considerably.

The remanence directions thus obtained served as a basis for calculating site means (Table I. sites 4, 6, 8, 13, 24, 12_1). At site 12 the component with the higher blocking temperature was further tested by repeating the demagnetization at the same temperature twice, first placing the specimen in the oven in one direction, then in the other, i.e. with X and Z in two opposite orientations; finally, the results of four cleaning steps — two at 450° C and two at 475° C – were averaged. This was done because of the moderate increase in susceptibility (20 per cent on average above 250–350° C, relative to the initial value).

Table 1[1] summarizes the ChRM directions before and after tilt (sites 19 and 25) or full tectonic correction — first for the *b*-axis tilt, then for the schistosity position, the latter being assumed to be parallel to the bedding for most sites.

[1] All samples bear the code of HA (for Hungary and Austria)

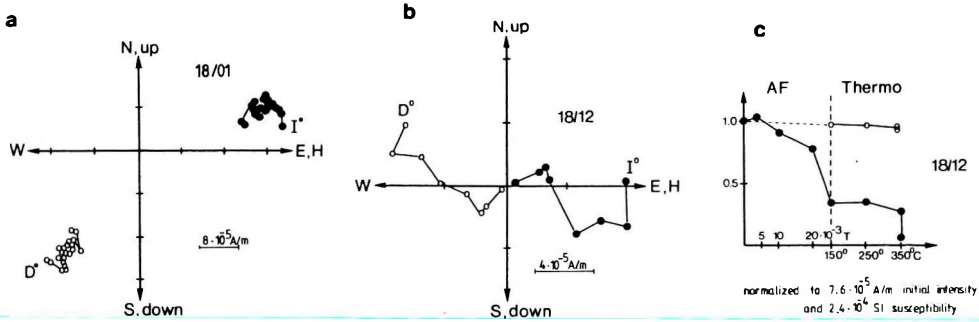

Fig. 2. Comparison of the behaviour of the NRM on AF (a) and on the combined AF and thermal (b, c) demagnetization. Rechnitz window, Penninic at Steinwandriegel (site 18): a) and b) are orthogonal plots (demagnetization steps in a): NRM to 1×10^{-2}T, in b) as in c)), c) is a normalized intensity (dots) and susceptibility (circles) diagram

2. ábra. Az NRM viselkedésének összehasonlítása váltóáramú (a) és kombinált váltóáramú- és termo- (b és c) lemágnesezésre. Rohonci ablak, Steinwandriegel, Penninikum (18. mintavételi hely): a) és b) ortogonális vetület (lemágnesezési lépések a)-ban: NRM-től 1×10^{-2}T-ig, b) és c) azonos), c) normalizált intenzitás (teli körök) és szuszceptibilitás (üres körök) diagram

Рис. 2. Сопоставление поведения NRM при чистке переменным током (a), а также комбинацией переменного тока с нагреванием (b и c). Рехницкое окно, Штайнвандригель, Пеннинский покров (пункт пробоотбора 18): a) и b) прямоугольная проекция; ступени чистки в a) от NRM до $1 \cdot 10^{-2}$ T; b) и c) одинаковы; c) диаграмма нормированной интенсивности (залитые кружки) и восприимчивости (полые кружки)

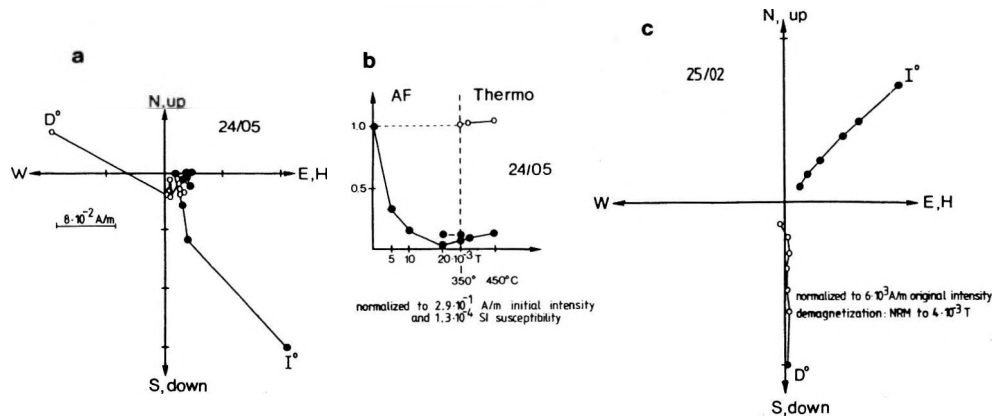

Fig. 3. Fast reduction of the NRM intensity on AF demagnetization. a) and b) Bernstein window, serpentinite (site 24) c) Badenian sediment (site 25). For explanation, see Fig. 2. (demagnetization steps: NRM to 4×10^{-3}T)

3. ábra. Az NRM gyors csökkenése váltóáramú lemágnesezésre. a) és b) Bernstein ablak, szerpentinit (24), c) bádeni üledék (25).
Jelmagyarázatot lásd a 2. ábrán (lemágnesezési lépések: NRM-től 4×10^{-3}T-ig)

Рис. 3. Быстрое убывание NRM при чистке переменным током. a) и b) Бернштайнское окно, серпентиниты (24), c) баденские отложения (25). Условные обозначеня см. на рис. 2. Ступени чистки — от NRM до $4 \cdot 10^{-3}$T

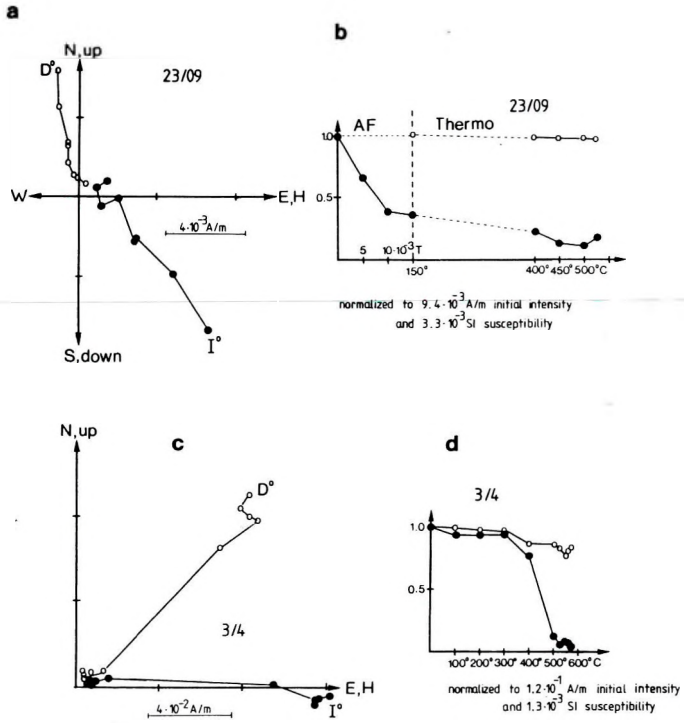

Fig. 4. Fast reduction of the NRM intensity on thermal demagnetization. a) and b): Wechsel unit, St. Corona, amphibolite (site 23); c) and d) Penninic, Markthodis, calcareous schist (site 3). For legend see Fig. 2

4. ábra. NRM gyors csökkenése hőkezelésre a) és b): Wechsel egység, St. Corona, amfibolit (23); c) és d) Penninikum, Markthodis, mészpala (3). Jelmagyarázat a 2. ábrán

Рис. 4. Быстрое убывание NRM при термической чистке. a) и b) Вехсельский покров, Ст. Корона, амфиболиты (23); c) и d) Пеннинский покров, Марктгодис, известковистые сланцы (3). Условные обозначения см. на рис. 2

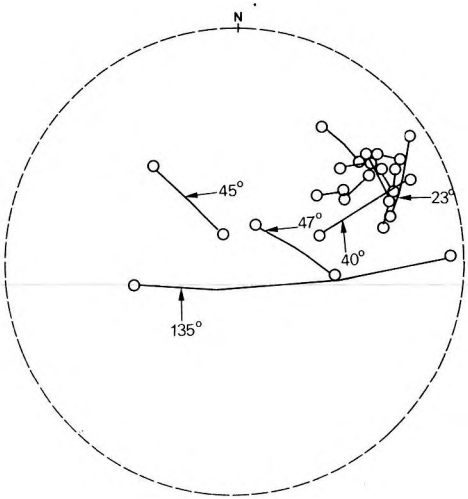

Fig. 5. Characteristic remanences for sister specimens. Wechsel unit, albite-chlorite schist (site 22). Stereographic projection, negative inclinations. ChRMs of sister specimens are joined and angular distances close to or higher than 25° marked

5. ábra. Ikerminták jellegzetes remanenciája. Wechsel egység, albit–klorit pala (22). Sztereografikus vetület, negatív inklinációk. Az ikerminták jellegzetes remanenciái össze vannak kötve és a 25°-nál nagyobb szögtávolságok megjelölve.

Рис. 5. Характерная остаточная намагниченность двойных проб. Вехсельский покров, альбит-хлоритовые сланцы (22). Стереографическая проекция, отрицательные наклонения. Значения характерной остаточной намагниченности соединены между собой с обозначением угловых расстояний свыше 25°

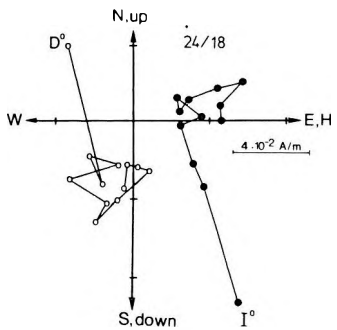

Fig. 6. Moderate instability of the NRM on thermal demagnetization. Penninic unit, Bernstein window, serpentinite (site 24)

6. ábra. Az NRM közepes instabilitása hőkezelésre. Penninikum, Bernstein ablak, szerpentinit (24)

Рис. 6. Средняя нестабильность NRM при термической чистке. Пеннинский покров, Бернштайнское окно, серпентиниты (24)

Site	rock type	n/n_o	D° D_c°	I° I_c°	k	α_{95}	cleaning
Rechnitz, Penninic, upper unit							
3	greenschist	5/11	43	−6	6	33.6	300° C
			53	+33	6	33.6	
4	greenschist	6/10	319	−57	4	40.8	300° C
			333	−34	4	40.8	
6	carbonatic	10/13	301	−37	11	15.2	150–300° C
	schist		327	−25	11	15.2	
18	calcareous schist	14/17	214	−29	18	9.6	300° C, 20–60 mT
	and phyllites		193	−35	18	9.6	
Rechnitz, Penninic, lower unit							
8	carbonatic	13/17	95	−2	5	19.6	300–400° C
	schist		98	+8	5	19.6	
10	calcareous	12/25	113	−3	7	11.7	150–400° C
	phyllite		115	+14	7	11.7	
Eisenberg, Penninic, lower unit							
12_1	greenschist	7/26	232	−23	18	14.4	250–350° C
			228	−23	18	14.4	
12_2	greenschist	17/26	286	−24	17	8.8	450–475° C
			283	−31	17	8.8	
14	greenschist	19/26	89	+2	4	18.9	150° C
			91	+20	4	18.9	
Palaeozoic of Graz							
13	greenschist	4/8	133	+47	84	10.0	50–150° C
			60	+64	84	10.0	
Bernstein, Penninic, upper unit							
24	serpentinite	19/19	287	+54	8	12.9	NRM
			–	–	–	–	
		14/19	139	−24	6	19.9	300–425° C
			–	–	–	–	
Wechsel unit							
22	albite-chlorite	9/13	58	−19	73	6.1	250–525° C
	schist		56	+9	73	6.1	
Tertiary sediments							
19	Karpathian	5/9	123	−36	11	23.9	300° C
	sandstone		133	−54	11	23.9	
25	Badenian	7/12	167	−42	7	25.0	20 mT
	sediment		165	−36	7	23.9	

Table 1. Palaeomagnetic data

n – number of samples used for evaluation; n_o – number of collected samples; D° – declination; I° – inclination, before tectonic correction; D_c°, I_c° – same after tectonic correction; k and α_{95} statistical parameters [FISHER 1953]

I. táblázat. Paleomágneses adatok

n — értelmezésbe bevont minták száma; n_0 — begyűjtött minták száma; D° – deklináció; I° — inklináció tektonikai korrekció előtt; D_c°, I_c° — ugyanaz tektonikai korrekció után; k és α_{95} — statisztikai paraméterek [FISHER 1953]

Таблица 1. Палеомагнитные данные

n — количество проб, использованных в интерпретации; n_0 — количество отобранных проб; D° I° — склонение и наклонение до тектонической поправки; D_c°, I_c° — то же с тектонической поправкой; к и α_{95} — статистические параметры, по Фишеру (FISHER 1953)

7. ábra. Normalizált IRM felvétele: a)–d) és szuszceptibilitás-hőmérséklet görbék: e)–h). Teli körök — normalizált intenzitás, üres körök — szuszceptibilitás

Рис. 7. Съемка нормированной IRM: a)–d) и кривые восприимчивость–температура e)–h). Залитые кружки — нормированная интенсивность, полые кружки — восприимчивость

3. Magnetic mineralogy and susceptibility anisotropy

The vector plots indicate composite NRM in most cases. The magnetic minerals responsible for the different components of the NRM were not identified precisely. The behaviour of the NRM on cleaning, that of the susceptibility on heating, IRM experiments and the inspection of polished sections, however, permit one to make some conclusions about the magnetic minerals in the samples.

Normally the IRM curves show fast saturation *(Fig. 7/a, b, c)*; the decay of the NRM on heating is also rapid while the susceptibility may increase *(Fig. 7/e)*, decrease *(Fig. 7/f)* or remain constant *(Fig. 7/g)*. Thus the magnetically soft mineral may be iron sulphide, as identified in the polished sections (sites 12 and 14) and/or maghemite (e.g. sites 3, 19). When the susceptibility remains stable, titanomagnetite is likely to carry the NRM (e.g. sites 18, 22, 24) since this mineral often occurs in the Penninic [KOLLER 1985].

In addition to a soft component, some specimens contain a phase which does not reach saturation in a field of 1.5 T. This is not likely to contribute to the NRM because the NRM versus temperature curve (*Fig. 7/h*) is similar to those with one soft component only.

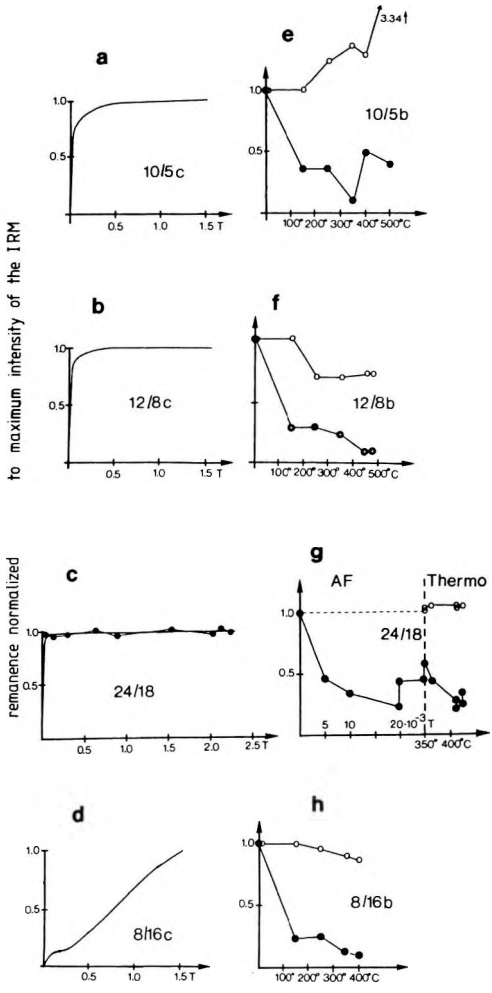

Fig. 7. Normalized IRM acquisition: a)–d) and susceptibility versus temperature curves: e)–h). Dots — normalized intensity, circles — susceptibility

Magnetic fabric was studied by measuring directional susceptibility in a low magnetic field. By analysing the magnitudes and orientations of the principal susceptibility axes and their relationship to the direction of the ChRM and the macroscopically observable schistosity planes we hoped to estimate the deflection of the directions of the ChRM of the ancient magnetic field due to anisotropy and the degree of complexity of the fabric.

Concerning the possible influence of magnetic anisotropy on the direction of the remanent magnetization, the observations can be summarized as follows. The degree of anisotropy is usually not high enough to cause considerable deflection from an external magnetic field due to magnetic anisotropy (*Table II*). Moreover, combined high and low field measurements indicate that the observed anisotropy is due largely to paramagnetic minerals (e.g. at site 12 entirely, at site 10, 90 per cent: ROCHETTE, personal communication).

The relationship between the orientation of the principal susceptibility axes and that of the fabric observable in the field is not straightforward.The directions of the principal susceptibility axes may be randomly distributed; if not, the minimum axes cluster, or define a great circle. In the last case, the great circle contains the pole of the macroscopically observable schistosity plane (*Figs. 8 and 9*). Such distribution may be explained by assuming that the minimum susceptibility directions, originally coinciding with the pole of the dominant schistosity, became displaced by adding a second 'component' to the original one during a later deformation process, or that the sampled rocks changed orientation in a constant stress field. The composite nature of the susceptibility is proved by the drastic reduction of the distance between extreme points along the great circle after heating, i.e. after having practically destroyed one of the magnetic minerals (*Fig. 9*).

A similar model may account for the fact that the statistically well-defined minimum susceptibility site mean directions often cluster away form the pole of the schistosity (*Fig. 10*). In this case, however, the deformation process responsible for the dominant fabric is totally overprinted.

Thus we may conclude that the magnetic fabric in itself or in relation to the texture of the studied metamorphics suggests that the rocks were subjected to complex tectonic and metamorphic processes. Our results, however, are indifferent to the timing, i.e. we cannot tell with any certainty whether the magnetic fabric was formed during one or during more metamorphic events.

In order to estimate the actual influence of the anisotropy on the direction of the remanence, remagnetization experiments were carried out. Some AF cleaned specimens were given IRM (*Fig. 11*) or ARM (*Fig. 12*), then stepwise heated and cooled in a laboratory field of controlled direction with the X (*Fig. 11*) or the Z (*Fig. 12*) axis parallel to the applied field. Remagnetization was complete or nearly complete at 435° C during a short heating run. The results of this experiment imply that

a) the directions of minimum susceptibility are close to the IRM directions (25/−3 and 349/−8) and the ARM directions (337/86, 340/57, 356/31, 180/31) respectively, i.e. the deflection from an external field due to the anisotropy of

Site	azimuth/dip		susceptibility anisotropy				ChRM
	b-axis	plane of schistosity	degree ($\kappa_{max}/\kappa_{min}$) per cent			mean direction of min. (field system)	$D°/I°$
			average	max.	min.	azimuth/dip	
Rechnitz window, lower unit							
1	150/12	240/54	10	12	4	(120/54)	–
2	170/20	253/49	9	13	6	86/33	–
5	358/10	280/63	–	–	–	–	–
6	335/22	204/35	–	–	–	–	301/–37
7	160/18	135/15	–	–	–	–	–
10	340/3	260/20	5	8	1	•	(113/–3)
15	190/9	275/35	22	37	13	(67/6)	–
16	200/10	280/72	20	32	13	(143/55)	–
17x	10/10	320/40	20	25	13	160/61 97/60	–
Rechnitz window, upper unit							
3	205/29	187/31	38	72	4	108/71	(43/–6)
4	240/14	170/25	6	8	4	337/54	(319/–57)
8	310/18; 225/26	223/16	–	–	–	–	(95/–2)
9	60/10	125/16	–	–	–	–	–
11	230/10	260/13	–	–	–	–	–
18	358/17	282/41	9	28	3	•	214/–29
Eisenberg window, lower unit?							
12	275/95	320/9	6	8	4	•	286/–24 232/–23
14	–	245/20	–	–	–	–	(89/2)
Bernstein window, upper unit							
24	–	–	6	9	2	(39/71)	(287/54) (139/–24)
Graz Palaeozoic							
13	–	350/46	–	–	–	–	–
Wechsel unit							
21	50/25	50/30	–	–	–	–	–
22	220/20	248/28	12	16	7	94/62	58/–19
23	255/22	240/32	9	15	4	(185/47)	–
Karpathian Sandstone covering Grobgneiss unit							
19	–	10/20	3	9	1	(130/71)	123/–36

Table II. Oriented fabric: field observations and data from magnetic fabric analysis Direction in brackets: poorly defined statistically ($k < 10$ and/or $\alpha_{95} > 15°$); asterisk: minimum susceptibility directions define a great circle

II. táblázat. Irányított szövet: terepi megfigyelések és a mágneses szövetanalízis eredményei Irányok zárójelben: statisztikailag gyengén meghatározott ($k < 10$ és/vagy $\alpha_{95} > 15°$); csillag: minimum szuszceptibilitás irányok egy főkört határoznak meg

Таблица II. Ориентированная текстура на основании полевых наблюдений и магнитного текстурного анализа Направления в скобке — статистически мало значимые ($k < 10$ и/или $\alpha_{95} > 15°$); звезда — направлениями минимальной восприимчивости определяется дуга большой окружности

the susceptibility is indeed not significant;

b) under geological conditions any previously existing NRM must have been totally overprinted during the last phase of metamorphism.

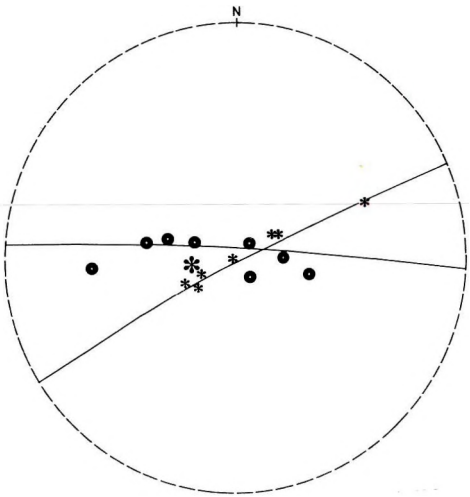

8. ábra. A minimum szuszceptibilitás irányok eloszlása egy főkörön (Hétforrásörs, mészfillit, 10). Sztereografikus vetület. Kör: a minimum szuszceptibilitás irányok gyürődés nélküli rétegekben; kis csillag: palásság (és rétegződés) pólusa kismértékü gyürődésekben; nagy csillag: ugyanez az általános palásságra.

Рис. 8. Распределение направлений минимальной восприимчивости вдоль дуги большой окружности (Хетфоррашёрш, известковистые филлиты, 10). Стереографическая проекция. Кружки — направления минимальной восприимчивости в нескладчатых прослоях; малые звезды — полюс сланцеватости (и слоистости) в небольших складках; крупные звезды — то же для общей сланцеватости

Fig. 8. Distribution of the directions of the minimum susceptibility along a great circle (Hétforrásörs, calcareous phyllite, site 10). Stereographic projection. Dots: directions of the minimum susceptibility in beds without small-scale folding; asterisks: poles of schistosity (and bedding) in small-scale folds (small asterisks) and that for the general schistosity (larger asterisk)

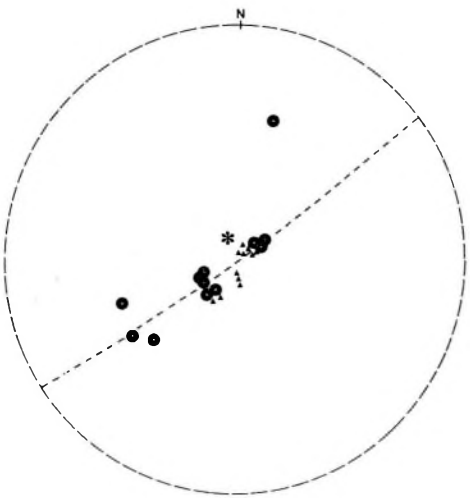

9. ábra. A minimum szuszceptibilitás irányok eloszlása egy főkörön (Felsőcsatár, zöldpala, 12). Sztereografikus vetület. Kör: a minimum szuszceptibilitás irányok a természetes állapotban; csillag: az általános palásság pólusa; háromszög: a minimum szuszceptibilitás irányok a minták 475° C-ra való hevítése, azaz a pirrhotit lebontása után

Рис. 9. Распределение направлений минимальной восприимчивости вдоль дуги большой окружности (Фельшёчатар, зеленые сланцы). Стереографическая проекция. Кружки — направления минимальной восприимчивости в естественном состоянии; звезды — полюса общей сланцеватости; треугольники — направления минимальной восприимчивости после нагрева проб до 475°, то-есть после разложения пирротина

Fig. 9. Distribution of the directions of the minimum susceptibility along a great circle (Felsőcsatár, greenschist, site 12). Stereographic projection. Dots: directions of the minimum susceptibility in the natural state; asterisk: pole of the general schistosity; triangles: directions of the minimum susceptibility after heating the specimens at 475° C, i.e. destroying pyrrhotite

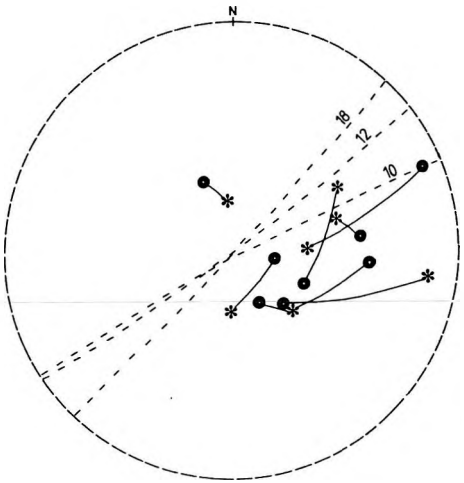

10. ábra. A palásság pólusának és a minimum szuszceptibilitás irányok összekötése a Penninikumra (1–11 és 15–17). Sztereografikus vetület, minden vektor lefelé mutat. A főkörök, amelyek mentén a minimumszuszceptibilitás irányok eloszlanak (10, 12 és 18) szaggatott vonallal vannak jelölve.

Рис. 10. Соединение полюсов сланцеватости и направлений минимальной восприимчивости по Пеннинскому покрову (1–11 и 15–17). Стереографическая проекция. Все векторы направлены вниз. Дуги больших окружностей, вдоль которых распределены направления минимальной восприимчивости (10, 12 и 18), обозначены пунктирной линией

Fig. 10. Position of the pole of schistosity joined to the direction of minimum susceptibility(ies) for the Penninic unit (sites 1–4, 15–17). Stereographic projection, all vectors pointing downwards. The great circles along which the directions of minimum susceptibility are distributed at sites 10, 12, 18, respectively, are shown in dotted lines

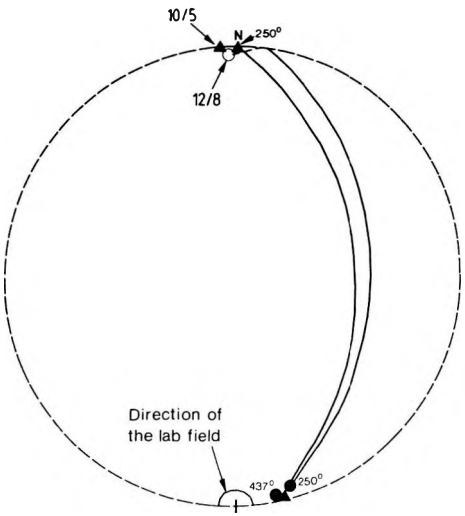

11. ábra. A 10. és 12. mintavételi hely mintái IRM-jének újramágnesezése szabályozott laboratóriumi mágneses térben történő hevítéssel és hűtéssel. Sztereografikus vetület. Fekete jelek: lefelé mutató vektorok; üres jelek: felfelé mutató vektorok

Рис. 11. Перемагничивание IRM проб пунктов 10 и 12 при нагреве и остывании в регулируемом лабораторном магнитном поле. Стереографическая проекция. Жирные значки — векторы, направленные вниз; полые значки — векторы, направленные вверх

Fig. 11. Remagnetization of IRM of samples from sites 10 and 12 by heating and cooling them in a controlled laboratory field. Stereographic projection. Solid symbols: vectors pointing downwards; hollow symbols: vectors pointing upwards

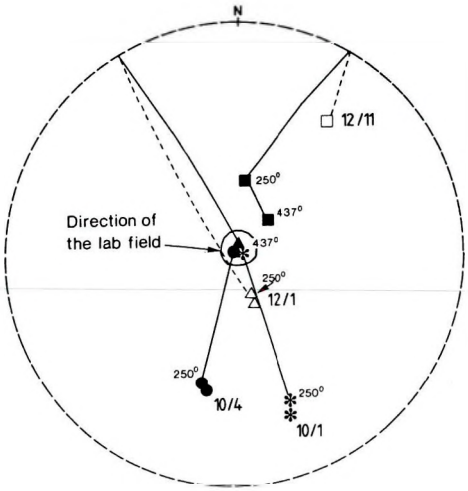

12. ábra. A 10. és 12. mintavételi hely mintái ARM-jének újramágnesezése szabályozott laboratóriumi mágneses térben történő hevítéssel és hűtéssel. Sztereografikus vetület. Fekete jelek: lefelé mutató vektorok, üres jelek: felfelé mutató vektorok

Рис. 12. Перемагничивание ARM проб пунктов 10 и 12 при нагреве и остывании в регулируемом лабораторном магнитном поле. Стереографическая проекция. Жирные значки — векторы, направленные вниз; полые значки — векторы, направленные вверх

Fig. 12. Remagnetization of ARM of samples from sites 10 and 12 by heating and cooling in a controlled laboratory field. Stereographic projection. Solid symbols: vectors pointing downwards; hollow symbols: vector pointing upwards

4. Tectonic implication

Due to high between-site scatter for all the studied units — both before and after tectonic correction — precise palaeomagnetic directions cannot be defined for any of the units. Nevertheless, certain rotation trends can be recognized.

The main problem in interpretation is caused by the spread in inclination (*Fig. 13*). It may be argued that a metamorphic rock at the time of acquisition of the ChRM might have been oriented differently from both the present and the tectonically corrected position.

It stands to reason, however, that the position at the critical time interval be assumed as constrained by the present horizontal on the one hand, and by the plane of schistosity (stratification) observed in the field, on the other. As Table I shows, the tectonic correction has but little effect on the direction of the ChRM. Thus the low inclinations are difficult to account for, once the mid-Tertiary age of the last metamorphic event is accepted, and the composite or deflected nature of the ChRM is ruled out. In fact, some of the inclinations are so shallow, both before and after tectonic correction, that they are indicative of a pre-Tertiary, probably Palaeozoic magnetization (sites 8, 10, 14). It is interesting to note, therefore, that previously Palaeozoic was the age assigned to the Rechnitz and Eisenberg windows [FÖLDVÁRI et al. 1948, SZEBÉNYI 1948].

Apart from sites 8, 10, and 14, the Rechnitz window is characterized by large to moderate clockwise declination rotations. Sites 3 (fully or partly corrected for tectonic position), 18, and 12_1 form a moderately rotated group together with 13 (Graz Palaeozoic, corrected), while 6 and 12_2 show excess

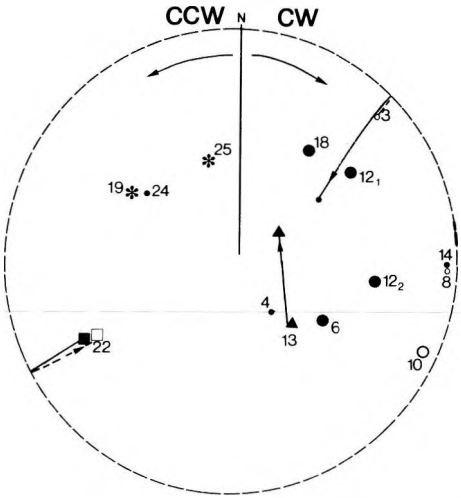

13. ábra. Paleomágneses inklinációk tektonikai korrekció előtt a Keleti Alpok keleti részében. Sztereografikus vetület. Fekete jelek: pozitív inklináció, üres jelek: negatív inklináció. Kör: Penninikum, háromszög: grazi paleozoikum, négyzet: Wechsel egység, csillag: harmadkori üledék. Kis jelek: $\alpha_{95} > 15°$, nagy jelek: $\alpha_{95} \leqq 15°$

Рис. 13. Палеомагнитные наклонения до тектонических поправок на восточном окончании Восточных Альп. Стереографическая проекция. Жирные значки — положительные наклонения; полые значки — отрицательные наклонения. Кружки — Пеннинский покров, треугольник — грацский палеозой, квадрат — Вексельский покров, звезды — третичные отложения. Малые значки — $\alpha_{95} > 15°$, крупные значки — $\alpha_{95} \leqq 15°$

Fig. 13. Palaeomagnetic inclinations before tectonic correction in the eastern part of the Eastern Alps. Stereographic projection. Full symbols: positive inclination; hollow symbols: negative inclination. Circles are for the Penninic unit, triangle for the Palaeozoic of Graz, square for the Wechsel unit, asterisks for Tertiary sediments. Small symbols: $\alpha_{95} > 15°$, larger symbols: $\alpha_{95} \leqq 15°$

rotation. The declination at sites 8, 10, 14 also deviate by a large angle from the north which may be interpreted as clockwise rotation. It is possible that on the CW side of Fig. 13 we see an older magnetization with more and a younger one with less declination rotation, since at site 12 the component with higher unblocking temperature (12_2) shows large deviation, the less resistant one (12_1) only moderate deviation from the present north.

The rotation angle for a single site from the Wechsel unit (Fig. 13, 22) is high, though the sense of rotation is undecided.

A single site from the highest level of the Rechnitz unit (24), and Tertiary sediments (sites 19, 25) covering the Grobgneiss unit (which is in turn underlain by the Wechsel) show counterclockwise rotation. The similarity of the directions observed for sites 24 and 19 implies Miocene rotation for the first of these.

The timing of the rotations observed for the rest of the metamorphics is less straightforward. Some of the ChRMs may predate the Miocene metamorphism (e.g. sites 8, 10, 14). This idea is supported, for instance, by observations on the metamorphic texture in the Eisenberg window by LELKES-FELVÁRI (personal communication) who suggests that the high-pressure low-temperature Eo-Alpine metamorphism was not everywhere overprinted by a younger greenschist facies metamorphism. Even if some of the ChRMs are older, there are others which are of Miocene age, implying that significant clockwise rotations took place between 20 Ma and the magnetization of the Styrian volcanics — that show no rotation [MAURITSCH and BECKE 1987]. The young age of the rotations in the Rechnitz area is supported in an indirect way by the orientation of the magnetic fabric.

As we have already noted the pole of the plane of schistosity (oriented by the strongest metamorphism) and the directions of the minimum susceptibilities (oriented by the last metamorphism) for the same site define a great circle. These great circles always deviate from north–south orientation (Fig. 10). When corrected for the measured palaeomagnetic rotations, these great circles become N–S oriented, thus reflecting a stress field which is expected in the Neogene as a consequence of the collision between stable Europe and the African plate.

Acknowledgement

We are grateful to P. Rochette for the high-field anisotropy measurements and evalution. We thank R. Bordás for assistance with the low-field anisotropy measurements and F. Heller for the critical reading of the manuscript.

REFERENCES

FISHER R. A. 1953: Dispersion on a sphere. Proc. Roy. Soc. Lond. A., **217,** pp. 295–305

FÖLDVÁRI A., NOSZKY J., SZEBÉNYI L. and SZENTES F. 1948: Geological observations in the Kőszeg area (in Hungarian). Report of the Hungarian Finance Ministry, 1947–1948, pp. 5–31

GRATZER R. 1985: Vergleichende Untersuchungen an Metabasiten im Raum Hannersdorf, Burgenland. Aus den Sitzungsberichten der ÖAW, Mathematisch-Naturwissenschaftliche Klasse, Abt. I, **194,** 6–10, pp. 132–148, Wien

KOLLER F. 1985: Petrologie und Geochemie der Ophiolite des Penninikums am Alpenostrand. Jahrbuch d. Geol. Bundesanstalt **128,** 1, pp. 83–150, Wien

LELKES-FELVÁRI Gy. 1982: A contribution to the knowledge of the Alpine metamorphism in the Kőszeg–Vashegy area. Neues Jb. Geol. Palaont. Monatshefte 5, pp. 297–305

MAURITSCH H. J. and BECKE M. 1987: Paleomagnetic Investigations in the Eastern Alps and the Southern Border Zone. In Geodynamics of the Eastern Alps, Flügel H. W. and Faupl P. (eds), pp. 282–308 Deuticke, Vienna

PAHR A. 1980: Die Fenster von Rechnitz, Bernstein, und Möltern. *in* OBERHAUSER R.: Der Geologische Aufbau Österreichs, pp. 320–326, Wien

SCHMIDT W. J. 1951: Überblick über geologische Arbeiten in Österreich. Zeitschrift d. Deutschen Geol. Gesellschaft **102,** Hannover, pp. 311–316

SCHÖNLAUB H. P. 1973: Schwamm-Spiculae aus dem Rechnitzer Schiefergebirge und ihr stratigraphischer Wert. Jahrbuch d. Geol. Bundesanstalt **116,** pp. 35–49, Wien

SZEBÉNYI L. 1948: Geology of the Hungarian part of the Eisenberg (in Hungarian). Report of the Hungarian Finance Ministry, 1947–1948, pp. 45–50

ERŐSEN METAMORFIZÁLT KŐZETEK PALEOMÁGNESES VIZSGÁLATA: KELETI ALPOK (AUSZTRIA ÉS MAGYARORSZÁG)

Herman J. MAURITSCH, MÁRTONNÉ SZALAY Emő és Alfred PAHR

Tektonikailag bonyolult terület paleomágneses vizsgálatát végeztük elsősorban erősen metamorfizált kőzetek mintázásával. Kilenc mintavételi hely esett a Penninikumra, egy a grazi paleozoikumra és egy a Wechsel egységre. Mindezek jellegzetes remanens mágnesezettséget adtak, amelyet tovább ellenőriztünk a metamorfózis okozta lehetséges torzítás korának és nagyságának felbecslésével. Arra az eredményre jutottunk, hogy a tanulmányozott metamorf kőzetek teljesen átmágneseződtek a metamorfózis utolsó szakaszában és az orientált mágneses szövetnek csak elhanyagolható hatása lehetett a remanens mágnesezettség irányára.

A jellegzetes remanencia-irányok — mind tektonikai korrekció előtt, mind után — határozottan eltérnek a terület jelenlegi mágneses terétől. A szórás túl nagy, így egyetlen tektonikai egységre sem tudtunk paleomágneses irányokat definiálni. Ennek ellenére a deklináció-rotációk tendenciái felismerhetők és mint tektonikai rotációk értelmezhetők. A Penninikum óramutató járásával megegyező, a Penninikum teteje viszont — a kárpáti és bádeni fedővel együtt — óramutató járásával ellentétes rotációt szenvedett. A Wechsel egység rotációja bizonytalan az igen lapos inklinációk miatt. A megfigyelt rotációk elsősorban középső-miocén tektonikai mozgásokhoz köthetők, amelyek mind a kárpáti üledék, mind a metamorfózis legutolsó fázisa (20 Ma) koránál fiatalabbak.

ПАЛЕОМАГНИТНОЕ ИЗУЧЕНИЕ СИЛЬНО МЕТАМОРФИЗОВАННИХ ПОРОД: ВОСТОЧНЫЕ АЛЬПЫ (АВСТРИЯ И ВЕНГРИЯ)

Герман И. МАУРИЧ, Змё МАРТОН-САЛАИ, Альфред ПАР

Было проведено палеомагнитное изучение района со сложным тектоническим строением путем опробования в первую очередь сильно метаморфизованиых пород. Девять пунктов пробоотбора были в пределах Пенниского покрова, один — грацского палеозоя, и один — Вехсельского покрова. Во всех обнаружена характерная остаточная намагниченность, которая была проверена путем оценки возраста и масштаба искажений, возможных вследствие метаморфизма. Был сделан вывод о том, что изученные метаморфические породы были целиком перемагничены в последнюю стадию метаморфизма и что ориентированная магнитная структура могла оказать лишь пренебрегаемое влияние на направление остаточной намагниченности.

Характерные направления остаточной намагниченности — как до, так и после тектонической поправки — существенно отличаются от современного магнитного поля региона. Разброс значений слишком велик, так что палеомагнитные направлания не могли быть определены для каждой тектонической единицы в отдельности. Несмотря на это, тенденции к повороту склонений могут быть установлены и интерпретированы в качестве тектонических. Пеннинский покров обнаруживает поворот по часовой стрелке, а его верхи — совместно с карпатским и баденским чехлом — против часовой стрелки. Поворот Вехсельского покрова устанавливаетсь ненадежно в связи с малыми наклонениями. Наблюдаемые повороты могут быть связаны в первую очередь со среднемиоценовыми тектоническими движениями, проявившимися как после накопления карпатских отложений, так и после последней фазы метаморфизма (20 млн. лет).

GEOPHYSICAL TRANSACTIONS 1991
Vol. 36. No. 1–2. pp. 67–79

GEOMAGNETIC INVESTIGATIONS IN THE AUSTRIAN–HUNGARIAN BORDER ZONE: THE KŐSZEG–RECHNITZ MTS. AREA

Egon HOFFER*, László SCHŐNVISZKY* and Georg WALACH**

From 1985 to 1988 a geomagnetic survey (total field and vertical component) was carried out along the border between Austria and Hungary by a combined team from the Eötvös Loránd Geophysical Institute of Hungary and the Institute of Geophysics of the Mining University, Leoben. In this paper the results of the geomagnetic survey of the Austrian topographic map-sheet 138 (Rechnitz), are reported. Comparison of the results — presented in isoanomaly maps — with the distribution of susceptibilities shows that Penninic serpentinites with locally occurring metagabbro, ophicalcite and blue schist are the characteristic magnetic rocks of the investigated region. Therefore the geomagnetic anomaly pattern can be interpreted qualitatively as an indicator of the distribution of the Penninic ophiolite complex in the eastern part of the Kőszeg–Rechnitz Mts.

Keywords: Austria, Hungary, Penninic, Rechnitz window, geomagnetic survey, magnetic susceptibility

1. Introduction

If one studies the geomagnetic maps of the border area between Austria and Hungary, e.g. the ΔZ map of Hungary 1 : 500,000 [HAÁZ–KOMÁROMY 1966] or the aeromagnetic ΔT map of the Styrian basin — South Burgenland Rise, 1 : 200,000 [SEIBERL 1989] — it appears that in the area of the Kőszeg–Rechnitz Mts. there are significant anomalies on both sides of the border. Moreover, the helicopter-borne aeromagnetic measurements organized by the Geologische Bundesanstalt in 1983/84 [SEIBERL et al. 1986] also found anomalies in the Rechnitz area: the continuation of these anomalies is assumed to be in Hungary.

For the above reasons at a meeting of geophysicists from Austria and Hungary, an interest in joining and completing the geomagnetic maps was declared. In particular, a detailed ΔT and ΔZ survey along the border area was suggested. The necessary measurements were performed between 1985 and 1988 by a combined field group of the Eötvös Loránd Geophysical Institute of Hungary and of the Institute of Geophysics, Mining University, Leoben.

The project had basically two main parts: (i) a detailed ΔT and ΔZ survey of the Austrian map sheet 138, Rechnitz covering two-thirds Austrian, one-third Hungarian territory; (ii) and the establishment of a regional geomagnetic base network for the whole of the common border section. It is intended that the results of the second part be submitted for publication at a later date.

* Eötvös Loránd Geophysical Institute of Hungary, Budapest, POB 35, H–1440, Hungary
** Institute of Geophysics, Mining University, Leoben, Franz-Josef Street 18, A–8700, Leoben, Austria
Manuscript received: 28 August, 1990

In 1984 the Austrian party — as the first step of planning the detailed survey — collected all available geomagnetic data for South-Burgenland — mainly measurements of the vertical component — and checked, completed and transformed them into a standardized reference system. The next step was to estimate the costs and then to come to an agreement on the division of the tasks: on the basis of this, the Hungarian party were required to perform the ΔT measurements, the Austrian party the ΔZ survey.

The location map of the study area showing general topographic and geologic surroundings is shown in *Fig. 1.* As can be seen, the ΔZ map covers the whole mapsheet, while the ΔT map — as a direct continuation of the helicopter-borne aeromagnetic survey to the east — covers only the direct border area, i.e. the Hungarian part of the Kőszeg–Rechnitz Mts. Altogether there are 1650 ΔZ points and 700 ΔT points available. The average station density is 3 points/km^2 for both the 540 and 240 km^2 survey areas *(Fig. 2).*

2. Geological and petrophysical overview

According to PAHR [1980], and FÜLÖP–DANK [1987] the Kőszeg–Rechnitz Mts. are mainly built up of epizonal metamorphic crystalline schists (calc-, quartz-, graphite phyllites, calc-serizite schists and quartzite) with interbedded metamorphic ophiolites (greenschists, chlorite phyllite, serpentinite, metagabbro). As the Kőszeg–Rechnitz Mts. lie along the border, the geological prospecting was carried out by Hungarian as well as by Austrian geologists.

The rocks called 'Rechnitz series' by WIESENEDER [1932], according to their composition [SCHMIDT 1950], tectonic [PAHR 1960] and stratigraphic position [SCHÖNLAUB 1973] belong to the Penninicum. Therefore PAHR [1980] gave these rocks the name 'Rechnitz Penninnicum'.

As one can see from the geological sketch of Fig. 1. the Rechnitz Penninicum is overlain by the Lower East-Alpine Wechsel and Grobgneiss units and surrounded on all sides by young Tertiary sediments. The geomagnetic survey presented in this paper covers the eastern part of the Kőszeg–Rechnitz Mts. and large parts of the Tertiary surroundings, while the helicopter-borne aeromagnetic survey covers the western parts.

Within the framework of the International Geodynamics Project [WALACH 1977, WEBER et al. 1975, 1981] and later on in mineral exploration projects [WEBER and WALACH 1981, 1986–88], petrophysical studies were carried out on rock samples from the Nordostspron area in the Central Alps, from the Kőszeg–Rechnitz Mts. and the South-Burgenland Rise. Therefore the magnetic susceptibility distribution of the examined area is well-known. A comprehensive paper on palaeo- and rock-magnetic studies was published by MÁRTON et al. [1987].

The magnetic key rocks in the Kőszeg–Rechnitz Mts. *(Table I.)* are ophiolites, primarily serpentinites with a susceptibility of $35–160 \cdot 10^{-3}$ SI units.

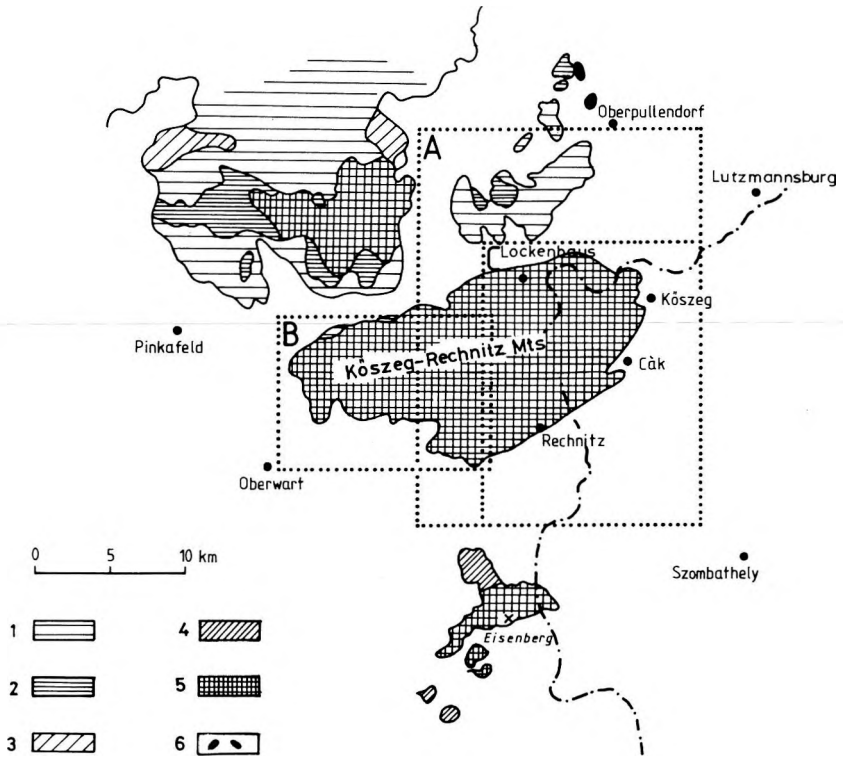

Fig. 1. Geological and geographical sketch of the survey area
1 — Grobgneiss unit (Lower East-Alpine); 2 — Wechsel unit (Lower East-Alpine); 3 — Crystalline (Middle East-Alpine); 4 — Palaeozoic (Upper East-Alpine); 5 — Rechnitz unit (Penninic); 6 — basalt (Pliocene); A — area of ΔZ ground mapping; B — area of helicopter-borne ΔT mapping; C — ΔT ground mapping

1. ábra. A kutatási terület földtani és földrajzi vázlata
1 — Grobgneisz egység (alsó kelet-alpi); 2 — Wechsel egység (alsó kelet-alpi); 3 — kristályos (középső kelet-alpi); 4 — paleozoos (felső kelet-alpi); 5 — rohonci egység (Pennini); 6 — bazalt (Pliocén); A — földi ΔZ-térképezés; B — helikopteres légi ΔT-térképezés; C — földi ΔT-térképezés

Рис. 1. Геолого-географическая схема района работ
1 — покров грубых гнейсов (нижне-австроальпийский); 2 — Вексельский покров (верхне-австроальпийский); 3 — кристаллические комплексы (средне-австроальпийские); 4 — палеозой (верхне-австроальпийский); 5 — Рехницкий покров (пеннинский); 6 — базальты (плиоцен); А — наземная съемка ΔZ; В — аэромагнитная съемка ΔT с вертолета; С — наземная съемка ΔT

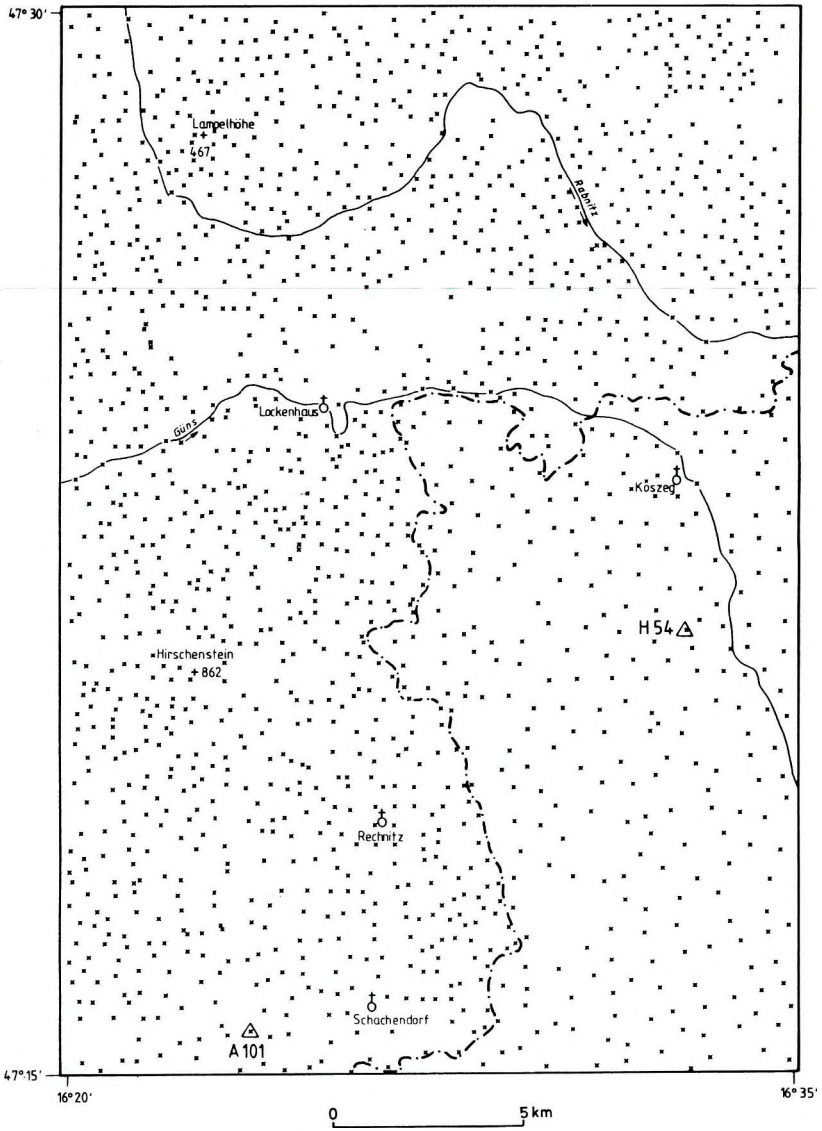

Fig. 2. Location map of the geomagnetic survey (Rechnitz)
A101 — 1st order basepoint Dürnbach; H54 — 1st order basepoint Kőszegdoroszló

2. ábra. A földmágneses mérések helyszínrajza
A101 — I. rendű alappont, Dürnbach; H54 — I. rendű alappont, Kőszegdoroszló

Рис. 2. План ситуации измерений магниторазведки A101 — опорный пункт 1-го класса, Дюрнбах; H54 — опорный пункт 1-го класса, Кёсегдоросло

Geological unit	Rock Type	Bulk density ($kg \cdot m^{-3}$)	Magnetic susceptibility (10^{-3} SI-unit)
RECHNITZ (Penninikum)	sericite phyllite	2670	1.0
	quartz phyllite	2660	0.1
	carbonate phyllite	2700	0.2
	marble (partly foliated)	2720	0.1
	conglomerate (Cák)	2750	0.1
	greenschist	2960	0.7
	ophicalcite	2780	5.0
	blueschist	2850	5.0
	metagabbro (a)	2980	30
	metagabbro (b)		0.8
	serpentinite (Fe_3O_4-poor)	2610	36
	serpentinite (Fe_3O_4-rich)	2980	160
	"Edelserpentin"	2680	0.3
WECHSEL (L. East Alpine)	albitegneiss	2700	0.6
	albitechlorite schist	2730	0.8
	mica schist	2680	0.6
	amphibolite	2920	0.7
	greenschist	2870	50
GROBGNEISS–COARSE GNEISS (L. East Alpine)	aplite gneiss	2620	0.3
	granite gneiss	2680	0.3
	mica schist	2700	0.2
	metagabbro	2950	0.6
	biotite schist	2860	0.6
	pegmatite	2650	0.1
PERMOMESOZOIC	quartzite	2660	0.1
	carbonate	2720	0.1
SIEGGRABNER S. (M. East Alpine)	paragneiss	2630	0.3
	serpentinite	2530	32
	amphibolite	2880	24
	eclogite	3360	2
HANNERSDORF –EISENBERG (U. East Alpine)	dolomite	2760	0.1
	"Rauhwacke"	2280	0.1
	shale	2680	0.6
	greenschist (a)	2860	0.6
	greenschist (b)		35
Young Tertiary volcanics		—	12–40
Quarternary and young Tertiary sediments		—	0.1–1

Table I. Bulk density and magnetic susceptibility of the most important rocks in the eastern margin of the Alps and the South-Burgenland Rise (WEBER et al. 1981, with additions)

1. Táblázat. A Keleti Alpok és a dél-burgenlandi küszöb legfontosabb kőzetfajtáinak térfogatsúlya és mágneses szuszceptibilitása (WEBER et al. 1981, kiegészítéssel)

Таблица I. Обёмный вес и магнитная восприимчивость важнейших порог Южных Альп и Южно Бургенландского порога (WEBER et al. 1981, с добовлениями)

Further locally occurring key rocks are ophicalcite, blue schists and some metagabbros with susceptibilities of $5–30 \cdot 10^{-3}$ SI. Detailed petrological and geochemical investigations were carried out on these Penninic rocks by KOLLER [1985] and by KISHÁZI and IVANCSICS [1986], respectively. Although slightly beyond the survey area the Upper East-Alpine greenschists of Hannersdorf ($35 \cdot 10^{-3}$ SI) as well as the young Tertiary volcanites ($12–40 \cdot 10^{-3}$ SI) of the Stool–Oberpullendorf area and of Pauliberg [SEIBERL 1978] should also be mentioned.

The susceptibilities of the Quaternary and Tertiary sediments are very low according to the numerous in situ and laboratory measurements: from $0.1 \cdot 10^{-3}$ SI (young Tertiary sand, Sinnersdorf Conglomerate) to $1.0 \cdot 10^{-3}$ SI (Quaternary loam). Therefore, neither they nor the carbonate- and quartz schists ($\kappa = 0.1–1.0 \cdot 10^{-3}$ SI) have any significance in the interpretation of magnetic maps. A special case is the area of the small streams coming from the serpentinites on the south flank of the Kőszeg–Rechnitz Mts. Their small sediment load may cause local anomalies because of the parent rocks some of which are highly magnetized. For example west of Rechnitz (Zuberbach) $\kappa = 5 \cdot 10^{-3}$ SI susceptibilities were measured on stream sediments. Therefore, in the survey the measurement points were located far from any rivers.

3. Measurement and interpretation methodology

The survey of the Hungarian part of map sheet 138, including the common frontier zone, was prepared in 1985 and executed in 1986. The magnetometer measurements were carried out by repeated readings and observations that were repeated three-five times daily at one of the basepoints. The co-ordinates of the survey points were read from topographic maps: 1 : 25,000 for Austria, and 1 : 10,000 for Hungary. Random checks at fixed geodetic points proved there to be no greater error than ± 20 m in the local positioning. This corresponds to an error of ± 0.15 nT in the normal field correction and can be neglected.

The ΔT measurements were carried out by a proton-precession magnetometer (GeoMetrics G 816) with a reading accuracy of 1 nT, while the ΔZ measurements by torsion magnetometers (ASKANIA GfZ and GfZ–M) with a reading accuracy of about 3 and 1 nT respectively. The second type of instruments (i.e. the torsion magnetometers) is based on the mechanical balance principle, and has already been used for 50 years. Therefore at the beginning of the program the drift and the calibration of the instruments [WALACH 1986] were checked, and for observations a mean square error of ± 5 nT was obtained.

To calculate the ΔT and ΔZ anomalies the values of the Hungarian normal field (epoch 1980.0) were taken into account by the following equations:

$$\Delta T = T - T_o \pm \delta T(t) \tag{1}$$

and

$$\Delta Z = Z' - Z'_B \pm \delta Z_o \pm \delta Z(t) \tag{2}$$

where

T = measured absolute value at the observation point
T_o = normal value at the point
Z' = measured relative value at the observation point
Z'_B = relative value at the basepoint
δZ_o = normal field correction
$\delta T(t)$, $\delta Z(t)$ = correction for daily variation

In compiling the ΔZ map, the problem of time variations arose; some of the data originated from as long ago as 10 years during which time the value of the vertical component changed by about +300 nT. It is pointed out, however, that in ΔZ anomaly map compilation, the absolute values are not very important. What is more important is the effect of the areal variation of the secular variation of the geomagnetic field. This was checked by repeated measurements on the basepoints A100 (Strem) and A101 (Dürnbach): For the epoch 1970.0 PÜHRINGER et al. [1975] obtained a difference between the two points of

$$\delta Z/(\text{Strem–Dürnbach})\ (1970.0) = 42.037 - 42.138 = -101\ \text{nT}$$

and, based on a repeat measurement in 1985, for the epoch 1980.0, approximately

$$\delta Z/(\text{Strem–Dürnbach})\ (1980.0) = 42.309 - 42.413 = -104\ \text{nT}$$

was obtained. This change of 3 nT is in the range of the observation error of the equipment utilized. Regarding the separation of the two base stations in the N–S direction (about 26 km), the 3 nT means a 0.12 nT/km N–S gradient difference in the normal field between 1970.0 and 1980.0. which is practically negligible, especially if the N–S extent of the survey area is less than 30 km. It was therefore concluded that the 1970 values are still valid, at least approximately, for 1980 as well. In view of this for anomaly calculations according to Eq. (2) — the normal field partial gradients defined by PÜHRINGER et al. [1975] were applied

$$\delta Z/\delta\varphi = 5.13\ \text{nT/km}, \qquad \delta Z/\delta\lambda = 0.80\ \text{nT/km}$$

To test this assumption, 16 stations along the Austrian–Hungarian border originally measured in 1977–79 were reobserved in 1985. Their location was unambiguously recoverable. Comparison of the ΔZ values led to a mean difference of ±5.2 nT, without any systematic error — e.g. a N–S trend. So — within the given limits of measurements error — a homogeneous data set was assured.

The reference anomaly values for basepoints A101 (Dürnbach) = +161 nT and H54 (Kőszegdoroszló) = +270 nT necessary for Eq. (2) were defined by connecting the base network in 1985 [WALACH 1986], and fitting them to the Hungarian national geomagnetic repeat survey of 1980.0. In order to record the daily variations the Hungarian party set up a mobile registration station (total field) in the survey area for the whole duration of the field work. For final calculations the T and Z registrations of the magnetic observatories of Tihany, Nagycenk and Vienna were used.

For map construction the anomaly values were interpolated by the Krieging method to a Gauss–Krüger net of 750 m grid interval thereby suppressing the anomalies of wavelengths smaller than 1.5 km. Taking into account the maximum horizontal gradient of more than 300 nT/km (Kőszeg area) and the map scale, a contour interval of 25 nT was chosen. The anomaly maps were computed and plotted by the graphic software UNIRAS in the computer centre of the Forschungsgesellschaft Joanneum in Leoben. The digital processing was carried out by R. Mayer and E. Posch.

4. Geomagnetic isoanomaly maps

The part of the South-Burgenland Rise between the Kőszeg–Rechnitz Mts. in the north and the lowland of Weixelbaum (Jennesdorf–Szentgotthárd) in the south constituting the Austrian–Hungarian border area is regionally a large magnetic high zone. As a simple sketch of the anomalous area *(Fig. 3.)* shows, a generally NNE directed anomaly main axis — although several times interrupted, a little bit shifted and situated in the area of the east flank of the South-Burgenland Rise — can be followed for about 80 km. In Austrian territory the anomaly zone was geologically thoroughly documented by outcrops and borehole data in order to be able to find a connection with the distribution of the Penninic serpentinites. Model calculations by Oberladstätter et al. [1979] explain the regional anomaly by magnetized near-vertical dykes deeply penetrating the crust. Probably there is a relationship with the Penninic Ophiolite complex that has been described geologically and petrographically several times.

The prospected area, Austrian map sheet 138, lies on the northern flank of the described anomaly zone. A brief glance at the isoanomaly maps of *Figs. 3, 4* and *5* shows that the main anomaly between Güssing and Szombathely extends to the south of Rechnitz. Further to the north the maps show a more complicated anomaly pattern.

The Kőszeg–Rechnitz Mts. are crossed by two, almost parallel NNW directed, remarkable anomaly zones: one at Kőszeg and another on the western edge of the map sheet, west of Hirschenstein (Figs. 3 and 4). The western one (main part outside of the maps, see Seiberl 1989) is regarded by Pahr [1980, p. 323) — in connection with ophiolite outcrops indicating high-pressure low-temperature paragenesis — as part of a subduction zone possibly tectonically dislocated by younger shear movements. By virtue of the similar anomaly pattern this interpretation can also be accepted for the anomaly in the Kőszeg area.

Fig. 3. Sketch of the geomagnetic anomaly field in the Austrian–Hungarian border area (old reconnaissance survey). Dotted frame: map sheet 138

3. ábra. Földmágneses anomália térkép az osztrák–magyar határ területéről (régi áttekintő felmérés). Pontozott keret: a 138-as térképlap

Рис. 3. Карта магнитных аномалий по окрестностям австрийско-венгерской границы (старая обзорная съемка). Пунктирная рамка — контур листа 138

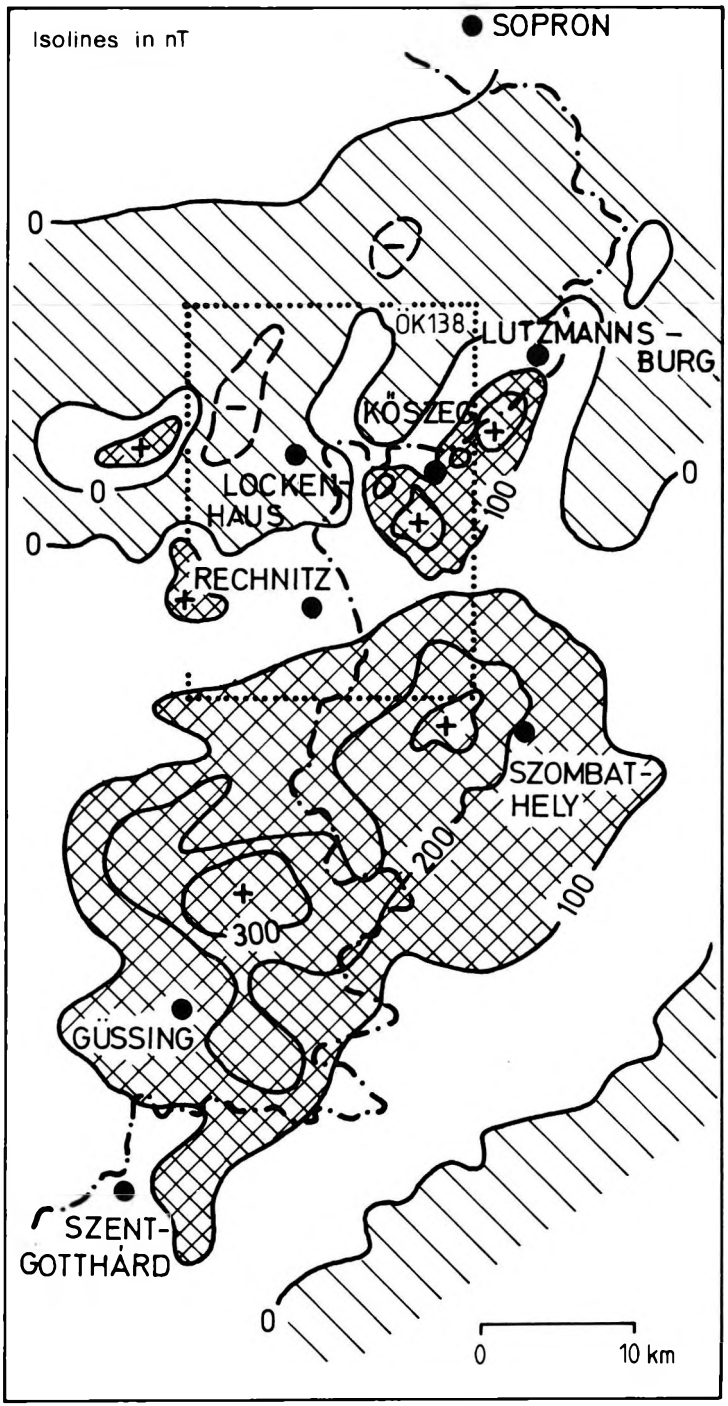
Isolines in nT
SOPRON
ÖK138
LUTZMANNS-
BURG
KŐSZEG
LOCKEN-
HAUS
RECHNITZ
SZOMBAT-
HELY
GÜSSING
SZENT-
GOTTHÁRD
0
100
200
300
0
10 km

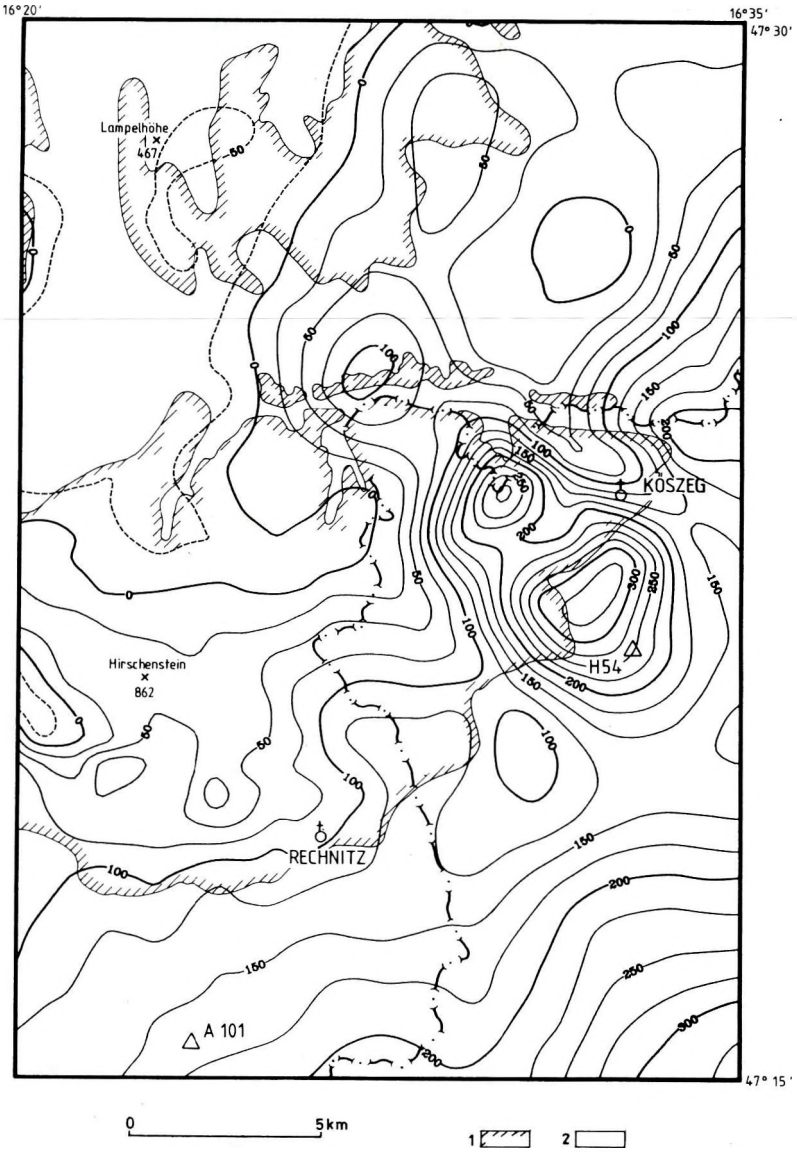

Fig. 4. Isoanomaly map of the vertical magnetic intensity, map sheet 138.
1 — basement outcrop; 2 — young sediments on the surface. Normal field:
$\delta Z/\delta\varphi = 5.13$nT/km; $\delta Z/\delta\lambda = 0.8$ nT/km. Basepoint values: A101 (Dürnbach):
$Z_{1980.0} = 42{,}413$ nT, $\delta Z = +161$ nT; H54 (Kőszegdoroszló): $Z_{1980.0} = 42{,}585$, $\delta Z = +270$ nT

4. ábra. A vertikális mágneses tér (ΔZ) izoanomália térképe, a 138-as térképlap területén
Normál tér: $\delta Z/\delta\varphi = 5{,}13$ nT/km; $\delta Z/\delta\lambda = 0{,}8$ nT/km. Alappont értékek: A101 (Dürnbach):
$Z_{1980.0} = 42.413$ nT, $\delta Z = +161$ nT; H54 (Kőszegdoroszló): $Z_{1980.0} = 42.585$ nT,
$\delta Z = +270$ nT. 1 — alaphegység-kibúvás; 2 — fiatal üledékek a felszínen

Рис. 4. Карта аномалий вертикальной компоненты магнитного ноля (ΔZ) по листу 138.
Нормальное поле: $\delta Z/\delta\varphi = 5{,}13$ нт/км, $\delta Z/\delta\lambda = 0{,}8$ нт/км. Значения в опорных пунктах:
A101 (Дюрнбах): $Z_{1980.0} = 42{,}413$ нт, $\delta Z = +161$ нт; H54 (Кёсегдоросло):
$Z_{1980.0} = 42{,}585$ нт, $\delta Z = +270$ нт
1 — выходы пород фундамента; 2 — молодые отложения на поверхности

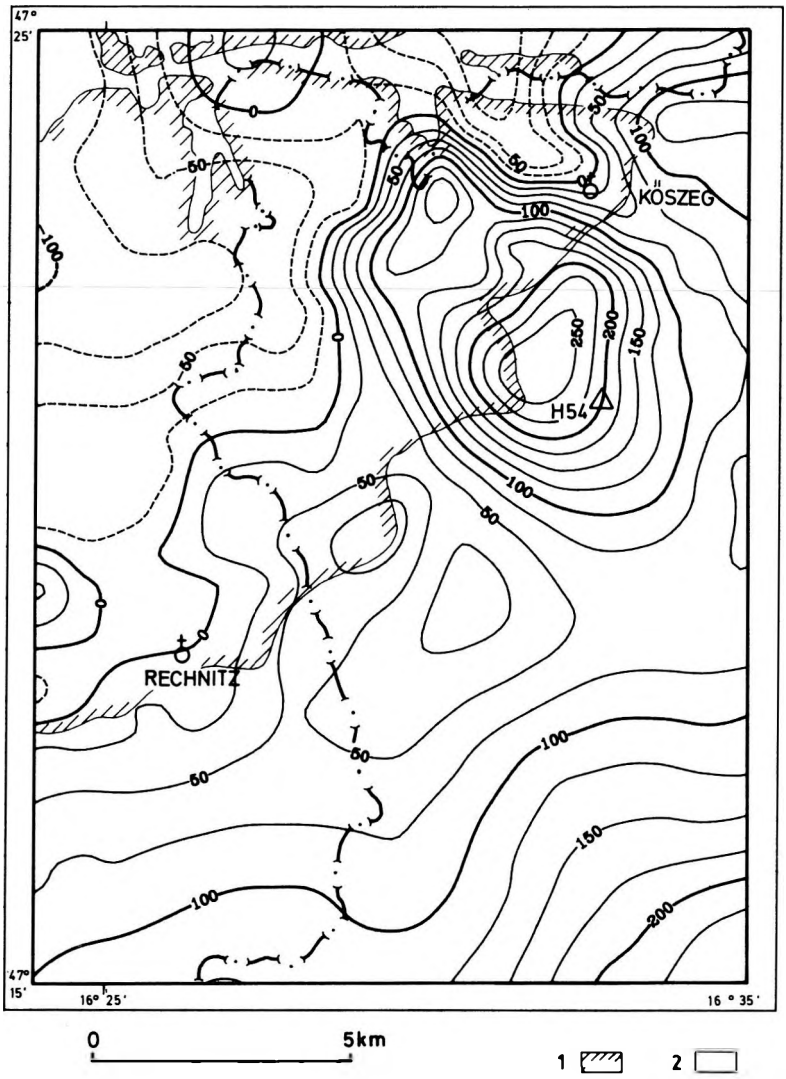

Fig. 5. Isoanomaly map of the geomagnetic total field, area of frame C in Fig. 1. Normal field: $\delta T/\delta\varphi$ = 2.51 nT/km, $\delta T/\delta\lambda$ = 0.75 nT/km. Basepoint values: H54 (Kőszegdoroszló): $T_{1980.0}$ = 47,581 nT, ΔT = +208 nT
1 — basement outcrop; 2 — young sediments on the surface

5. ábra. A totális mágneses tér (ΔT) izoanomália térképe az 1. ábrán C-vel jelzett területen. Normál tér: $\delta T/\delta\varphi$ = 2,51 nT/km, $\delta T/\delta\lambda$ = 0,75 nT/km. Alappont értékek: H54 (Kőszegdoroszló): $T_{1980.0}$ = 47.581 nT, δT = +208 nT. 1 — alaphegység-kibúvás; 2 — fiatal üledékek a felszínen

Рис. 5. Карта аномалий полного магнитного поля (ΔT) по району, обозначенному 'C' на рис. 1. Нормальное поле: $\delta T/\delta\varphi$ = 2,51 нт/км, $\delta T/\delta\lambda$ = 0,75 нт/км. Значения в опорных пунктах: H54 (Кёсегдоросло): $T_{1980.0}$ = 47,581 нт, δT = +208 нт
1 — выходы пород фундамента; 2 — молодые отложения на поверхности

North of the Lockenhaus–Kőszeg line, morphologically marked by the valley of the Güns river, the above-described eastern anomaly zone divides into two branches. With some offset from the anomaly at Kőszeg the main branch extends to the area north-east of Lutzmannsburg, where it decays [see WEBER and WALACH 1981]. The western branch runs approximately parallel to the main branch reaching the area of Oberpullendorf. The significantly lower amplitude and the flattening of the anomaly flanks of this branch mean greater depth and a small shift of the northern part of the magnetized body towards the west along an ENE line where the river Güns breaks through, east of Lockenhaus. From the regional anomaly distribution of Fig. 3 it seems that a similar north shifted element (shear body?) of the large ophiolite complex appears in the south, too.

In the NE corner of both isoanomaly maps an extended minimum zone can be seen. This is interpreted as the northern border of the ophiolites. Due to the bipolarity of the magnetic field this minimum zone (Fig. 3) is the northern accompanying minimum of the total Penninic (highly magnetized) basement complex. On the edge of the vertical intensity map (Fig. 4) the anomaly zone of the serpentinite outcrop of the Bernstein area starts just SW of Lampelhöhe.

The local anomalies on the southern flank of the Kőszeg–Rechnitz Mts. near Rechnitz area connected with the smaller serpentinite outcrops (Grosse Plischa, Budiriegel) of this area [PAHR 1980].

5. Conclusion and Acknowledgement

The results of the bilateral geomagnetic survey carried out in the border zone of Austria and Hungary proved the absolute necessity of further cooperation in the field of geophysics in order to solve the problems of geology — since geology is not concerned with state borders.

The authors wish to express their gratitude to both countries, for having permitted, promoted and covered all expenses of the joint project.

REFERENCES

FÜLÖP J. and DANK V. 1987: Geological map of Hungary without Cenozoic formations. Publication of the Hung. Geol. Survey, Budapest.

HAÁZ I. B. and KOMÁROMY I. 1966: Magyarország földmágneses térképe. A függőleges térerősség anomáliái. 1 : 500,000

KOLLER F. 1985: Petrologie und Geochemie der Ophiolite des Penninikums am Alpenostrand. Jb. Geol. Bundesanstalt **128**, pp. 83–150, Wien

KISHÁZI J. and IVANCSICS J. 1986: Bozsok Greenschist Formation. Magyarország geológiai alapszelvényei 86/166, Magyar Állami Földtani Intézet, Budapest

KRÖLL A., FLÜGEL H. W., SEIBERL W., WEBER F., WALACH G. and ZYCH D. 1988: Karten über der prätertiären Untergrund des Steirischen Beckens und der Südburgenländischen Schwelle (1 : 200,000), mit Erläuterungen. Geol. Bundesanstalt, Wien

MÁRTON E., MAURITSCH H. J. and PAHR A. 1987: Paläomagnetische Untersuchungen in der Rechnitzer Fenstergruppe. Mitt. Österr. Geol. Ges., **80**, pp. 185–205, Wien

OBERLADSTÄTTER M., WALACH G. and WEBER F. 1979: Geomagnetic measurements in the Alpine–Pannonic Boundary region. EOS–Transactions (Abstract), **60,** No. 32, Washington

PAHR A. 1960: Ein Beitrag zur Geologie des nordöstlichen Sporns der Zentralalpen. Verh. Geol. Bundesanstalt, Wien

PAHR A. 1980: Die Fenster von Rechnitz, Bernstein und Möltern. In: Der geologische Aufbau Österreichs, pp. 320–326, Springer Verlag, Wien–New York

PAHR A. 1987: Geologische Karte der Republik Österreich, Blatt 138, Rechnitz (mit Erläuterungen), 1 : 50,000, Geol. Bundesanstalt Wien

PÜHRINGER A., SEIBERL W., TRAPP E. and PAUSWEG F. 1975: Die Verteilung der erdmagnetischen Elemente in Österreich zur Epoche 1970. O. Z.–A. f. Met. u. Geodyn., Wien

SCHMIDT W. J. 1950: Überblick über geologische Arbeiten in Österreich. Z. Dt. Geol. Ges., **102,** Berlin

SCHÖNLAUB H. P. 1973: Schwamm Spiculae aus dem Rechnitzer Schiefergebirge und ihr stratigraphischer Wert., Jb. Geol. Bundesanstalt, **116,** Wien

SEIBERL W. 1978: Magnetische Modellrechenergebnisse an einem Basaltvorkommen (Pauliberg) im Burgenland. BHM, **123,** pp. 459–462, Wien

SEIBERL W. et al. 1986: Hubschraubergeophysikalische Karte der magnetischen Totalintensität, Rechnitzer Schieferinsel, 1 : 25,000, Wien (ÖAW)

SEIBERL W. 1989: Aeromagnetische Karte Steirisches Becken–Südburgenländische Schwelle, 1 : 200,000, Geol. Bundesanstalt, Wien

WALACH G. 1977: Geophysikalische Arbeiten im Gebiet des Nordostsporns der Zentralalpen I: Magnetische Traverse 1 (Neunkirchen–Hochwechsel–Pöllauer Bucht). Geol. Tiefbau der Ostalpen, Z.–A. Met. u. Geodyn., Wien

WALACH G. 1986: Bericht über die im Jahr 1985 durchgeführten Zusammenmessungen zwischen den erdmagnetischen Landesaufnahmen von Österreich und Ungarn. Unveröff. Bericht, 15 p. Leoben

WEBER F., ANTON H., HEIDINGER H., JANSCHEK H., KLAMMER W., MAURITSCH H. and WALACH G. 1975: Activities of the Institute of Petro-Geology and Applied Geophysics of the University of Mining, Leoben. In: Report of the Austrian National Committee for the International Geodynamics Projekt, 1972–1975, Wien

WEBER F., JANSCHEK H., MAURITSCH H., OBERLADSTÄTTER M., SCHMÖLLER R. and WALACH G. 1981: Activities of the Institute of Geophysics of the University of Mining, Leoben. In: Austrian Investigations in the International Geodynamics Projekt 1972–1979, BMfWF, Wien

WEBER F. and WALACH G. 1981: Gravimetrische und magnetische Detailmessungen der seichten Teile des Südburgenländischen Beckens und seiner kristallinen Umrahmung. Geophysik der Erdkruste (Projekt BA 10), unveröff. Endbericht 1980, ÖAW, Wien

WEBER F. and WALACH G. 1986–88: Bodenmagnetische Detailuntersuchungen im Südburgenland und im österreichisch–ungarischen Grenzgebiet. Geophysik der Erdkruste (Projektgruppe BC–2e), unveröff. Endberichte 1985–1987, ÖAW, Wien

WIESENEDER H. 1932: Studien über die Metamorphose im Altkristallin des Alpenostrandes. Min. Petr. Mitt., N. F. **42,** Leipzig

FÖLDMÁGNESES KUTATÁS AZ OSZTRÁK–MAGYAR HATÁRZÓNÁBAN A KŐSZEGI HEGYSÉG TERÜLETÉN

HOFFER Egon, SCHÖNVISZKY László és Georg WALACH

1985-től 88-ig az Eötvös Loránd Geofizikai Intézet és a Leobeni Bányászati Egyetem közös terepi csoportja az osztrák–magyar határ mentén földmágneses (ΔT és ΔZ) méréseket végzett. Jelen cikkben a 138-as (Rohonc) osztrák topográfiai térképlap földmágneses térképeit és értelmezésüket ismertetjük. Az izoanomália térképeken bemutatott eredményeket összehasonlítva a szuszceptibilitás eloszlással azt találjuk, hogy a pennini szerpentinitek helyi metagabbró, ophikalcit és kékpala előfordulásokkal a mágneses hatók. Ezért a jellegzetes földmágneses anomáliakép kvalitatíve úgy értelmezhető, mint a pennini ofiolit komplex terjedésének indikátora a Kőszeg–Rohonci hegység keleti részén.

МАГНИТОРАЗВЕДКА В ЗОНЕ АВСТРИЙСКО-ВЕНГЕРСКОЙ ГРАНИЦЫ В КЁСЕГСКО-РЕХНИЦСКИХ ГОРАХ

Эгон ГОФФЕР, Ласло ШЕНВИСКИ, Георг ВАЛАХ

В 1985–1988 годы совместной полевой партией Венгерского Геофизического института им. Л. Этвеша и Леобенского Горного института вдоль австрийско-венгерской границы выполнялась магниторазведка с измерением ΔT и ΔZ. В настоящей статье представляюстя геомагнитные карты по листу 138 (Рехниц) австрийской номенклатуры и их интерпретация. Путем сопоставления результатов, сведенных на картах аномалий, с магнитной восприимчивостью горных пород можно найти, что магнитовозмущающими телами являются пеннинские серпентиниты с локальными проявлениями метагаббро, офикальцитов и голубых сланцев. Поэтому характерные магнитные аномалии в восточной части Кёсегско-Рехницких гор могут быть качественно интерпретированы как индикаторы распространения пеннинских офиолитов.

GEOPHYSICAL TRANSACTIONS 1991
Vol. 36. No. 1–2. pp. 81–92

RESISTIVITY AND IP PARAMETERS USED FOR HYDROGEOLOGIC PURPOSES AND DIFFERENTIATION BETWEEN NONMETALLIC MINERALS*

József DUDÁS[+], Erich NIESNER[++], László VERŐ[+]

Some unusual applications of the IP method are discussed. Frequency domain resistivity and IP measurements were carried out over nonmetallic mineral deposits in Austria and East Germany. Because of the simple geologic models the parameters obtained can be considered — at least approximately — as in situ ones.

Time domain resistivity and IP measurements were carried out for hydrogeologic purposes in Hungary. In sedimentary sequences correlation between resistivity and IP values obtained from surface measurements varies from place to place. Numerous surface and in-hole measurements demonstrated that variations in the ϱ_a–P_a values are connected with lithological changes. Using a carefully designed crossplot a third parameter can be determined from the ϱ_a–P_a values: grain size, referring to lithology. Lithological maps corresponding to different depth intervals can be constructed from these values providing basic hydrogeological information on the area.

Keywords: IP, resistivity, water prospecting, nonmetallic minerals, geoelectric survey, in-hole measurements

1. Introduction

The induced polarization method is mainly used in ore prospecting. Improvements achieved in measurements accuracy and reliability, and a broader choice of measurable IP parameters have enabled us to solve tasks that earlier seemed to be hopeless. From this perspective reliable measurement of very low — only a few per cent or even less — polarizability of PFE values, measurement of rapid decay curves or effects appearing at relatively high frequencies only, and curve shape analysis are some of the most important results. Another Austro–Hungarian paper dealing with these questions can be found in this volume [AIGNER and DRASKOVITS 1991].

The aim or dream of geophysicists involved in electrical methods is to differentiate between buried geologic formations based on their geoelectric parameters measured from the surface. The feasibility of this has significantly been improved by developments in field techniques; the basis for any kind of differentiation can be established by experiments, laboratory investigations or in situ measurement of the parameters characterizing different rocks.

* Paper presented at the 49th EAEG Meeting, Belgrade, 1987
[+] Eötvös Loránd Geophysical Institute of Hungary, H–1440 Budapest, POB 35, Hungary
[++] Institute of Geophysics, Mining University, Leoben, Franz-Josef Street 18, A–8700, Leoben, Austria
Manuscript received (revised version): 5 November, 1990

2. Electric parameters of nonmetallic minerals

First the geoelectrical properties — resistivity and induced polarization parameters — obtained by surface measurements over some unusual, nonmetallic IP targets will be discussed. These measurements were carried out in Austria and East Germany with a Phoenix IPV–3 receiver and a 3 kW transmitter. In most cases a dipole-dipole array with an electrode separation between 1 and 10 m was used, from $n=1$ to $n=6$; some measurements were also made with a gradient array. The frequency domain IP parameter determined with high accuracy was the PFE value between 0.25 and 4 Hz.

Geologic models of the investigation sites can be considered as simple ones. Thus the parameters are influenced only by the formation in question: the effect of other rocks and inhomogeneities can be neglected. We assumed that the measured apparent resistivities and polarizabilities were very near to the intrinsic values. Obviously, many factors of varying importance are neglected in such qualitative interpretations. But parameters characterizing different rocks are never discrete values: they are, rather, a narrow or even wide range of values. This range might become wider than the real one if results of such measurements and interpretation are used, i.e. partly in situ, partly apparent parameters. Trends in the resistivity-polarizability crossplots might become obscure. When crossplots are used for differentiation or geologic interpretation, these features should be remembered. In *Fig. 1* such a resistivity – PFE (polarizability) crossplot is shown.

Some words about the sites, with emphasis on the rock types discussed in the second part of the paper (the numbers refer to Fig. 1).

Gravel at a location south of the Alps (1) has very low PFE values; the highest is about 0.3%. Depending on water saturation, the resistivity varies between 200 and 1000 Ωm.

If the gravel is mixed with sand and clay, such as in a Quaternary deposit in Southern Styria (2), the resistivity range is lower (between 50 and 100 Ωm), but the polarizability is higher (between 2 and 3%).

In Regis, East Germany (3), very high PFE values (up to 30%) were measured in an open pit mine. The Upper Eocene – Lower Miocene coal is underlain by a layer of mud or silt contaminated with coal. The resistivity of this layer is about the same as that of the coal — 30–50 Ωm — the PFE values, however, are definitely higher.

Different clay types show a wide variety of electric parameters. Kaolinite at Kriechbaum (4) is of low resistivity and polarizable, PFE values lie between 10 and 13%. Another kaolinite deposit, at Mallersbach (5), is more resistive — 50–100 Ωm — and less polarizable, 1–5%.

Bentonite (6) has resistivities from 30 to 50 Ωm and PFE values up to 5%. From sample measurements a direct proportionality was obtained between montmorillonite content and PFE values.

Clay at Stoob (7) has moderate resistivities but rather low, less than 2%, PFE values.

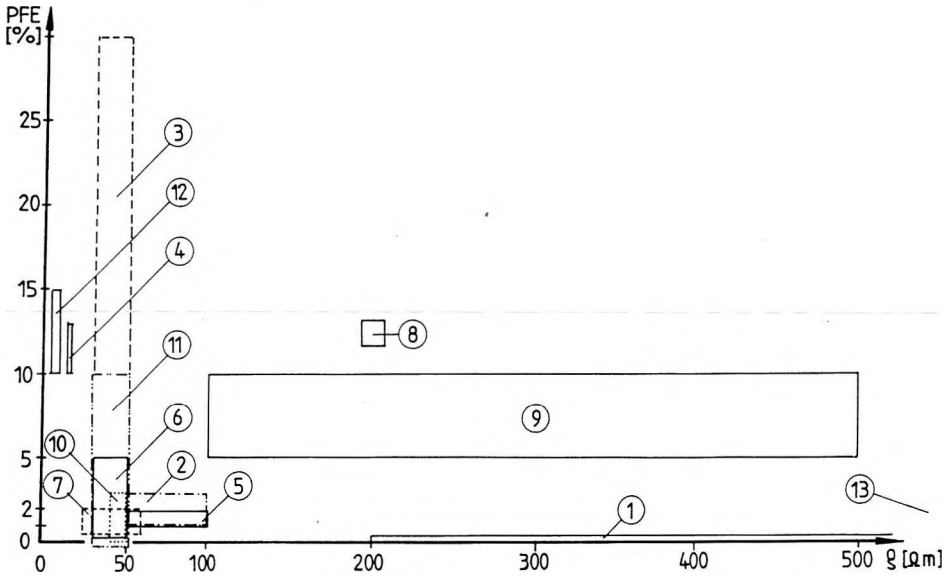

Fig. 1. ϱ_a–PFE crossplot for some nonmetallic minerals in Austria and East Germany
1 — gravel (Bodenbauer); 2 — sand + gravel + clay (Großsteinbach); 3 — silt + coal (Regis); 4 — kaolinite (Kriechbaum); 5 — kaolinite (Mallersbach); 6 — bentonite; 7 — clay (Stoob); 8 — coal (Sollenau); 9 — coal (Langau); 10 — coal (Profen); 11 — coal (Regis); 12 — infusorial earth (Aflenz); 13 — gypsum (Preinsfeld)

1. ábra. ϱ_a–PFE diagram néhány ausztriai és kelet-németországi nem-fémes ásványra
1 — kavics (Bodenbauer); 2 — homok + kavics + agyag (Großsteinbach); 3 — kőzetliszt + szén (Regis); 4 — kaolinit (Kriechbaum); 5 — kaolinit (Mallersbach); 6 — bentonit; 7 — agyag (Stoob); 8 — szén (Sollenau); 9 — szén (Langau); 10 — szén (Profen); 11 — szén (Regis); 12 — diatomit (Aflenz); 13 — gipsz (Preinsfeld)

Рис. 1. Диаграмма ϱ_a–PFE по некоторым нерудным минералам из Австрии и Восточной Германии
1 — галечник (Боденбауэр); 2 — песок + галька + глина (Гросштейнбах); 3 — алеврит + уголь (Регис); 4 — каолинит (Крихбаум); 5 — каолинит (Маллерсбах); 6 — бентонит; 7 — глина (Штоб); 8 — уголь (Золленау); 9 — уголь (Лангау); 10 — уголь (Профен); 11 — уголь (Регис); 12 — диатомит (Афленц); 13 — гипс (Прайнсфельд)

Summarizing the trends of resistivity and PFE values we may say that gravel has the highest resistivity and lowest polarizability; resistivity decreases towards finer grain sizes, while polarizability has a maximum at the grain size corresponding to silt or mud. Clays have low to moderate resistivites, and their polarizability covers a wide range. Similar trends in parameters of other nonmetallic minerals cannot be recognized.

Measurements were carried out over three coal deposits. At Sollenau (8), in the southern part of the Vienna Basin the Upper Miocene low quality clayey brown coal has a sulphur content of 2.2%, and the ash content is 43%. It can be characterized by high PFE and moderate resistivity values.

The resistivity of the Lower Miocene low quality brown coal at Langau (9), Northern Austria, varies between 100 and 500 Ωm, its PFE is between 5 and 10%.

The Upper Eocene – Lower Miocene coals at Profen (10) and Regis (11), East Germany, have lower resistivities — 30–50 Ωm — and, on average, lower PFE values as well. It would be too early to speak about any definite relationship between the geophysical and geologic parameters.

The two extremes in the figure are: an infusorial earth or diatomite deposit at Aflenz, Austria (12), has the lowest resistivity (5–20 Ωm) and the highest PFE (10–15%) except for the silt layer underlying the coal at Regis (3). Gypsum at Preinsfeld, Austria (13), on the other hand, is the most resistive (600–700 Ωm) and least polarizable.

Although such a crossplot might be of interest in itself, in the second part of our paper we make another step forward. An attempt to use these and many other data to translate geophysical parameters into the language of hydrogeology will be discussed.

3. The utilization of electric parameters in hydrogeology

It is true in Hungary and in the time domain too, that gravel, pure sand, different mixtures of sand and clay, and pure clay have different resistivities and polarizabilities — similarly to the results shown in Fig. 1. Polarizability of these unconsolidated sediments depends, inter alia, on the grain size, fluid saturation and pore fluid salinity, type of dissolved ions and concentration ratio of ions. For the most common ions up to ion concentration of 3 g per litre there is only a slight change in polarizability, while at concentrations higher than this limit polarizabilities are very low and independent of other parameters. Resistivity depends on the same factors, but in a different way, see *Fig. 2.* This diagram was constructed on the basis of published data [Lipskaya and Ryapolova 1970], as well as field and laboratory measurements carried out in Hungary. In these measurements, soundings with gradient array, ELGI's time domain resistivity and IP systems — DIAPIR — were used with a 4 kW transmitter. The IP parameter is the polarizability, measured with a delay time of 0.125 s. Extreme and mean values of two electric parameters, resistivity and polarizability, are plotted as a function of grain size.

It can be seen that resistivity increases continuously with increasing grain size (i.e. porosity), while polarizability reaches a maximum at grain size corresponding to silt and fine sand. A very similar trend was observed in the frequency domain for selected sediments, from gravel to clay, as shown in Fig. 1. This diagram cannot directly be used in practice for grain size determination because of the implicit effect of salinity. Further assumptions and experimental results are needed.

In the Eötvös Loránd Geophysical Institute of Hungary the relationship between resistivity and polarizability of sediments has been studied for a long

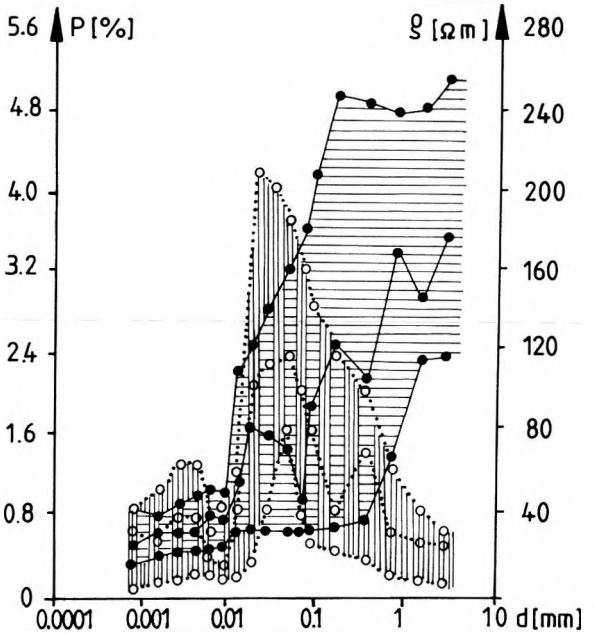

Fig. 2. Connection between resistivity, polarizability and grain size of unconsolidated sediments. Extreme and mean values in the literature and obtained from field and laboratory measurements are plotted. Filled circles: resistivity; empty circles: polarizability values.

2. ábra. Kapcsolat az ellenállás, a polarizálhatóság és a szemcseméret között, laza üledékekre. Az irodalomban közölt, valamint terepi és laboratóriumi mérésekből kapott szélsőértékeket és átlagokat ábrázoltuk. Betöltött körök: ellenállás; üres körök: gerjeszthetőség értékek

Рис. 2. Взаимосвязь между сопротивлением, поляризуемостью и зернистостью в рыхлых отложениях. Представлены экстремальные и средние значения по литературным данным, а также по результатам полевых и лабораторных измерений. Залитые кружки — сопротивления, полые кружки — поляризуемость

time. On a crossplot of resistivity and polarizability values obtained from in-hole measurements, points representing layers of similar composition cluster in separate parts of the crossplot, as can be seen in *Fig. 3* [Draskovits and Новот 1983]. This means that in different parts of Hungary where the sandy–clayey sedimentary complex is thick, these loose sediments are not dry but water saturated and the salinity is low. Thus ϱ_a and P_a values depend first of all on grain size. Because of the effect of other parameters a range of ϱ_a and P_a values belongs to a given grain size; within the saturation limits existing in our investigations the combinations ϱ_{min} and P_{max}, ϱ_{max} and P_{min} are the corresponding value pairs. For this simplified but not very special case the diagram shown in Fig. 2 can be transformed to the nomogram shown in *Fig. 4*. With the use of this diagram a dominant or apparent grain size can be determined from the measured ϱ_a–P_a values.

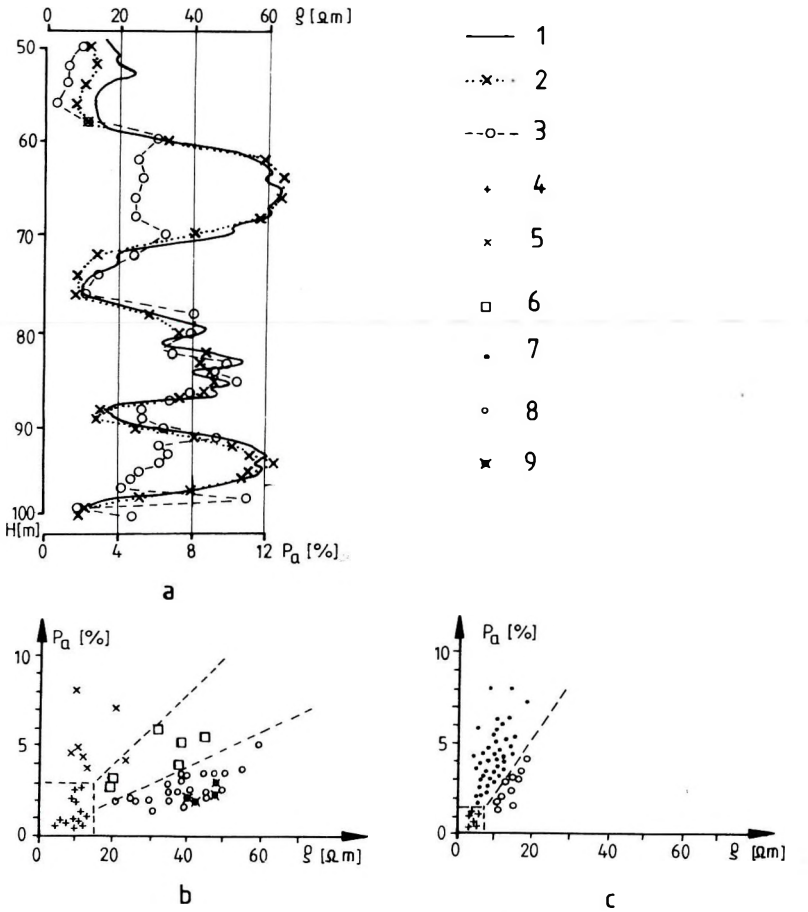

Fig. 3. Results of in-hole resistivity and IP measurements.
a) Comparison of stationary measurements with well-logging.
Resistivity-polarizability crossplots obtained
b) in a favourable and c) in a less favourable part of an alluvial cone.
1 — resistivity log; 2 — stationary resistivity measurements; 3 — stationary IP measurements;
4 — clay; 5, 7 — sandy clay; 6 — silt, fine grained sand; 8 — sand; 9 — sandy gravel

3. ábra. Lyukbeli ellenállás és GP mérések eredményei
a) Pontonkénti és folyamatos szelvényezés összehasonlítása
b) és c) Ellenállás – gerjeszthetőség diagramok egy törmelékkúp kedvező és kevésbé kedvező részéről
1 — ellenállás szelvény; 2 — pontszerű ellenállás mérések; 3 — pontszerű GP mérések;
4 — agyag; 5, 7 — homokos agyag; 6 — kőzetliszt, finomszemű homok; 8 — homok;
9 — homokos kavics

Рис. 3. Результаты скважинных измерений сопротивления и поляризуемости
а) Сопоставление результатов точечных и непрерывных профильных измерений
b) и c) Диаграммы сопротивление–поляризуемость по благоприятному и менее благоприятному участкам конуса выноса
1 — профиль сопротивления; 2 — точечные измерения сопротивления; 3 — точечные измерения вызванной поляризации; 4 — глины; 5, 7 — песчанистые глины;
6 — алевриты, тонкозернистые пески; 8 — пески; 9 — гравийники

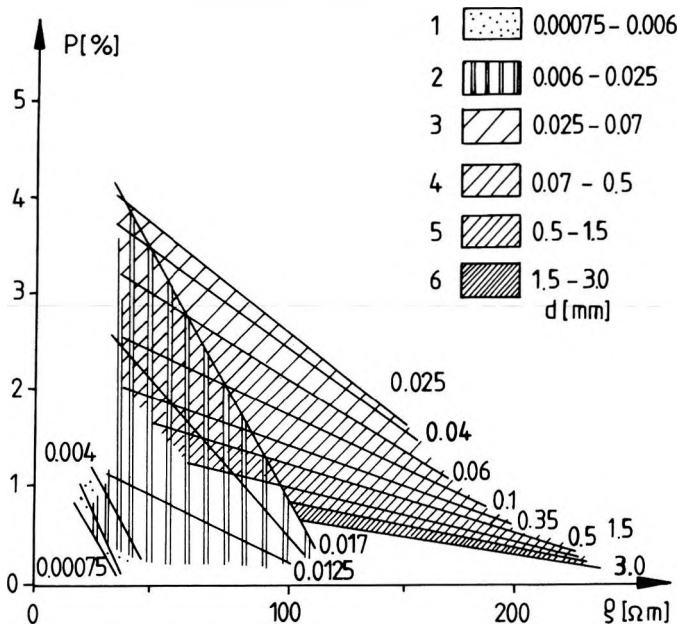

Fig. 4. Nomogram for dominant or apparent grain size determination using resistivity (ϱ_a) and polarizability (P_a) data (parameter: grain diameter in mm)
Grain size of sediments: clay 0.00075–0.006, silt 0.006–0.025, fine sand 0.025–0.07, medium grained sand 0.07–0.5, coarse sand 0.5–1.5, sandy gravel 1.5–3.0

4. ábra. Az uralkodó vagy látszólagos szemcseméret meghatározására szolgáló nomogram az ellenállás (ϱ_a) és gerjeszthetőség (P_a) felhasználásával (paraméter: szemcseátmérő mm-ben). Szemcseátmérők közettani megfelelői: agyag 0,00075–0,006, közetliszt 0,006–0,025, finom homok 0,025–0,07, közepes szemcséjű homok 0,07–0,5, durva homok 0,5–1,5, homokos kavics 1,5–3,0

Рис. 4. Номограмма для определения преобладающей или кажущейся зернистости с использованием сопротивления (ϱ_a) и поляризуемости (P_a) (параметр: диаметр зерен в мм). Литологические эквиваленты размеров зерен в мм: глина — 0,00075 – 0,006, алеврит — 0,006–0,025, тонкий песок — 0,025–0,07, среднезернистый песок — 0,07–0,5, грубый песок — 0,5–1,5, гравий — 1,5–3,0

Lithologic logs of wells obtained from the ϱ_a–P_a values and by other methods agreed closely. Two problems should be mentioned: if other polarizable materials, first of all pyrite, can be found in the sediments, the nomogram should not be used. In some cases very fine-grained pyrite increased the polarizability of pure sand to 5–6%. The effect of organic materials, e.g. coal, can be similar. Unambiguous determination of silt itself is always difficult because of the overlapping values of the parameters as shown in Fig. 4.

The next logical step in the development of a combined geoelectric method for ground-water prospecting is the use of ϱ_a and P_a values obtained from surface surveys. The usefulness of these parameters in locating water wells has been demonstrated in other parts of Hungary too [Draskovits and Hobot 1983]. As simultaneous study of two or three maps — e.g. resistivity, polarizabil-

ity and thickness — is not convenient, it would be desirable to combine the information from the individual maps into a single map or section. This can be performed by using the nomogram of Fig. 4 and the measured ϱ_a–P_a values. The results of the process can be plotted in different ways. These are demonstrated using the results of a reconnaissance survey in northwestern Hungary.

The measured ϱ_a and P_a data, or interpreted parameters (e.g. layer resistivities) are generally plotted in the form of maps. In our case cross sections and maps of average resistivity and apparent polarizability were constructed. In *Fig. 5* three forms of section display are presented. The top section (a) divides the sediments of the uppermost 100 m into four intervals and represents the average lithology by the given key. The medium section (b) shows the weighted averaged lithology, while the bottom one is a conventional geoelectric section. The averaged section is constructed from the apparent grain size values in the four depth intervals weighted by the thickness of these intervals. Similarly to these sections a summarized lithologic map, or map of the dominant grain size can be constructed. Such a map is shown in *Fig. 6*. The maximum depth to which this kind of hydrogeologic interpretation can be applied is determined by the available IP values. The largest AB separation used for IP measurements was 800 m. From the viewpoint of ground-water prospecting the thickness of the water-bearing layers is the other important parameter. It would be possible to include the thickness in the interpretation too and to calculate some kind of combined parameter, e.g. favourability. In our opinion, however, it is better to study these two kinds of maps — a lithologic map and a thickness map — separately. These together provide a good basis for locating water wells.

The geologic formations distinguished on the lithologic map are given in Table I. with the resulting hydrogeologic characteristics.

It can be explained by deposition conditions that areas of the most favourable hydrogeologic characteristics and greatest thickness of water-bearing formations coincide.

4. Conclusions

Frequency domain measurements in Austria and East Germany revealed the usefulness and limitations of the IP method in investigating nonmetallic minerals. A qualitative relationship between resistivity, PFE and grain size was found. A similar relationship based on a large data set can be considered as quantitative for Quaternary sediments in Hungary. This explains why the combined use of resistivity and polarizability values for hydrogeological characterization of the Quaternary sediments has proved successful. It is mentioned, however, that the basis for transformation of geophysical parameters ϱ_a and P_a — or any other IP parameter — to a hydrogeologic feature — grain size, sediment type or permeability — is experimental, therefore it should be checked prior to application on geologically different areas.

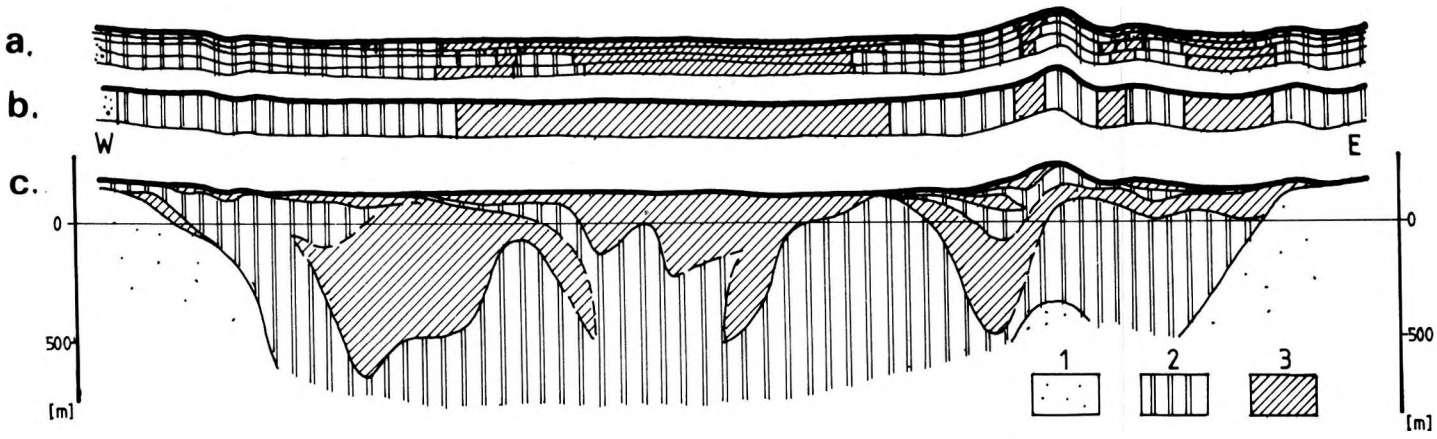

Fig. 5. Section display of geoelectric parameters
a) Four lithologic intervals constructed from ϱ_a and P_a values
b) Weighted average lithology section obtained from a).
c) Geoelectric section along the E–W profile shown in Fig. 6
1 — clay; 2 — silt; 3 — sand and sandy gravel

5. ábra. Geoelektromos paraméterek szelvényszerű ábrázolása
a) ϱ_a és P_a értékekből szerkesztett négy litológiai intervallum
b) a)-ból súlyozott összegzéssel kapott litológiai szelvény
c) Hagyományos geoelektromos szelvény a 6. ábrán jelölt K–Ny-i szelvény mentén
1 — agyag; 2 — kőzetliszt; 3 — homok, homokos kavics

Рис. 5. Представление геоэлектрических параметров в виде профиля
а) четыре литологических интервала, составленные по значениям ϱ_a и P_a
b) литологический профиль, полученный из а) путем суммирования по весам
c) Традиционный геоэлектрический разрез по широтному профилю, обозначенному на рис. 6
1 — глины; 2 — алевриты; 3 — пески и гравийники

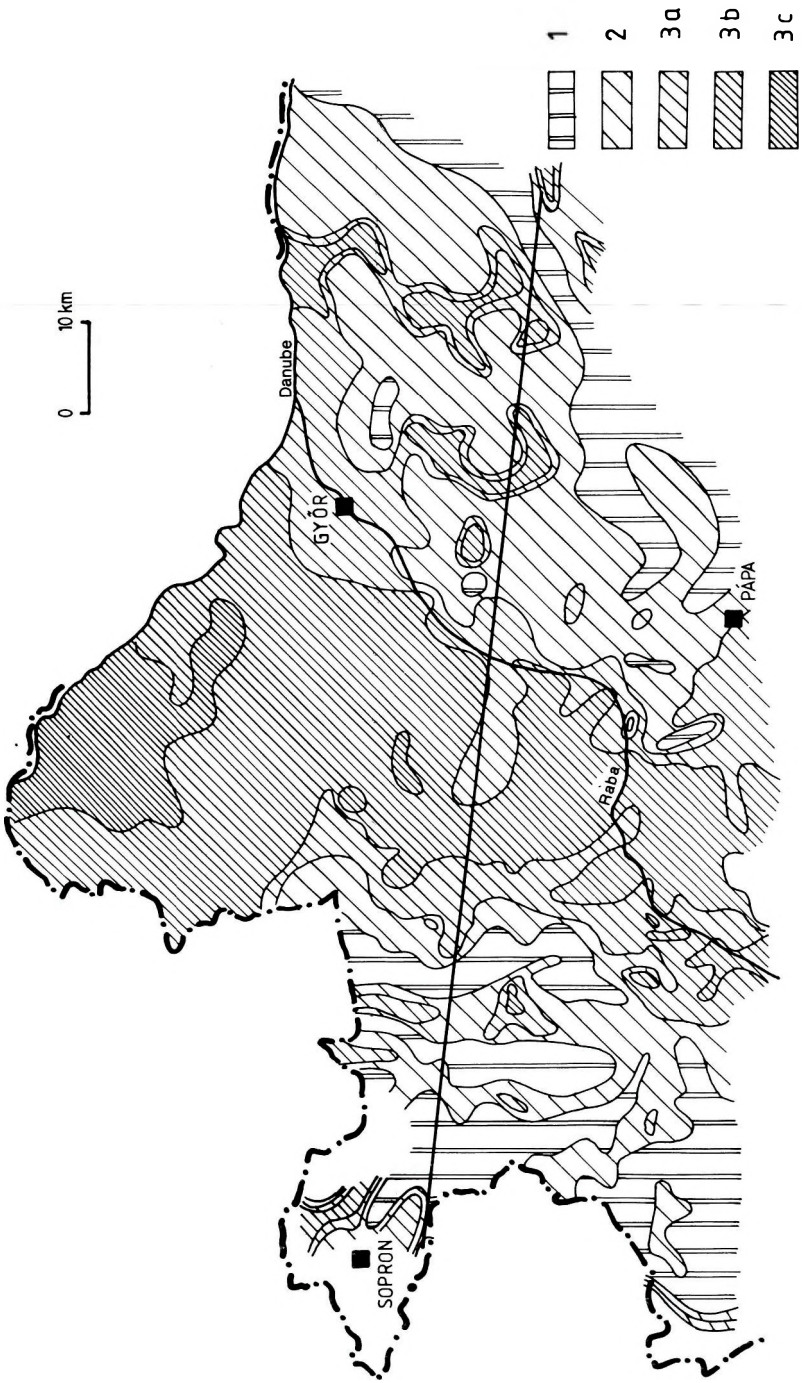
1
2
3a
3b
3c
0
10 km
Danube
GYŐR
PÁPA
Rába
SOPRON

Fig. 6. Lithologic map of the sediments down to 150 m (for explanation see Table I)

6. ábra. Az üledékek litológiai térképe 150 m mélységig (jelmagyarázatot lásd az I. táblázatban)

Рис. 6. Литологическая карта до глубины 150 м (условные обозначения см. в табл. I)

	Resistivity	Polarizability	Rock type	Characteristics
1	low	low to high	clay to silt	unfavourable to weak
2	medium	medium	clay to fine sand	medium
3	a higher than medium	lower than medium	fine sand to sand	favourable
	b high	low	sand to gravel	excellent
	c high	varying	?	favourable

Table I.

I. Táblázat.

Таблица I.

REFERENCES

see AIGNER E., DRASKOVITS P. (in this volume)

DRASKOVITS P., HOBOT J. 1983: Geophysical exploration of the alluvial cone of River Maros. *in:* Annual Report of the Eötvös Loránd Geophysical Institute of Hungary for 1982, Budapest, pp. 191–192

LIPSKAYA A. E., RYAPOLOVA V. A. 1970: Application of induced polarization method in engineering geologic studies. *in:* Application of geophysical methods in hydrogeologic and engineering geologic investigations (in Russian) pp. 30–37, Moscow

ELLENÁLLÁS ÉS GP PARAMÉTEREK FELHASZNÁLÁSA HIDROGEOLÓGIAI CÉLOKRA ÉS NEM-FÉMES ÁSVÁNYOK MEGKÜLÖNBÖZTETÉSÉRE

DUDÁS József, Erich NIESNER és VERŐ László

A GP módszer néhány szokatlan felhasználását tárgyaljuk. Frekvencia tartománybeli ellenállás- és GP méréseket végeztünk nemfémes ásványtelepeken Ausztriában és Kelet-Németországban. Az egyszerű földtani modellek miatt a kapott paraméterek közelítőleg in situ értékeknek tekinthetők.

Hidrogeológiai célból időtartománybeli ellenállás és GP méréseket végeztünk Magyarországon. Üledékes sorozatokban a felszíni mérésekből kapott ellenállás- és GP értékek közti korreláció területenként változó. Számos felszíni és lyukbeli mérés igazolta, hogy a ϱ_a–P_a értékek változása a litológiai változásokkal van kapcsolatban. Egy gondosan megszerkesztett crossplot felhasználásával egy harmadik paramétert lehet meghatározni a ϱ_a–P_a értékekből, a litológiával kapcsolatos szemcseméretet. Ezen paraméter alapján különböző mélységintervallumokra lehet litológiai térképeket szerkeszteni, amelyek hidrogeológiai információt adnak a területről.

ПРИМЕНЕНИЕ ПАРАМЕТРОВ СОПРОТИВЛЕНИЯ И ВЫЗВАННОЙ ПОЛЯРИЗАЦИИ ДЛЯ РЕШЕНИЯ ГИДРОГЕОЛОГИЧЕСКИХ ЗАДАЧ И ДЛЯ ОПРЕДЕЛЕНИЯ НЕРУДНЫХ МИНЕРАЛОВ

Йожеф ДУДАШ, Эрих НИЗНЕР, Ласло ВЕРЁ

Рассматриваются некоторые необычные области применения метода вызванной поляризации. Измерения сопротивления и вызванной поляризации в частотном диапазоне были выполнены на месторождениях нерудных полезных ископаемых в Австрии и Восточной Германии. В связи с простотой геологического строения полученные параметры могут рассматриваться как приблизительно совпадающие с таковыми в массиве.

Для решения гидрогеологических задач в Венгрии были выполнены измерения сопротивления и вызванной поляризации во временном диапазоне. Корреляция между значениями сопротивления и вызванной поляризации, полученная при наземных измерениях на осадочных толщах, меняется от участка к участку. Многочисленными наземными и скважинными измерениями подтверждено, что изменение значений ϱ_a–P_a связано с литологической изменчивостью. На основании тщательно разработанной прямоугольной диаграммы по значениям ϱ_a–P_a можно определить и третий параметр — зернистость, характеризующую литологические особенности. На базе этого параметра можно составить литологические карты по различным интервалам глубин, дающие гидрогеологическую информацию по площади работ.

GEOPHYSICAL TRANSACTIONS 1991
Vol. 36 No. 1-2. pp. 93-102

IP METHOD AS A MEANS OF IMPROVING THE SITING OF WATER WELLS

Heinrich AIGNER* and Pál DRASKOVITS**

In order to determine the optimum sites for drilling water wells, the IP method was used combined with a resistivity survey. Initially resistivity and polarizability characteristics of recent river sediments of different grain size were studied by laboratory model measurements. Interpretation of field data was based on these laboratory results. In order to support the interpretation of field measurements, in-hole resistivity and IP measurements (both in the time- and frequency domain) were carried out. For this purpose the instruments had to be adapted to borehole conditions. In a water prospecting project in SE-Hungary, the quantity and distribution of porous formations were determined qualitatively. These data were later checked by test pumping. On this basis in alluvial basins the best water-bearing formations can be expected in areas characterized by high resistivity and low or medium polarizability.

Keywords: IP-method, water prospecting, water wells, resistivity, polarizability, sand reservoir

1. Introduction

In hydrogeologic investigations of clastic sediments the sand/shale ratio is of prime importance as high permeability zones can only be expected in areas of high sand content. In water supply projects the various resistivity methods are generally used as the leading geophysical method. The limitations of the dc methods become obvious when sand and different sand–clay mixtures have similar resistivities. Therefore it is necessary to find another geoelectric method which, without considerably increasing the costs, might help to solve the problems. Judging from the technical literature, induced polarization might be the method sought [AIGNER 1986, BERTIN and LOEB 1976, BODMER et al. 1968, NIESNER and WEBER 1985].

In sedimentary rocks, at the phase boundary between the matrix and the electrolyte, there is a state of equilibrium (electric neutrality). If a current is turned on (or off), this equilibrium of charges breaks down and polarization phenomena occur. The amplitude, frequency and phase characteristics of this polarization are utilized in the induced polarization method [AIGNER 1986, KELLER and FRISHKNECHT 1970].

There are two ways to measure the IP effects. In time-domain measurements, direct current is passed into the ground and in a certain time it is interrupted. The current can be turned off practically instantaneously whereas the decay of potential between the electrodes is a relatively long process. Time-domain IP measurements mean the analysis of this decaying potential.

* Forschungsgesellschaft Joanneum, Roseggerstrasse 17, A–8700 Leoben, Austria
** Eötvös Loránd Geophysical Institute of Hungary, Budapest, POB 35, H–1440, Hungary
Revised version of a paper presented at the 49th EAEG Meeting in Belgrade, 1987

In frequency-domain measurements, charging is effected by ac current and the resistivity of the rocks (the amplitude of the potential) and the phase shift between the charging current and the measured potential will be studied as a function of the frequency.

The work was carried out co-operatively, the basis for co-operation — between Joanneum (Leoben, Austria) and ELGI (Budapest, Hungary) — being provided by the former's expertise in frequency-domain IP, while the latter's in time-domain IP. ELGI had, in 1982, completed a large water supply project when the idea for co-operation in using the IP method in hydrogeological problems arose. In that the results were available of a 4-year systematic VES + IP (time-domain) survey together with the pumping tests of the subsequent drilling project [DRASKOVITS et al. 1990], an ideal test area was at hand for comparing different methods.

2. Instrumentation

Induced polarization has been the leading method in ore prospecting for about 25 years. The possibility of using the method for other purposes was opened up by the development of the instruments [KELLER and FRISHKNECHT 1970, SUMNER 1976, VACQUIER et al. 1957] increasing their accuracy significantly, first of all by introducing the microprocessor technique. In the 1980s a large amount of IP measurements were carried out both in the field and in the laboratory [DRASKOVITS 1986, KELLER and FRISHKNECHT 1970, LIPSKAYA and RYAPOLOVA 1970, ROY— ELLIOTT 1980]. Several attempts were made to extend the method to in-hole measurements which resulted in further problems mainly of a technical nature (e.g. electromagnetic coupling through the cable, or limitations caused by the small hole diameter and large depths, etc.) [DRASKOVITS 1986, WEBSTER 1986]. In the first stage of Austrian–Hungarian co-operation, field and laboratory measurements were carried out in the time domain, and in-hole measurements were performed both in the time and frequency domains.

For time domain measurements the DIAPIR–18 resistivity and polarizability equipment (ELGI, Budapest) was used. It samples the first 1.5 s of the decay curve in 100 ms steps, and uses longer sampling intervals for the time range up to 30–40 s. The length of the current pulses can be varied in accordance with the formula $T = 1.6 \times 2^k$ s where $k = 0, 1, 2, \ldots, 9$.

For frequency domain measurements the instrument (Joanneum, Austria) contains a sine generator which produces current pulses of varying frequency; these pulses are converted to dc by a potential-to-current transformer. The measured potentials reach a two-phase lock-in analyser where the potential synchronized to the frequency is filtered and its amplitude and phase related to the charging current are determined. The instrument operates in the 0.1–10,000 Hz frequency range.

It must be underlined that the above instruments are not well loggers.

Either the standard field units are connected to the sondes or they are modified to some extent (e.g. built-in preamplifier), and standard well-logging winches, depth indicators, etc. are used.

3. Model studies

For model measurements Danube sand was used. By passing the sand through a series of sieves, different grain size samples were obtained (0.63–0.32 mm, 0.32–0.20 mm, 0.2–0.1 mm, 0.1–0.06 mm). They were saturated with fresh water and with a solution of NaCl of various concentrations. The resistivity and polarizability curves (100 ms after turn-off) for fresh and brackish water (0.01 n NaCl) saturation are presented in *Fig. 1*. This shows, in agreement with published data, that

— whereas resistivities of different grain size fractions differ slightly, their polarizabilities show considerable differences;

— the best conditions for high polarizability (first of all for electrolytic polarization) occur in the grain size fraction below 0.1 mm.

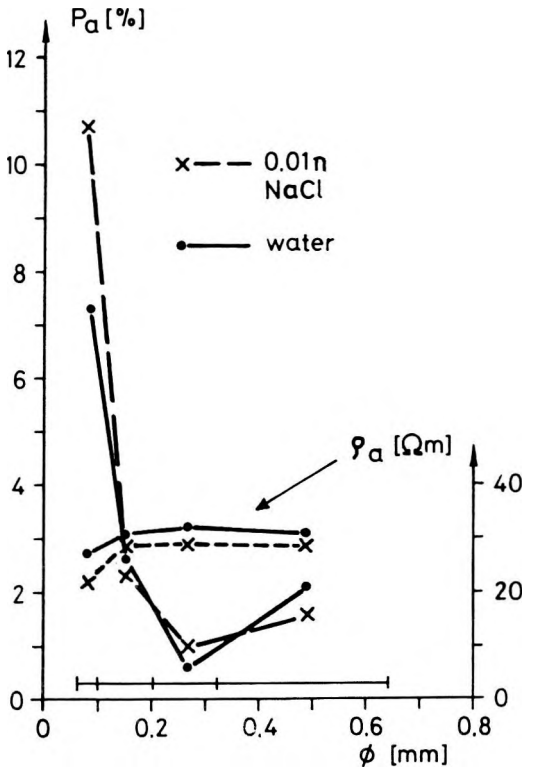

Fig. 1. Resistivity and polarizability measured in sands of different grain size

1. ábra. Különböző szemcseméretű homokban mért ellenállás és polarizálhatóság adatok

Рис. 1. Значения сопротивления и поляризуемости, полученных в песках различной зернистости

These results of laboratory measurements prove that the induced polarization method provides valuable additional information for water prospecting in a sand/shale sequence.

4. Field measurements

The next step in the co-operation was field work with the frequency-domain instrument of the Austrian team in an area which had formerly been prospected by ELGI. The test area chosen was an alluvial fan of the river Maros (SE Hungary). The task was to search for the coarse sediments of paleo-rivers running in Upper Pliocene and Pleistocene times. The whole alluvial fan is located on Pannonian clays of considerable thickness. An integrated geoelectric survey was carried out in 1978–82 over an area of 1500 km^2. Two promising depth intervals could be traced between the surface and near-surface formations of extremely variable resistivity and the low-resistivity Pannonian clays, named upper and lower water-bearing horizons. The areal resistivity and polarizability distribution of the upper water-bearing horizon are presented in *Fig. 2.* Depth to this horizon varies between 5 and 30 m — while the thickness of the water-bearing sequence between 100 and 300 m, decreasing from E to W. On the resistivity map there are definite highs of similar resistivity (Fig. 2a), interpreted as local accumulation of the coarse-grain fraction (areas marked by 1–2–3). So on the basis of this single parameter the hydrological value of these areas can be taken as near to equal. Anomaly No 1 can be judged more favourable because of its large extent.

The polarizability distribution of the same depth interval (Fig. 2b) shows a totally different character: areas having identical or similar resistivity show different polarizability.

5. In-hole measurements

Figure 3. shows a comparison between point-like in-hole measurements performed with a 40 cm Wenner probe attached to a time-domain surface instrument and the resistivity log obtained with a 40 cm potential probe on drilling 1. The two resistivity curves match perfectly and enable us to construct the sand/clay variation in the lithologic column. The polarizability values are
— small (below 4%) in clays (e.g. 50–56 m);
— medium (4–6%) in clean sands (62–68 m);
— high (8–11%) at sand/clay boundaries (60 m, 70 m, 91 m, 98 m).

Fig. 2. Resistivity (a) and apparent polarizability (b) maps of the alluvial fan of river Maros

2. ábra. A Maros hordalékkúpjának ellenállás- (a) és látszólagos polarizálhatóság- (b) térképe

Рис. 2. Карты сопротивления (а) и кажущейся поляризуемости (в) по конусу выноса р. Марош

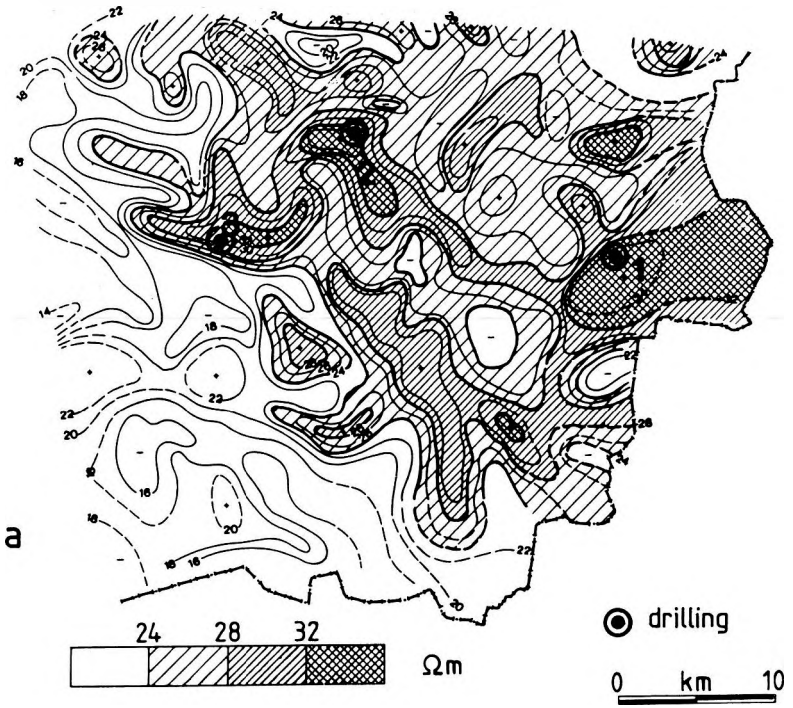
a
24 28 32
Ωm
drilling
0 km 10

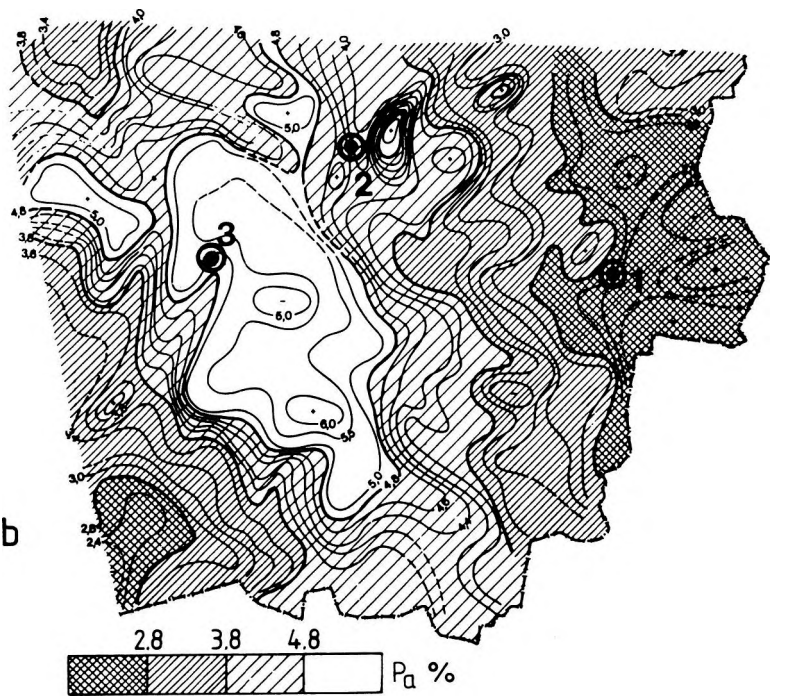
b
2
3
2.8 3.8 4.8
Pa %

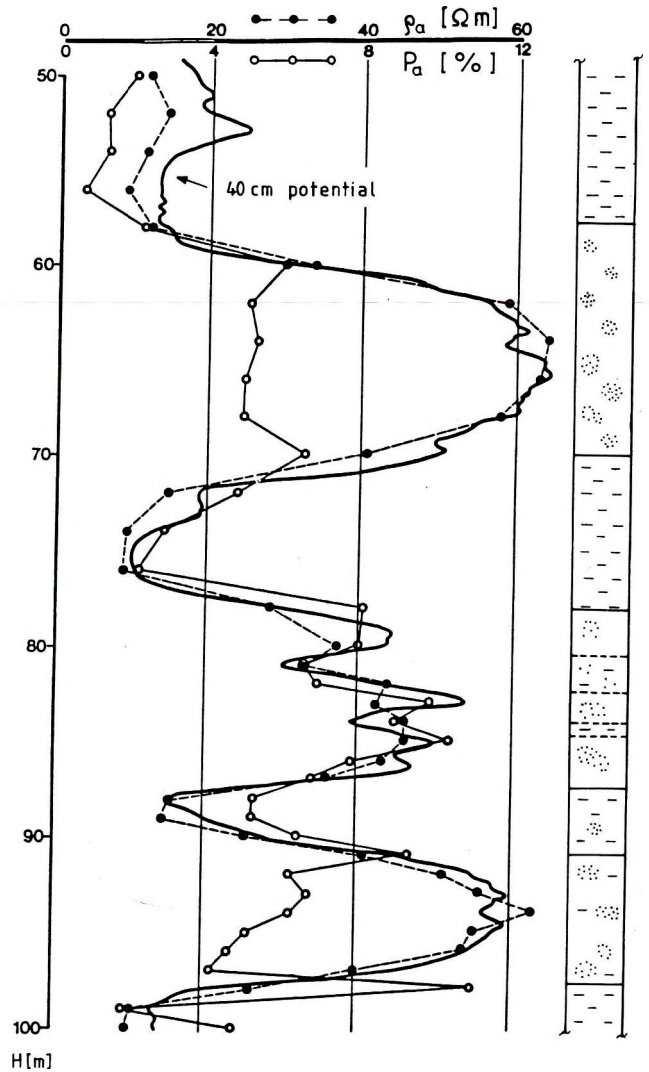

Fig. 3. In-hole resistivity and polarizability values measured in SE-Hungary

3. ábra. DK-Magyarországon mért fúrólyukbeli ellenállás- és polarizálhatóság értékek

Рис. 3. Значения сопротивления и поляризуемости, измеренных в скважинах юго-восточной Венгрии

These results suggest that induced polarization takes place mostly at sand/clay boundaries. Therefore the average level of polarizability becomes high where thin individual sand and shale layers alternate (e.g. between 78 and 86 m).

At the same time, the average resistivity level is only slightly lower than in the case of a clean sand layer (between 62 and 68 m). From these data it may be suggested that the resistivity value determined by surface measurements is linked with the total quantity of sand in the depth interval studied, while the polarizability value is linked with the distribution of this sand. Thus thick clean sand layers may be expected in areas of high resistivity and low polarizability, i.e. in our case in the eastern anomaly marked by 1. In areas of similarly high resistivity but high polarizability (anomalies marked by 2 and 3), variation of thin sand and clay layers are to be expected. This conclusion is supported by borehole data and pumping tests.

Time domain and frequency domain in-hole measurements were compared in the framework of another water supply project (Western Hungary). Frequency domain measurements were carried out in the frequency range of 0.1 to 1000 Hz, at 11 discrete frequencies. One point in clean clay (24 m) was taken as reference, and measurements at other points were normalized to this value. Normalized resistivity and phase curves obtained in clay *(Fig. 4a)* differ both for shape and amplitude from the respective curves obtained in sand (Fig. 4b).

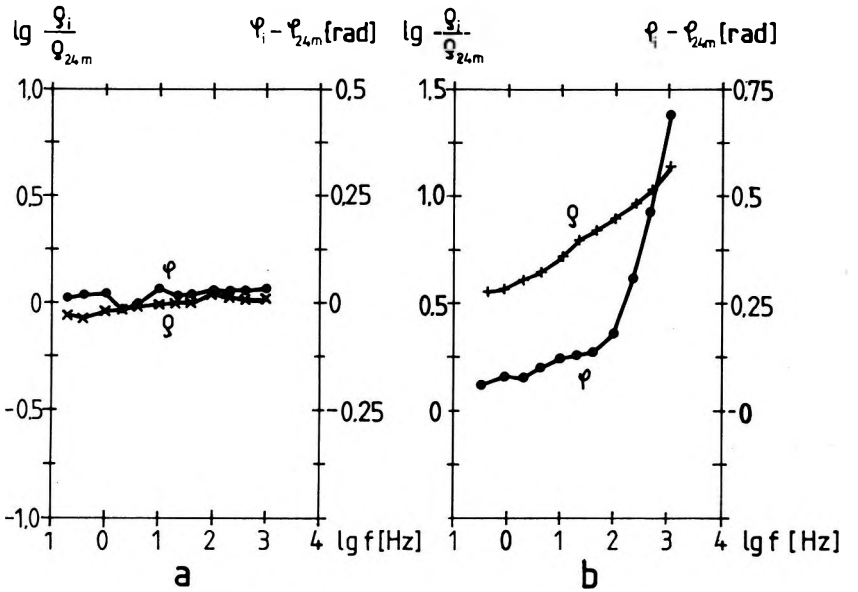

Fig. 4. Normalized resistivity ($\varrho_1/\varrho_{24\,m}$) and phase shift ($\varphi_1-\varphi_{24\,m}$) values versus frequency
a) Sonde in 25 m, clay; b) Sonde in 30 m, sand

4. ábra. Normalizált ellenállás ($\varrho_1/\varrho_{24\,m}$) és fáziseltolás ($\varphi_1-\varphi_{24\,m}$) értékek a frekvencia függvényében
a) 25 m mélyen lévő szonda, agyag; b) 30 m mélyen lévő szonda, homok

Рис. 4. Значения нормированного сопротивления ($\varrho_1/\varrho_{24\,м}$) и фазовых смещений ($\varphi_1-\varphi_{24\,м}$) как функции частот
а) зонд на глубине 25 м, глина; b) зонд на глубине 30 м, песок

Although the experiment comprises a short section of the well, it includes the boundary of a layer of dominating sand fraction around 28–29 m. This is reliably indicated both by dc and ac resistivity measurements *(Fig. 5c)* and the time-domain polarizability measurements indicate the same boundary (Fig. 5a). Figure 5b shows the phase shift as a function of depth and frequency. Sand appears with high phase shift and the contrast between sand and clay increases with increasing frequency. This is favourable from the viewpoint of both time demand and economy of measurements. In the middle part of the section it is interesting that ac and dc resistivity correlate well with the phase shift. A local polarizability maximum at a depth of 28 m indicates the same boundary.

Summarizing, we found that clay and sand can be separated by other methods (well-logging) more quickly and more accurately than by in-hole resistivity and IP measurements. However, our experiments were aimed not at accurate separation of clay and sand but as a means of contributing to the interpretation of combined resistivity and IP surveys. In this respect our results are of help in explaining IP phenomena in sand/clay sequences.

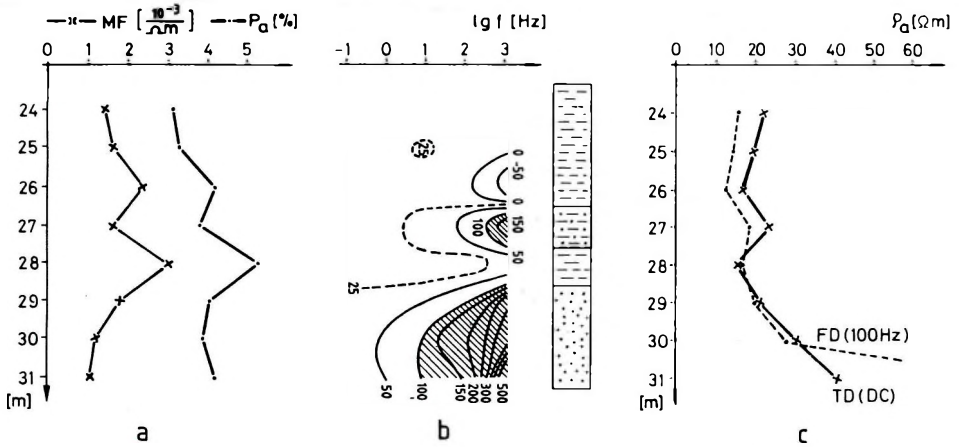

Fig. 5. In-hole resistivity, time and frequency domain polarizability measurements
a) Apparent polarizability in time domain (P_a) and frequency domain (MF)
b) Phase shift in mrad versus depth and frequency
c) ac and dc resistivity values

5. ábra. Fúrólyukbeli ellenállásmérések összehasonlítása idő- és frekvenciatartománybeli polarizálhatóság mérésekkel
a) Látszólagos polarizálhatóság az idő- (P_a) és frekvenciatartományban (MF)
b) Fázistolás mrad-ban a mélység és frekvencia függvényében
c) Váltóáramú és egyenáramú ellenállás értékek

Рис. 5. Сопоставление результатов скважинных измерений сопротивления с измерениями поляризуемости во временно́м и частотном диапазонах
a) Кажущаяся поляризуемость во временно́м (P_a) и частотном диапазонах (MF)
b) Фазовое смещение в мрад как функция глубин и частот
c) Значения сопротивления постоянного у перененного тока

6. Conclusion

In hydrogeologic prospecting of basins filled with young clastic sediments the use of the IP method is found to be a good means of complementing resistivity surveys. Anomalies of similar resistivity can be distinguished or even classified with the help of their apparent polarizability. The best water-bearing layers occur in areas characterized by high resistivity and low or medium polarizability judging from our results in several water-prospecting projects. This conclusion is supported by laboratory and in-hole resistivity and IP measurements, and by pumping tests.

REFERENCES

AIGNER H. 1986: Methode der Induzierten Polarisation. Angewandte Geophysik, Bd. II., Springer Verlag Wien, Akademie Verlag Berlin, pp. 186–207

BERTIN J., LOEB J. 1976: Experimental and theoretical aspects of induced polarisation. Bd. II, Gebrüder Borntrager, Berlin,

BODMER R., WARD S. H., MORRISON H. F. 1968: On induced polarisation and ground water. Geophysics **33,** 5, pp. 805–821

DRASKOVITS P. 1986: Study on hydrogeological application of the induced polarization method. (in Hungarian) Project report, ELGI, Budapest (manuscript) 10 p.

DRASKOVITS P., HOBOT J., SMITH B. D., VERŐ L. 1990: Induced polarization surveys applied to evaluation of ground water resources, Pannonian Basin, Hungary. *in:* Induced polarization: Application and Case Histories, Society of Exploration Geophysicists, Tulsa

KELLER G. V., FRISHKNECHT F. C. 1970: Electrical methods in geoelectric prospecting. Pergamon Press, New York

LIPSKAYA, A. E., RYAPOLOVA, V. A. 1970: Application of induced polarization method in engineering geologic studies (in Russian). *in:* Application of geophysical methods in hydrogeologic and engineering geologic investigations, Moscow, pp. 30–37

NIESNER E., WEBER F. 1985: Anwendung der induzierten Polarization auf nichtmetallische Materialien, Projectbericht StA–60/84 und StA–60/85, Forschungsgesellschaft Joanneum, Leoben

ROY K. K., ELLIOT M. M. 1980: Model studies on some aspects of resistivity and membrane polarization behaviour over a layered earth. Geophysical Prospecting **28,** 5, pp. 759–775

SUMNER J. S. 1976: Principles of induced polarization for geophysical exploration. Elsevier, Amsterdam

VACQUIER V., HOLMES C. R., KINTZINGER P. R. and LAVERGNE M. 1957: Prospecting for ground water by induced electrical polarization. Geophysics **22,** pp. 660–687

WEBSTER B. 1986: Time domain IP borehole logging. *in:* Borehole geophysics for mining and geotechnical applications, ed. P. G. Killeen, Geological Survey of Canada, Paper 85–27, pp. 107–118

VÍZKUTAK TELEPÍTÉSÉNEK OPTIMALIZÁLÁSA A GERJESZTETT POLARIZÁCIÓS MÓDSZER ALKALMAZÁSÁVAL

Heinrich AIGNER, DRASKOVITS Pál

Vízkutak optimális telepítése céljából az ellenállás méréseket gerjesztett polarizációs mérésekkel kombináltuk. Először laboratóriumi modellmérésekkel meghatároztuk a különböző szemcseméretű folyóvízi üledékek ellenállás- és polarizálhatóság jellemzőit. A terepi adatok értelmezése a laboratóriumi mérések eredményein alapul. A felszíni mérések értelmezésének alátámasztása céljából fúrólyukbeli ellenállás- és GP méréseket végeztünk az idő- és a frekvenciatartományban. E célból a mérőműszereket alkalmassá kellett tenni a fúrólyukbeli viszonyokra. Egy DK-magyarországi vízkutatás során kvalitatíve meghatároztuk a porózus képződmények mennyiségét és eloszlását. Ezeket az adatokat később próbaszivattyúzásokkal ellenőrizték. Mindezek eredményeképp megállapítható, hogy alluviális medencékben a legjobb víztároló képződmények a nagy ellenállással és kicsi, vagy közepes polarizálhatósággal jellemezhető körzetekben várhatók.

ОПТИМАЛИЗАЦИЯ ВЫБОРА ПУНКТОВ ПОД ГИДРОГЕОЛОГИЧЕСКИЕ СКВАЖИНЫ С ПРИМЕНЕНИЕМ МЕТОДА ВЫЗВАННОЙ ПОЛЯРИЗАЦИИ

Гейнрих АИГНЕР, Пал ДРАШКОВИЧ

С целью выбора оптимальных пунктов для гидрогеологических скважин электроразведка методом сопротивлений была поставлена в комплексе с методом вызванной поляризации. При этом на лабораторных моделях были определены параметры сопротивления и поляризуемости аллювиальных отложений различной зернистости. Интерпретация данных полевых работ основана на результатах лабораторных измерений. Для подтверждения интерпретации наземных данных были выполнены измерения сопротивления и поляризуемости в скважинах в частотном и временно́м диапазонах. Для этой цели измерительная аппаратура была приспособлена к скважинным измерениям.

В ходе гидрогеологических работ в Юговосточной Венгрии были качественно определены количество и распределение пористых пород. Эти данные впоследствии были проверены путем испытательных откачек. В результате проведенных работ можно установить, что в аллювиальных бассейнах отложения, наиболее насыщенные водой, можно ожидать на участках высокого сопротивления и малой до средней поляризуемости.

GEOPHYSICAL TRANSACTIONS 1991
Vol. 36. No. 1–2 pp. 103–111

EM SOUNDINGS IN WATER- AND BROWN-COAL PROSPECTING. CASE HISTORIES

I. FARKAS[+], P. KARDEVÁN[+], G. REZESSY[+], CH. SCHMID*, L. SZABADVÁRY[+], F. WEBER*

The possibility of applying electromagnetic (EM) soundings in solving tectonic problems in water- and brown-coal exploration when EM measurement complement or substitute seismics is discussed in the paper. It is shown that buried faults can successfully be detected by EM method which, thus, can substitute even reflection seismics in shallow prospecting. In favourable cases information on changing lithology along profiles can be obtained from EM soundings. This is, however, strongly hindered by structural effects. Detection of conductive clay layers by EM measurement is a valuable contribution to seismic data in most water prospecting problems.

Keywords: water prospecting, electromagnetics, seismics, case history

1. Introduction

The Institute of Applied Geophysics in Leoben has been using electromagnetic frequency sounding as part of integrated geophysical surveys for solving groundwater- and coal prospecting as well as structural mapping problems since 1982. *Fig. 1* shows the locations of the survey areas discussed in this paper. The application of high frequency reflection seismics in combination with electromagnetic (EM) frequency soundings represents a novel application of geophysics.

We present case histories discussing the possibilities for such applications, where the seismic and electromagnetic methods complement or substitute each other. The data from the EM soundings carried out along seismic profiles considerably improve the chances of lithologic or age classification in the course of the multiparametric geological interpretation. The recognition of the lithologic changes (such as increasing clay content) or, say, the detection of impermeable clay layers are extremely important in hydrogeology. On the other hand, EM frequency soundings can be used alone as well. They may be used in some types of geological build-up to determine the tectonics of the high-resistivity basement (crystalline or dolomite) enabling the replacement of seismics — since the latter has recently often caused environmental problems.

The co-operation between the Austrian and Hungarian parties consisted in field work and interpretation of the EM frequency soundings by the Eötvös Loránd Geophysical Institute, while all other geophysical methods were carried out by the Institute of Applied Geophysics, Leoben.

* Institut für Angewandte Geophysik, Rosegger str. 17, A–8700 Leoben, Austria
+ Eötvös Loránd Geophysical Institute of Hungary, Budapest, P.O.B. 35, H–1440, Hungary
Manuscript received (revised version): 30 November, 1990

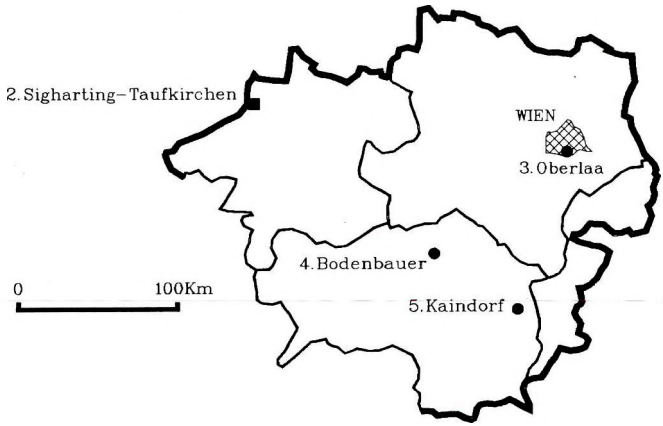

Fig. 1. Survey areas of electromagnetic soundings in Austria discussed in the paper (square — brown-coal prospecting, circle — water prospecting)

1. ábra. A dolgozatban tárgyalt elektromágneses szondázások kutatási területei Ausztriában (négyzet — barnakőszén-kutatás, kör — vízkutatás)

Рис. 1. Районы работ методом электромагнитного зондирования в Австрии (квадрат — работы на бурые угли, кружок — гидрогеологические работы)

The electromagnetic measurements discussed here were carried out with the Maxi–Probe EMR–16 frequency sounding system using an approximately vertical magnetic dipole source in the inductive zone of the dipole. For details of the Maxi–Probe EMR–16 frequency sounding system see SINHA [1979, 1983].

As a result of multifrequency measurements depth sections of resistivity are obtained with a depth coverage from 20 to 80 per cent of the separation between the transmitter and the receiver. The definition of the apparent resistivity used here [see also SINHA 1979] is similar to that described by WILT and STARK in 1982.

Direct comparison of a transformed sounding curve with the geologic log of the corresponding borehole and the correlation of curve patterns extends the geological information obtained at the drill site along the profile. The pattern of the transformed curves, i.e. the way apparent resistivity changes with depth, shows higher stability against lateral variation of the near-surface rocks or against the variations of resistivity contrasts of the layers than the apparent resistivity values themselves. Thus, this way of obtaining geological information means a powerful filtering out of geological noise and considerably increases the reliability of geophysical interpretation of depth sections.

A similar approach is described by PRITCHARD and RENICK [1981], in which it was proposed that residual resistivity sections be used in structural mapping.

2. Brown coal prospecting in the Molasse zone of Upper-Austria (Sigharting–Taufkirchen)

In the course of a brown-coal prospecting project near Sigharting–Taufkirchen, reflection seismic measurements were carried out to solve tectonic problems; the Bouguer-anomaly map of the area was available for interpretational purposes. The aim of the electromagnetic soundings thereafter was to recognize the lithology in the given geologic–geoelectric model in which a high resistivity crystalline basement was underlying a low-resistivity series of Tertiary sediments of the Molasse-zone characterized by Upper-Eocene sandstones, Oligocene clayey marls, and Miocene sanstones containing brown coal seams.

Although there are no pronounced conductive key layers within the approximately 300 m thick Tertiary complex, the EM soundings can still be correlated as they are some hundred meters apart from each other. In *Fig. 2* the correlatable break points appearing on the transformed sounding curves are connected by thin lines. The possible positions of faults can be determined in those parts of the section where curve patterns change remarkably, i.e. between stations T8 and T9 as well as T11 and T12. It can be seen that the sounding curve at station T12, which was about 400 m away from the outcrop of the crystalline rock, is of completely different type than those at stations inside the basin. The trend of increasing apparent resistivity with increasing depth in T12 indicates the elevated position of the crystalline basement.

The conclusions of the electromagnetic measurements were compared with gravimetry and reflection seismic measurements. In Fig. 2, the reflection seismic horizon transformed to depth, interpreted as the upper boundary of crystalline basement is plotted. It coincides with the breakpoints obtained from EM soundings, interpreted as the surface of the basement although this indication cannot be regarded as unambiguous north of the fault between points T9 and T10.

The Bouguer anomaly along the profile can be interpreted as unevenly deepening of the high-density basement to the South — possibly by faults.

Information on litholigic changes could not be obtained on the basis of EM soundings because of strong structural effects.

3. Water prospecting in the South-Vienna basin (Oberlaa)

In this area the basement is formed by Triassic Hauptdolomite, covered by several hundred meters of young Tertiary clayey and sandy sediments. Breccia and conglomerate are found at the lowermost part of the Tertiary series *(Fig. 3)*. Along deep fracture zones hot water characterized by the Kations Sodium, Calzium and the Anions Chloride, Sulfate, Hydrocarbonate (total mineralization 3.7 g/kg, 54 C° temperature) appears at some places. The most important sweet water aquifer is the basal conglomerate and the weathered, permeable upper part of the Hauptdolomite.

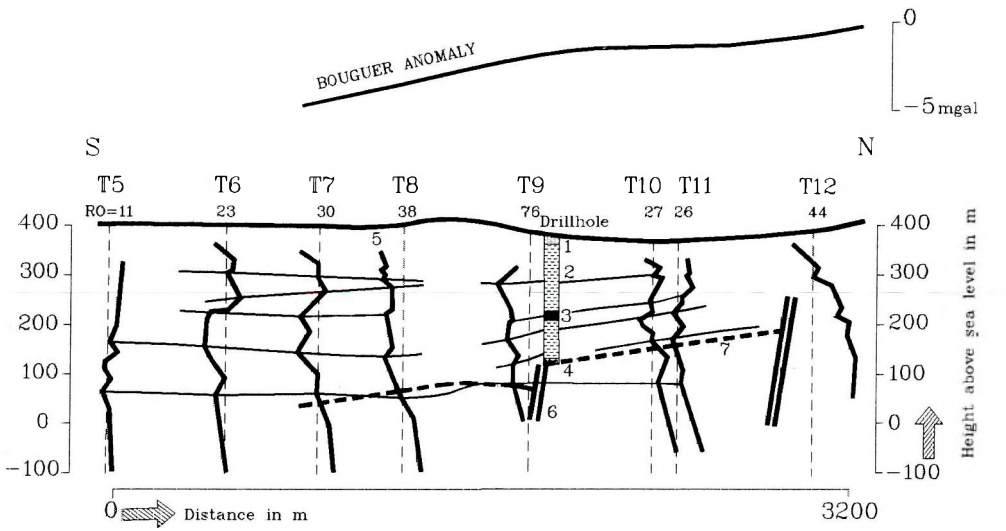

Fig. 2. Geophysical depth-section — including the results of reflection seismics and EM soundings — with Bouguer anomaly for solving structural problems in brown-coal prospecting in the Molasse Zone of Upper Austria (area: Sigharting–Taufkirchen)

1 — sand; 2 — clayey marl; 3 — gravel; 4 — crystalline basement; 5 — apparent resistivity versus depth curve of EM sounding; 6 — fault; 7 — crystalline basement from reflection seismics

2. ábra. Geofizikai mélységszelvény — a reflexiós szeizmika és az EM szondázások eredményei — és a Bouguer-anomália összevetése barnakőszén-kutatás során felmerülő szerkezetföldtani problémák megoldására Felső-Ausztria molasz övezetében. (Kutatási terület: Sigharting–Taufkirchen)

1 — homok; 2 — agyagos márga; 3 — kavics; 4 — kristályos aljzat; 5 — EM szondázásból kapott látszólagos ellenállás–mélység görbe; 6 — vető; 7 — reflexiós szeizmikából kapott kristályos alaphegység felszín

Рис. 2. Сопоставление глубинного геофизического разреза по результатам сейсморазведки методом отраженных волн и электромагнитного зондирования с аномалиями Буге для решения структурно-геологических проблем, возникающих в ходе работ на бурые угли в молассовой зоне Верхней Австрии (район работ: Сиггартинг–Тауфкирхен)

1 — пески; 2 — глинистые мергели; 3 — галечники; 4 — кристаллический фундамент; 5 — кривая зависимости кажущегося сопротивления от глубины, полученная по данным электромагнитного зондирования; 6 — разлом; 7 — поверхность кристаллического фундамента по сейсморазведке методом отраженных волн

Four marker horizons (*A* ,*B*, *C*, *D*) can be recognized in the electromagnetic soundings; the upper (*B*) and the lower (*C*) boundary of a low-resistivity layer overlying the conglomerate. Judging from electric well-logs the Badenian clays are of the lowest resistivity (2–3 Ωm), while the resistivity of the conglomerate ranges between 100 and 450 Ωm, depending on the cementing material. The Hauptdolomite may have even higher resistivities, although the resistivity of the fissured parts does not differ from that of the breccia. Numerous exploratory

drillings prove that the waterbearing rock complex (i.e. the conglomerate and the fissured dolomite) is by no means equally permeable. Therefore, the changes in apparent resistivity are of hydrological importance. It should be mentioned, however, that in many cases strong structural effects appear on the sounding curves and mask the inductive effects caused by lithological changes. The apparent resistivity decrease observable on the lowermost part of curve Oa–4 is caused, for instance, by the fault between Oa–4 and Oa–1 and not by lithologic changes of the basement.

The faults — such as that in Fig. 3 — were found by correlating the characteristics of the transformed sounding curves. This was done since reflection seismic measurements could not be performed due to reasons of environmental protection.

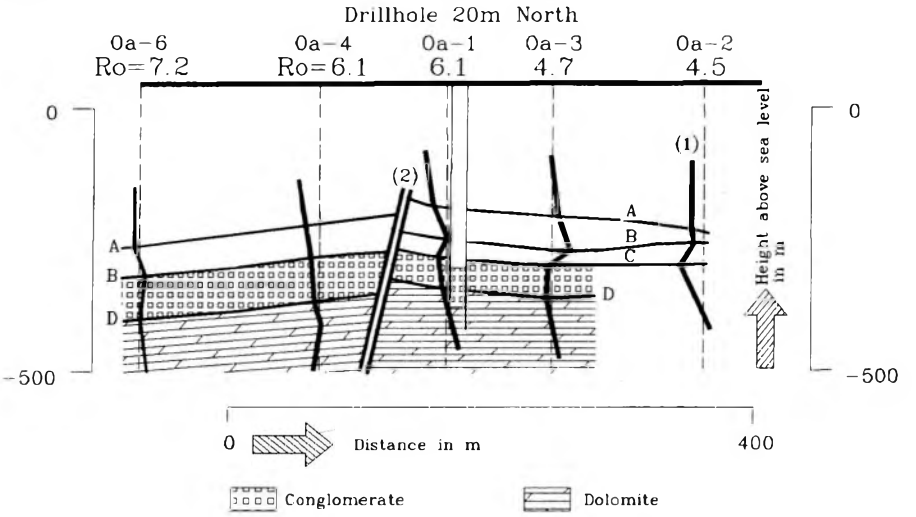

Fig. 3. Interpretation of EM soundings carried out in the Vienna Basin for water prospecting
1 — apparent resistivity versus depth curve of EM sounding; 2 — fault; *A*, *B*, *C*, *D* — correlated horizons of resistivity contrast

3. ábra. A bécsi medencében vízkutatási céllal végzett EM szondázások értelmezése
1 — EM szondázásból kapott látszólagos ellenállás–mélység görbe; 2 — vető; *A*, *B*, *C*, *D* — korrelált ellenállásváltozás

Рис. 3. Интерпретация данных электромагнитного зондирования в Венской впадине при гидрогеологических изысканиях
1 — кривая зависимости кажущегося сопротивления от глубины, полученная по данным электромагнитного зондирования; 2 — разлом; *A*, *B*, *C*, *D* — скоррелированные изменения сопротивления

4. Water prospecting in the region of Bodenbauer

Water prospecting is illustrated by the profile of *Fig. 4*, which was chosen from the results of the measurements performed in a narrow, mostly 300 m wide valley near Bodenbauer, at the southern foot of the massif of Hochschwab/ Northern Calcareous Alps.

Some drillings indicated 200 m Quaternary thickness underlain by Triassic limestone and dolomite and Werfenian shale. The seismic refraction measurements performed in 1971 mapped a refracting horizon with a velocity of about 3000 m/s (not indicated in Fig. 4), which was initially interpreted as the upper boundary of Werfenian beds at a depth of about 90 m. Judging from the hole drilled later, however, this horizon proved to be within the moraine.

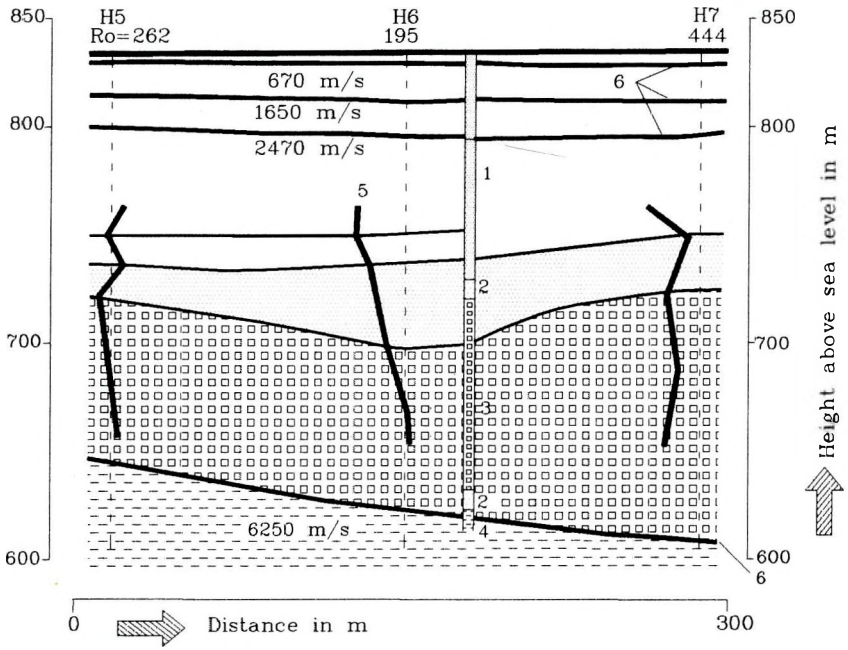

Fig. 4. Geophysical depth section of water prospecting carried out in an inner-Alpine valley
1 — gravel; 2 — silt; 3 — glacial rocks (moraine); 4 — Werfenian beds; 5 — apparent resistivity versus depth curve of EM sounding; 6 — refractor

4. ábra. Belső-alpi völgyben végzett vízkutatás geofizikai mélységszelvénye
1 — kavics; 2 — iszap; 3 — moréna hordalék; 4 — Werfeni pala; 5 — EM szondázásból kapott látszólagos ellenállás–mélység görbe; 6 — refraktáló határfelület

Рис. 4. Глубинный геофизический разрез по гидрогеологическим работам, выполненным в одной из альпийских долин
1 — галечники; 2 — илы; 3 — моренные отложения; 4 — верфенские сланцы; 5 — кривая зависимости кажущегося сопротивления от глубины, полученная по данным электромагнитного зондирования; 6 — отражающая граница

Because of the small width of the valley, neither refraction seismic nor dc sounding crosslines could use a spread ensuring the necessary penetration.

Investigations continued in 1987, when reflection seismics was used to clarify the structure of the supposed synclinal zone, while electromagnetic frequency soundings were aimed at providing lithological data on the sediments filling the valley. Clay layers and gravel with clayey cementing were of primary hydrological importance. The depth of penetration of the frequency soundings was set between 70 to 140 m.

As can be seen in Fig. 4, a resistivity decrease occurs within the moraine, this was interpreted as a consequence of higher clay content. The difference between the depth to the silt layer in the drillhole and in sounding curve H6 (see Fig. 4) is not more than 10 per cent. This important marker horizon could be mapped throughout the whole area.

5. Prospecting for deep aquifers in Southeastern Steiermark (Kaindorf)

In the region of South-eastern Steiermark, investigations with the purpose of water prospecting have been carried out with varying success for a long time for detecting deep-seated, thin sand layers. The maximum exploration depth was 300 m, because at greater depths higher water temperatures can be expected. In the course of the project, high frequency reflection seismics and electromagnetic frequency soundings were combined.

Reflection seismics provided a relatively good resolution of the alternating Tertiary sand–clay complex *(Fig. 5)* but in the lack of exploratory drillings no information was available to identify water-bearing sand layers. The task of EM soundings was to distinguish between the high-resistivity sand and conductive clay layers in the 150–300 m depth range.

In order to convert TWT into depth, the interval velocities obtained from the velocity analysis were used. The basement of the Tertiary sediment is at depths between 600 and 700 m (see the reflection horizon marked with a broken bold line in Fig. 5). Electromagnetic frequency soundings were performed at different places with different transmitter–receiver separations, thus with different penetration depths. The results are plotted in the seismic depth section of Fig. 5. The reflectors are marked with bold lines, the resistivity interfaces appearing in the electromagnetic frequency soundings are marked with thin lines. The three layers of low resistivity indicated by letters A, B, C can be interpreted as clay. These markers could be determined along the whole length of the profile (about 7 km). The lowermost resistivity interface D indicates the upper boundary of a resistive layer.

It is worth mentioning that in lack of any borehole the seismic depth values are subject to uncertainties due to the uncertainties of the velocity determinations. The errors of electromagnetic depth can be estimated to be about 10 per cent within the depth range of investigation ($2 < L/H < 3$, where H is the apparent depth, L is the separation between transmitter and receiver).

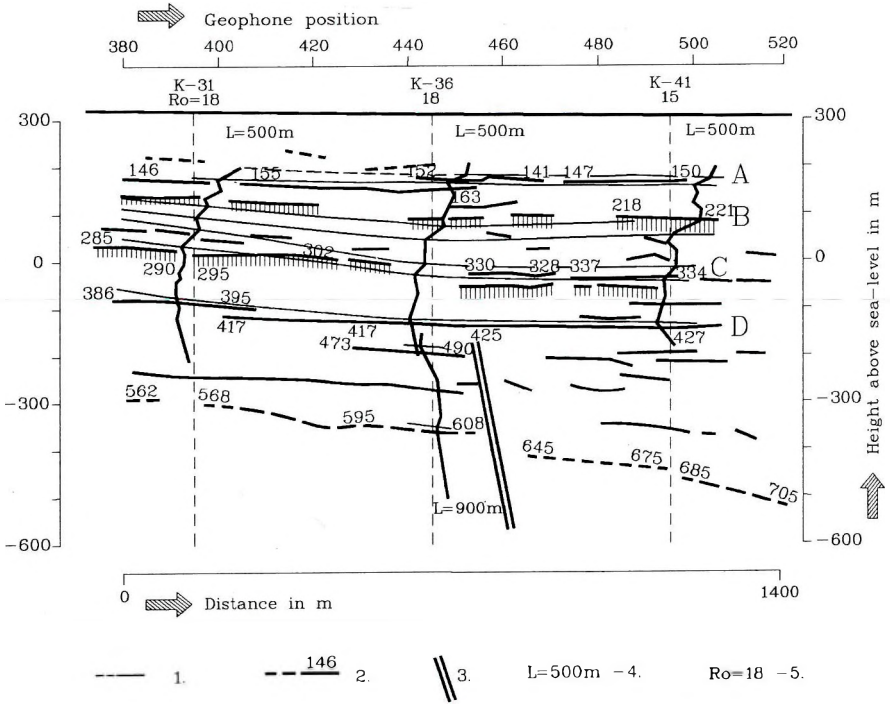

Fig. 5. Comparison of reflection seismic horizons and correlated electromagnetic interfaces (water prospecting in Southeastern Steiermark, area: Kaindorf)

1 — correlated EM resistivity contrast; 2 — reflectors; 3 — fault; 4 — separation of EM sounding; 5 — apparent resistivity value of the transformed sounding curve at the reference axis

5. ábra. Reflexiós szeizmikus reflektáló felületek és korrelált elektromágneses réteghatárok egybevetése (vízkutatás DK Steiermarkban, kutatási terület: Kaindorf)

1 — korrelált EM ellenállásváltozás; 2 — reflektálófelületek; 3 — vető; 4 — frekvenciaszondázás adó–vevő távolsága; 5 — a transzformált görbe referenciatengelyen felvett látszólagos ellenállás értéke

Рис. 5. Сопоставление отражающих сейсмических и скоррелированных электромагнитных границ (гидрогеологические изыскания в Юговосточной Штирии, район работ: Кайндорф)

1 — скоррелированные изменения сопортивления по данным электромагнитного зондирования; 2 — отражающие границы; 3 — разлом; 4 — расстояние между датчиком и приемником при частотном зондировании; 5 — значения кажущегося сопротивления, снятые с опорной оси преобразованной кривой

BIBLIOGRAPHY

GYURKÓ P., KARDEVÁN P., REZESSY G. and SZABADVÁRY L. 1984: Multifrequency electomagnetic soundings (MFS). Annual Report of ELGI for 1983. pp. 176–178

GYURKÓ P. and SZABADVÁRY L. 1983: MFS surveys in Upper Austria. Annual Report of ELGI for 1982. p. 249

PRITCHARD J. I. and RENICK Jr. 1981: Today's exploration capability of electrical method surveys. Presented at the 51st Annual International SEG Meeting, October 11–15, Los Angeles

SINHA A. K. 1979: Maxi-Probe EMR–16: A new wide-band multifrequency ground EM system. Current Research, Part B, Geological Survey of Canada, Paper 79–1B, pp. 23–26

SINHA A. K. 1983: Deep multifrequency E.M. sounding at a site near Bowmanville, Ontario. Current research, Part A, Geological Survey of Canada, Paper 83–1A, pp. 133–137

WILT M. and STARK M. 1982: A simple method for calculating apparent resistivity from electromagnetic sounding data. Geophysics **47**, pp. 1100–1105

EM SZONDÁZÁS ALKALMAZÁSA A VÍZ- ÉS BARNAKŐSZÉN-KUTATÁSBAN. ESETTANULMÁNYOK

FARKAS I., KARDEVÁN P., REZESSY G., CH. SCHMID, SZABADVÁRY L., F. WEBER

Víz- és barnakőszén kutatás során felmerülő szerkezetföldtani problémák elektromágneses szondázások alkalmazásánál történő megoldási lehetőségét vizsgáljuk a dolgozatban olyan esetekben, amikor az EM mérések kiegészítik vagy helyettesítik a szeizmikus mérést. Bemutatjuk, hogy az eltemetett vetők sikeresen detektálhatók EM módszerrel, amely még a reflexiós szeizmikát is helyettesítheti a sekély kutatásban. Kedvező esetben a litológia szelvény menti változására vonatkozó információt is kaphatunk az EM szondázásokból. Ezt azonban szerkezeti hatások erősen akadályozzák. A vezetőképes agyagrétegek detektálása EM szondázásokkal értékes hozzájárulás a szeizmikus adatokhoz a legtöbb vízkutatási feladatban.

ПРИМЕНЕНИЕ ЭЛЕКТРОМАГНИТНОГО ЗОНДИРОВАНИЯ ДЛЯ ПОИСКОВ И РАЗВЕДКИ ПОДЗЕМНЫХ ВОД И БУРЫХ УГЛЕЙ. КОНКРЕТНЫЕ ПРИМЕРЫ

И. ФАРКАШ, П. КАРДЕВАН, Г. РЕЗЕШИ, Х. ШМИД, Л. САБАДВАРИ, Ф. ВЕБЕР

В статье рассматриваются вопросы решения структурногеологических проблем, возникающих при проведении поисков и разведки подземных вод и бурых углей, путем применения электромагнитных зондирований в таких случаях, когда электромагнитными измерениями дополняется или заменяется сейсморазведка. Показано, что погребенные разломы могут быть успешно выявлены электромагнитным методом, который при малоглубинных исследованиях может заменить даже сейсморазведку методом отраженных волн. В благоприятном случае по данным электромагнитного зондирования можно получить информацию по литологической изменчивости вдоль профилей, чему однако серьезно препятствуют структурные эффекты. Выявление глинистых пачек высокой проводимости при электромагнитном зондировании дает существенный вклад к данным сейсморазведки в большинстве задач гидрогеологического типа.

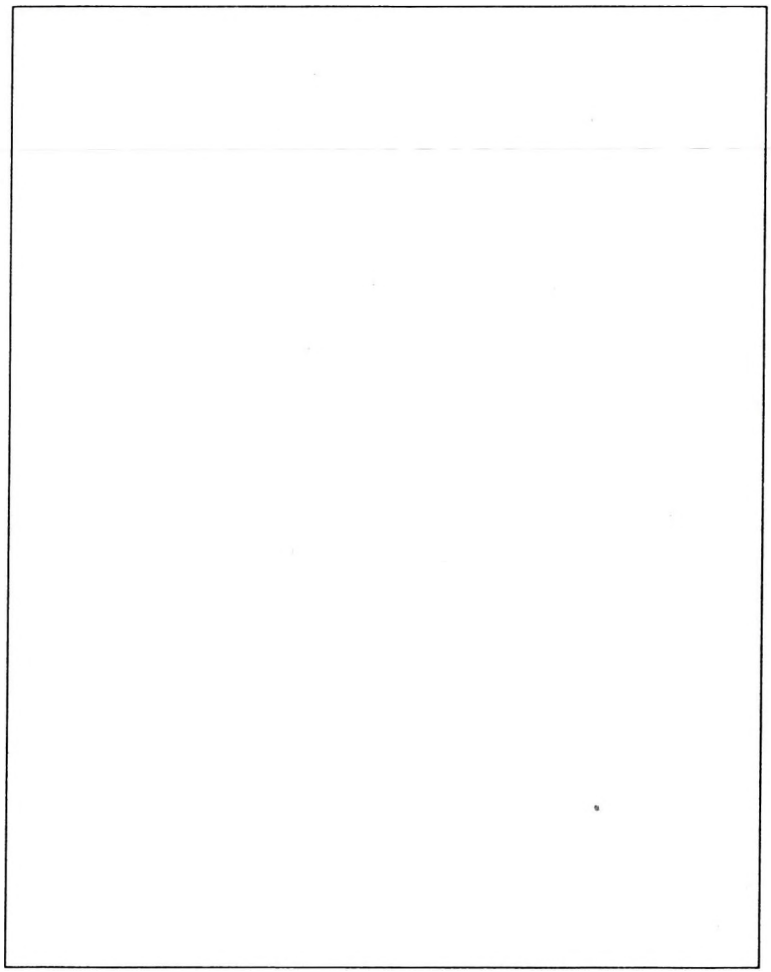

This page is waiting for you!

A NEW ADVERTISING MEDIUM AT YOUR COMMAND!

GEOPHYSICAL TRANSACTIONS OFFERS YOU ITS PAGES TO WIDEN THE SCOPE OF YOUR COMMERCIAL CONTACTS

Geophysical Transactions, as the leading English language quarterly of the CMEA countries, contains indispensible information to decision makers of the geophysical industry. It is distributed to 45 countries in 5 continents.

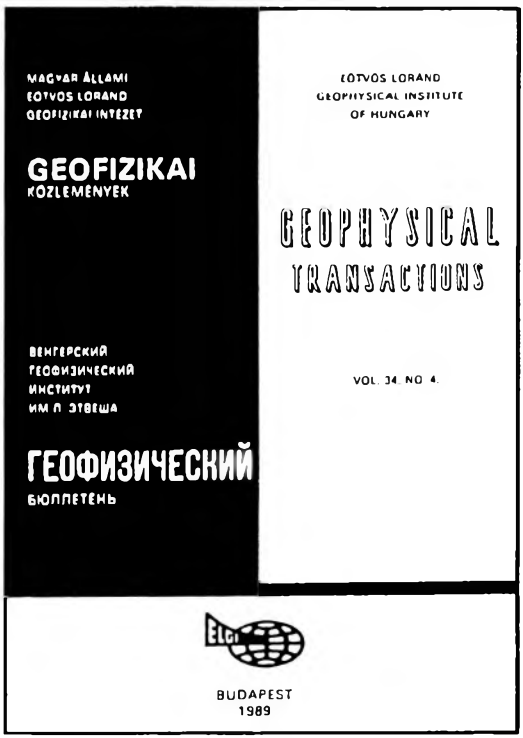

Advertising rates (In USD)

	Page	Half page
Black and white	400/issue	250/issue
Colour	800/issue	450/issue

Series discount: 4 insertions — 20%

For further information, please contact:
Geophysical Transactions, Eötvös Loránd Geophysical Institute of Hungary

P.O.B. 35, Budapest, H–1440, Hungary
tel: (36–1) 163–2835 telex: 22–6194

The proven technology to help you reduce risk and increase your success rate – worldwide.

HGS

Halliburton Geophysical Services

6909 Southwest Freeway Houston, TX 77074 Ph: (713) 774-7561 FAX: (713) 778-3487/Telex: 76-2781

A Halliburton Company

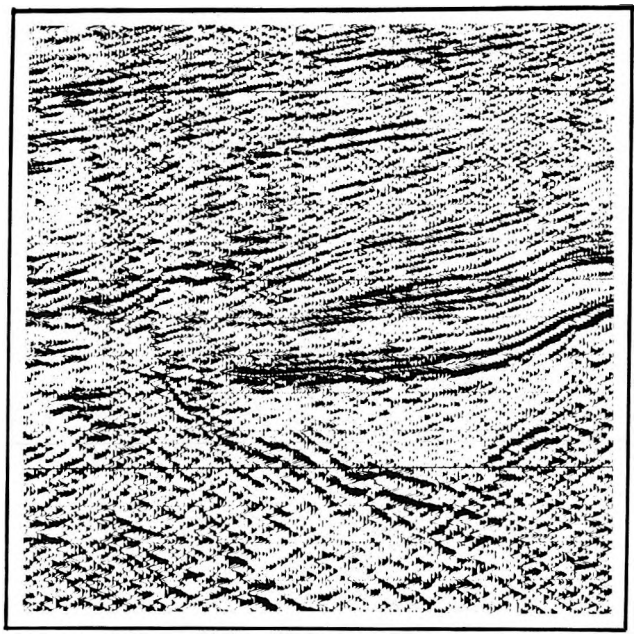

Land data example courtesy of OKGT

GECO is in the forefront of exploration technology with worldwide experience in:-

DATA ACQUISITION
DATA PROCESSING
INTERPRETATION
MAPPING
SEISMIC SOFTWARE
GEOCHEMICAL ANALYSIS
WORKSTATIONS

GECO OFFERS THE FULL RANGE OF GEOPHYSICAL SERVICES FROM SURVEY PLANNING TO BASIN EVALUATION

DATA ACQUISITION:
Our land crews operate with telemetry systems to ensure high productivity 2D and 3D surveys.

WORKSTATIONS:
GECO's CHARISMA work stations are acknowledged to be the finest in the industry providing unrivalled performance and functionality.

DATA PROCESSING:
Advanced algorithms coupled with high performance Vector Processors allow rapid delivery of quality data.

SEISMIC SOFTWARE:
GECO's portable package, STARPAK, runs on micros, minis, mainframes and supercomputers for 2D and 3D processing.

For further information please contact Chris Walker in England or John Christensen in Norway

HEAD OFFICE
GECO A.S.
Kjorbokollen
N-1300 Sandvika, NORWAY
Telephone: 47 (0) 2 47 55 00
Telefax: 47 (0) 2 47 55 55
Telex: 78623 geco n

EUROPE-AFRICA-MIDDLE EAST
GECO Geophysical Company Ltd.
The GECO Centre
Knoll Rise, Orpington
Kent BR6 0XG
UNITED KINGDOM
Telephone: 44 (0) 689 32133
Telefax: 44 (0) 689 22650

GECO

DON'T BUY EQUIPMENT OR SERVICES UNTIL YOU KNOW THE FACTS

ELGI's Well Logging Divison has put its 25 years of experience to work again in the new line of well logging technology in

water,

coal,

mineral,

geotechnical

prospecting

HERE'S WHAT WE OFFER

- Complete series of surface instruments from portable models to the PC controlled data logger
- Sondes for all methods: electrical, nuclear, acoustic, magnetic, mechanical, etc.
- Depth capacity down to 5000 m
- On-site or office computer evaluation
- International Metrological Base for calibration to true petrophysical parameters
- Training and in-house courses
- Design laboratory for custom-tailored assemblies

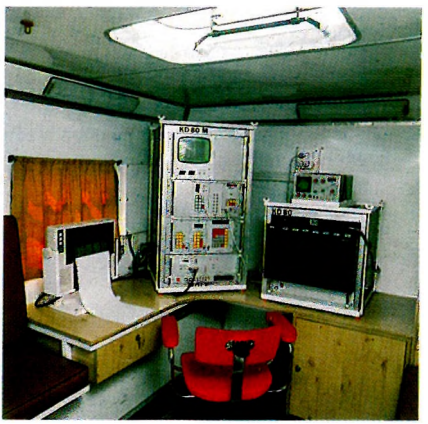

Just think of us as the scientific source of borehole geophysics you may never have heard of

SALES ✣ ✣ ✣ ✣ RENTALS ✣ ✣ ✣ ✣ SERVICES

Well Logging Division of ELGI
POB 35, Budapest, H-1440 Hungary
Phone: (361) 252-4999, Telex: 22-6194,
Fax: (361) 183-7316

CONTOUR MAP OF THE MOHOROVIČIĆ DISCONTINUITY BENEATH CENTRAL EUROPE

SCALE

1 : 1,000,000

0 10 20 30 40 50 km

Compiled by:

K. Posgay and I. Albu for Hungary

M. Mayerová, Y. Nakládalová, I. Ibrmajer, H. Herrmann and M. Bližkovsky for Czechoslovakia

K. Aric and R. Gutdeutsch for Austria

LEGEND

Contour lines in km b.s.l. reliable

estimated

52,5 50 47,5 45 42,5 40 38 36 34 32 30 28 26 24

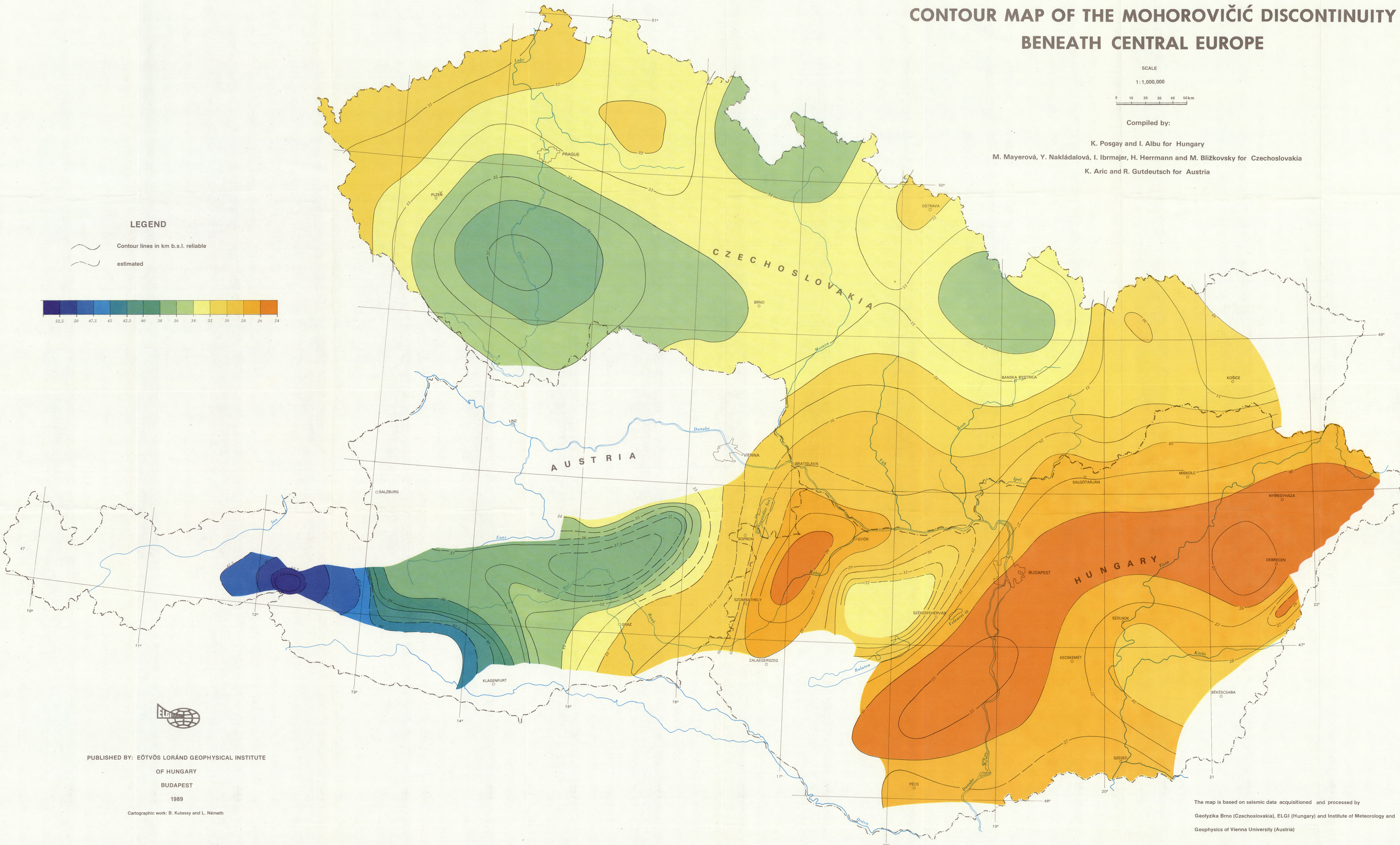

PUBLISHED BY: EÖTVÖS LORÁND GEOPHYSICAL INSTITUTE

OF HUNGARY

BUDAPEST

1989

Cartographic work: B. Kutassy and L. Németh

The map is based on seismic data acquisitioned and processed by Geofyzika Brno (Czechoslovakia), ELGI (Hungary) and Institute of Meteorology and Geophysics of Vienna University (Austria)

MH TÁTI 90-69

PRE-TERTIARY BASEMENT CONTOUR MAP OF THE CARPATHIAN BASIN BENEATH AUSTRIA, CZECHOSLOVAKIA AND HUNGARY

SCALE

1 : 500,000

0 10 20 30 40 50 km

Editors:

E. Kilényi (ELGI, Budapest) and
J. Šefara (Geofyzika Brno, Bratislava branch)

Mapping:

A. Kröll (ÖMV), P. Steinhauser (Vienna University) and
F. Weber (Mining University, Leoben) for Austria

D. Obernauer (Geofyzika Brno, Bratislava branch)
L. Pospíšil and A. Šutora (Geofyzika Brno) for Czechoslovakia

J. Rumpler (GKV, Budapest) and
Z. Szabó (ELGI, Budapest) for Hungary

Cartographic work: O. Kolačkovský (Geofyzika Brno, Bratislava branch)

PUBLISHED BY: EÖTVÖS LORÁND GEOPHYSICAL INSTITUTE OF HUNGARY

BUDAPEST 1989

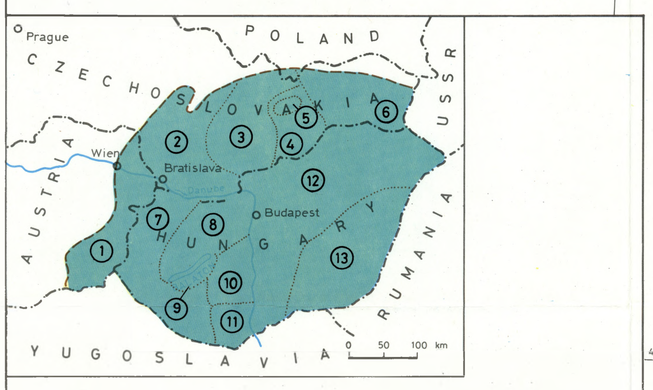

Mapping:

(1) A. KRÖLL, P. STEINHAUSER, F. WEBER for AUSTRIA.

(2) A. ŠUTORA, M. BIELIK; (3) J. ŠEFARA, R. VELICH; (4) J. BODNÁR; (5) M. KURKIN, J. MIKUŠKA;

(6) L. POSPÍŠIL, R. VELICH for CZECHOSLOVAKIA.

(7) a team led by B. BARDÓCZ; (8) A. PINTÉR; (9) S. MAJOROS; (10) L. NEMESI; (11) a team led by M. KASSAI; (12) E. KILENYI - Z. SZABÓ; (13) a team led by J. RUMPLER for HUNGARY.

0 5 10 15 20 25 30 35 40 45 50 km

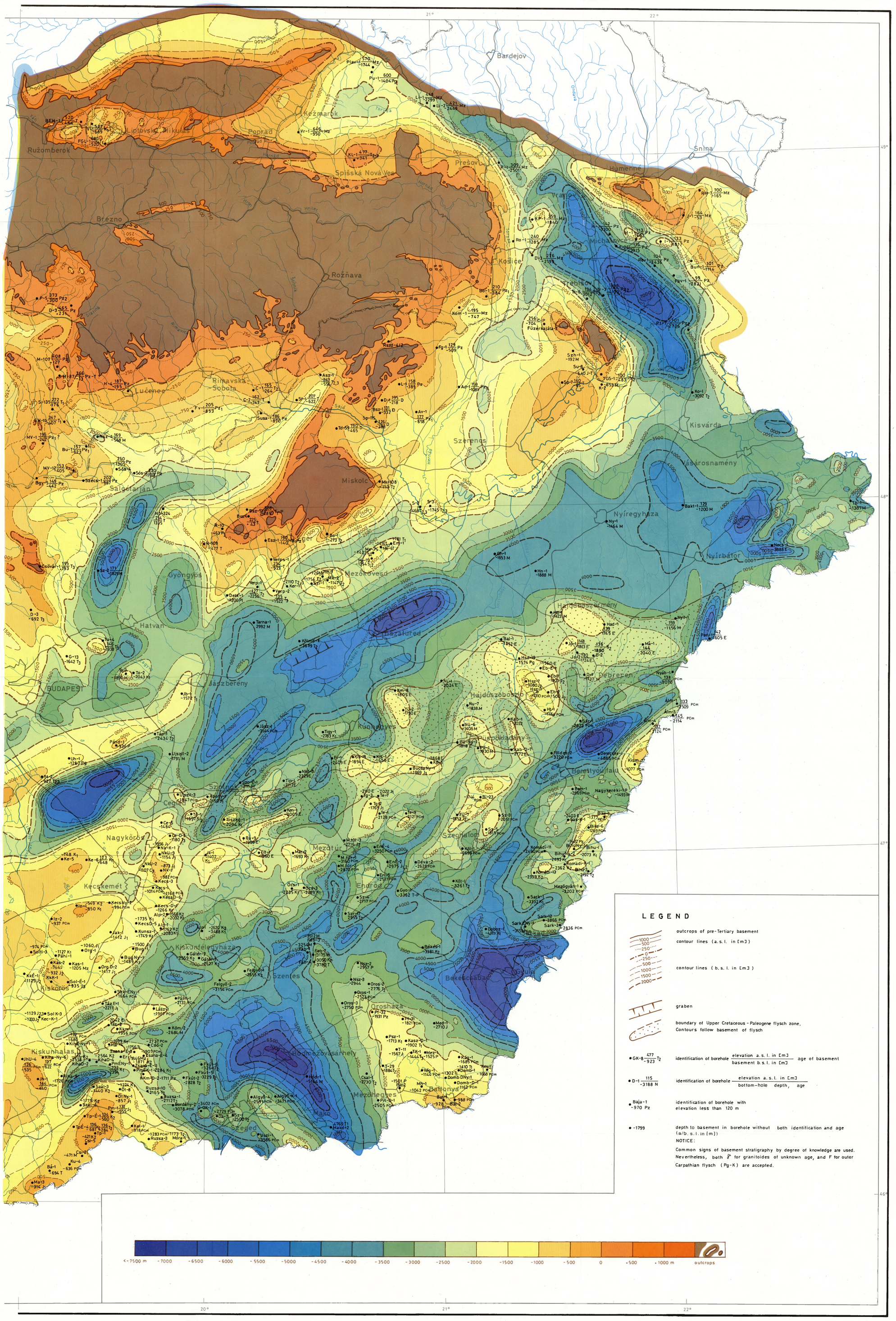

LEGEND

- outcrops of pre-Tertiary basement
- contour lines (a.s.l. in [m])
- contour lines (b.s.l. in [m])
- graben
- boundary of Upper Cretaceous - Paleogene flysch zone, Contours follow basement of flysch
- GK-8 $\frac{477}{-923}$ T_2 — identification of borehole $\frac{\text{elevation a.s.l. in [m]}}{\text{basement b.s.l. in [m]}}$ age of basement
- D-1 $\frac{115}{-3188}$ N — identification of borehole $\frac{\text{elevation a.s.l. in [m]}}{\text{bottom-hole depth,}}$ age
- Baja-1 / -970 Pz — identification of borehole with elevation less than 120 m
- -1799 — depth to basement in borehole without both identification and age (a/b. s.l. in [m])

NOTICE:

Common signs of basement stratigraphy by degree of knowledge are used. Nevertheless, both $\mathcal{G}$ for granitoides of unknown age, and F for outer Carpathian flysch (Pg-K) are accepted.

MH TÁTI 89-43